UNIVERSITY OF CALIFORNIA

Santa Barbara

Environmental and Geo-Social Factors in Alzheimer's Disease and Related Dementia Development

A dissertation submitted in partial satisfaction of the

requirements for the degree Doctor of Philosophy

in Geography

by

Gabrielle Eva Husted

Committee in charge:

Professor Susan Cassels, Chair

Professor Elizabeth Ackert

Professor Barbara Bendlin, University of Wisconsin-Madison

June 2026

The dissertation of Gabrielle Eva Husted is approved.

_____

Professor Elizabeth Ackert

_____

Professor Barbara Bendlin

_____

Professor Susan Cassels, Chair

May 2026

Environmental and Geo-Social Factors in Alzheimer's Disease and Related Dementia Development

DEDICATION

This dissertation is dedicated to Lev & Derek. Lev, you bring endless joy and reprieve to my long days caught up in my swirling thoughts. Derek, I cannot even come close to adequately conveying my gratitude for your presence in my life. You engage in my rambling fascinations, demonstrate incredible work ethic, and you help me cultivate comfort with the ebb and flow of the challenges that make for a great life.

ACKNOWLEDGEMENTS

Derek: You have been my source of confidence when I can't muster up any of my own. Over the years you somehow help me to see the progress I am making and take the time to acknowledge and celebrate it. Thank you for listening to all my practice TA sessions, my presentations for conferences and classes, and for reading my half-baked manuscript drafts. Thanks for picking up the slack on chores and helping me to be a little more flexible with what I prioritize. You have helped me stay nourished and active, balancing life and living amidst the never-ending work of a PhD program.

Susie: I still remember where I was when we had our first phone call about my interest in applying to work with you. It's one of those moments where I literally have a picture of what I was looking at imprinting in my eyes – it was such a pivotal moment! I was so motivated by your matter-of-fact guidance that it was *not* too much of a stretch for me to pivot from nursing; that clarity amidst my messy mind continued throughout my whole time at UCSB. You so kindly read numerous drafts of my work, talked through ideas and rabbit holes with me, helping me arrive at a feasible research agenda. You helped me learn how to network and develop collaborations, which has allowed me to engage in multi-disciplinary work. I am so grateful to have been advised by you; thank you for accepting me into the program! While the diploma is the tangible takeaway from these five years, the mentorship and positive work environment you provided is what has been the most impactful to me; it's set me on a trajectory I didn't even know was possible.

Liz – Connecting with you early on was such a gift. Working on your projects gave me a model for team research, provided a framework for how to structure a project, and exposed me to new methodologies. Thank you so much for investing in my

restricted use data clearance, inviting me to work with you in the UCLA RDC (I enjoyed being a part of that project, and honestly, I enjoyed the drives too!), and providing critical support for my work with the PSID.

Barb – I continue to be so appreciative (and even in awe) of your willingness to embrace my interest in ADRD work. Your openness to my research interests, connecting me with data to carry out my pilot study, and spending countless hours fielding my questions and pointing me in the right direction to learn more has been invaluable. I have learned so much from your research, your lab, and the resources you have connected me with. Thank you for making time for me just from such a chance encounter with your colleague, John Shadle, at an IAPHS conference (shoutout to him for introducing me to you!).

Rachel – Thank you so much for your enthusiasm for my project and demystifying chemistry and all the fancy instrumentation in the MRL. I had always revered that building, so it has been so cool to get to conduct research within it, with your expert guidance.

Monica – It has been such a privilege getting to know you through the GloCal application process, and beyond. I've thoroughly enjoyed working with you and learning from your approach to research questions, data wrangling, and funding, as well as your unique perspective as both a clinician and a researcher. Thank you for generously sharing your Lima social and cognitive population data with me, and for meeting with me regularly over the past year throughout this project.

Stuart – During my first year in 210C I had no idea how to work with R. Despite reading, going to class, working on the assignments, I needed tremendous support – thank you so much for taking the time to provide that extra, extensive support. It

meant so much to me that you met with me each week to re-explain and model how to navigate R, at the level I needed; I learned how to trouble shoot effectively, and what I learned during those sessions laid a solid foundation for my research.

Sigrid – You are an incredible friend and colleague. I feel so fortunate to have been office mates with you for four years, and you even showed up for me in my fifth year – whether that was via text or phone call or even showing up to conference with me! I enjoyed your company so much, learning about the latest teaching technique, equitable classroom practices, and data wrangling skills. Thank you for letting me turn our office into a play gym for Lev, too! You brought me into the UCSB-Geography-PHiG-academia fold; I knew next to nothing about graduate school when I started at UCSB, and you helped me get up to speed and find my way.

Silvana – How fun that we connected day one being TAs for GEOG 5, and despite having no overlap the rest of our time, we've been able to stay connected! Our friendship has been such a source of joy for me – whether its talking through our research to make sure it is translatable, playing tennis, going for walks, surveying the croissant scene of Santa Barbara, or chatting while Lev naps in the car! I love the perspective you bring to our conversations and the way you confidently approach challenges and opportunities.

Hannah Holman – Our morning workouts were so much more than an opportunity to move my body (which I also loved), they were a chance to ground myself, to reset, and set my day to the most positive tone. Your thoughtfulness, curiosity, and depth of genuine care for me, my family, and really everyone everywhere has been so comforting and inspiring. You've helped me maintain a healthy perspective, keep tabs on my priorities, and adjust to shifting roles and

responsibilities I've had over these five years. I'm so glad Bike Valet at the SB Bowl for CAAMP brought us together!

Fares – What a stand-up buddy you have been! I'm so glad our puppies had to pee all the time, leading to the beginning of our friendship! You provide support across the board, to me, Derek, Lev, and Siggi! I have loved all our co-working sessions, and having you as accountability to move my body, reinforcing that moving my body helps me do better work! It's been so fun to run, swim, bike, climb, and play tennis! Dancing is *not* on that list, but Derek and I did give it a go, just for you. Your passion for basically everything you engage with is admirable. Thank you for being such a constant in our lives. To be continued, please!

Madison – What a treat to cross paths with you in Susie's Geo-social determinants of health class! Thank you for all the individualized Stata tutoring sessions, and the collaboration as Broom Lab Managers. Your level-headed approach to academia, and our shared juggle to be grad students and present for our non-academic husbands was much more fun navigating it together. Thank you for all the above-and-beyond support when I was pregnant and in Lev's early months.

Population Health in Geography (PHiG) – Big shoutouts to all PHiG & PHiGlets, particularly to Bri, Hannah, Esaú, Katie, Sofia, Sophia, Sean, and Chelsie. It was such a treat to have a group of like-minded colleagues to meet with regularly, exchange ideas, and learn new skills in a supportive environment. Thanks, Bri for the lovely Saturday yoga and teatime meet ups. Hannah, it has been so nice working with you on the HEIRS project!

The Geography Department - I am grateful to the staff and administrative team in the Geography Department for their support throughout my graduate training.

Thank you for your help answering logistical questions, coordinating TA assignments, assisting with funding and applications to outside funding, and keeping the department organized and running smoothly. Your work behind the scenes made many parts of graduate school much easier to navigate, and I greatly appreciate it.

Mitchell – Thank you for encouraging me to be bold and go after what I seek; I've always admired your passion for learning and intense dedication to understand how processes and phenomena work. I still think back to the high school math class I was struggling in, and how you wouldn't let me wallow feeling defeated; thank you for believing in me then, and now!

Clarisse – Maybe this PhD is actually me subconsciously copying my big sister?! This clicked only recently in my mind - I think back to going to visit you during your undergrad, sitting in on your Reading Brains Lab meetings, interviewing your neuroscientist advisor for my high school project, and having such an exciting time being immersed in your studies! Possibly, that laid the foundation for my interest in ADRD. Beyond that foundational exposure you provided me, thank you for being such a support system to me for raising Lev and navigating competing demands on my time.

Mama – Who would've thought I would end up at your alma mater? It is such a treat to be finishing up my PhD at a place I grew up hearing you speak of so highly and happily! I have thoroughly enjoyed my time here and the full circle feel of spending time living and growing in a place that was so formative for you too. Thank you for all your love, encouragement, and support along this journey!

Deniene & Roy – I always enjoy our conversations; they make me think more creatively and help me to gather my thoughts. Talking through my research with you helps me identify any gaps in my understanding that I overlooked and also helps me to connect my research with other current events. Roy, I've enjoyed you keeping me in the loop with UCI researchers you've written stories about, and the news broadly – so fun to get the inside, expert journalists' scoop! Deniene, you have been instrumental from the beginning! Thank you for reading and providing valuable comments on my UCSB application!

UCSB – What an amazing place to complete a PhD! The resources and facilities are exceptional, the campus inspires balance, and there are many opportunities for interdisciplinary collaboration. I'm grateful to the Broom Center for the stimulating seminar series each quarter, and to the Geography Department for all the support and administrative assistance. UCSB has been such an amazing place to be rooted for 5 years; I've been able to progress not only in my academic studies, but also in my personal life goals through all the fantastic and accessible resources UCSB provides. A huge THANK YOU to the **University Children's Center**! Colleen, Alessandra, Olivia, and amazing teaching assistants, thank you all for helping Lev have such exciting and enriching days! I love reading the curriculum for the week and seeing the new interests and skills it cultivates within Lev. I am so grateful for the love and kindness Lev receives at school, and how intentional you all are in what you say and do. It is such a relief to know Lev is so well taken care of while we are at work. Special shoutout to Briza for her hours in the sandbox with Lev!

VITA OF GABRIELLE EVA HUSTED
June 2026

EDUCATION
Bachelor's of Science in Nursing, University of Portland, May 2018
Master of Arts in Geography, University of California-Santa Barbara, May 2023
Doctor of Philosophy in Geography, University of California-Santa Barbara, June 2026 (expected)
PhD Emphasis in Environment and Society
PhD Emphasis in Demography

PROFESSIONAL EMPLOYMENT
2021-2026: Teaching Assistant, Department of Geography, University of California-Santa Barbara
Oceans and Atmosphere, People Place and Environment, Sex Drugs and Geography, Geography of Surfing, Research Methods, Urban Geography, Population Geography, Channel Islands, Health Geography, Teaching Assistant Training
2021-2026: Graduate Student Researcher, Department of Geography, University of California-Santa Barbara
2023-2026: Laboratory Manager, Broom Center for Demography, University of California-Santa Barbara
2020-2021: Community Outreach Specialist I, Public Health Institute
2020-2021: Registered Nurse, BrightStar
2019-2020: Registered Nurse, MedStar Washington Hospital Center
2019: Registered Nurse, Compassionate Cancer Care Center

PUBLICATIONS
Gabrielle Eva Husted, Susan Cassels, Elizabeth Ackert, Stuart Sweeney (2024). "Socio-Demographic Patterning of Urinary Mono-ethyl Phthalate Levels among Children and Adults the U.S. (1999-2018)." Environmental Research Communications.

Sigrid Van Den Abbeele, Dan Grafton, Madison Avila, Gabrielle Eva Husted, Esau Casimiro Vieyra, Brianna Chan, Sofia Kaloper, Ben Moscona-Remnitz, Susan Cassels (2025). "Teaching and learning about geo-social determinants of health." Place & The Social-Spatial Determinants of Health. Springer.

AWARDS
Broom Center for Demography, Graduate Student Research and Travel Grant, 2022
Broom Center for Demography, Graduate Student Research and Travel Grant, 2024
Inter-university Consortium for Political and Social Research (ICPSR) Panel Study of Income Dynamics (PSID) Sponsored Workshop, 2024
Center For Feminist Futures, Gender, Race, and Health Fellowship, 2025
Healthy Communities Project, 2025

FIELDS OF STUDY
Major Field: Geography with Dr. Susan Cassels and Dr. Elizabeth Ackert
Studies in Neuroscience with Dr. Barbara Bendlin

Studies in Chromatography with Dr. Rachel Behrens

ABSTRACT

Environmental and Geo-Social Factors in Alzheimer's Disease and Related Dementia Development

by

Gabrielle Eva Husted

The broad question examined in this dissertation is how environmental exposures shape the risk of Alzheimer's disease and related dementias (ADRD). More specifically, this dissertation investigates socio-environmental inequalities, phthalate exposure, and air pollution as determinants of cognitive aging across multiple geographic and biological scales, drawing on methods from spatial epidemiology, environmental health, biomarker development, and population health research. Chapter 1 uses linked Panel Study of Income Dynamics (PSID), EPA Toxic Release Inventory (TRI), and U.S. Census data to examine whether long-term exposure to emissions from plastics and rubber manufacturing facilities is associated with ADRD risk in the United States. Using longitudinal modeling and logistic regression, this chapter finds that higher emissions intensity from plastics and rubber-related facilities is associated with increased ADRD risk, independent of individual socioeconomic characteristics and neighborhood disadvantage. Neighborhood disadvantage also emerges as a strong independent predictor of ADRD risk, underscoring the importance of structural and environmental determinants of cognitive aging. Chapter 2 develops a laboratory method for detecting phthalates in human fecal samples (n=10) using ultra-high-performance liquid chromatography-mass spectrometry (UPLC-MS), with data from the Microbiome in Alzheimer's Risk Study (MARS). This chapter demonstrates that phthalates are detectable in human

fecal samples and establishes a proof-of-concept for using fecal biomarkers in environmental exposure research, laying the groundwork for future studies examining relationships among phthalate exposure, gut microbiome function, and cognitive health outcomes. Chapter 3 investigates air pollution and cognitive health within an under-resourced population in Lima, Peru using secondary door-to-door survey data (n=1,066) paired with PurpleAir and OpenStreetMap data. This chapter examines the feasibility of integrating citizen-science air pollution monitoring with community-based cognitive health research in a region with limited environmental monitoring infrastructure. While no significant associations were observed between PM2.5 and cognitive outcomes, uniformly high exposure levels and limited within-population exposure variation likely complicate detection of exposure-response gradients. Secondary findings suggest that roadway proximity may reflect both pollution exposure and improved access to transportation, healthcare, social engagement, and socio-economic status, highlighting the complexity of disentangling environmental risks in urban, low-and-middle-income contexts. This chapter also underscores persistent data gaps in cognitive health and environmental research in LMICs. Together these chapters demonstrate that environmental exposures, from industrial emissions to chemical pollutants to air quality, are unequally distributed and may contribute to disparate ADRD risk across populations and geographies. This dissertation advances interdisciplinary methods for studying environmental contributors to cognitive aging and points to the need for more equitable environmental and public health policy.

CONTENTS

Introduction	1
Chapter 1	11
Chapter 2	66
Chapter 3	114
Conclusion	163
References	172
Appendix	199

LIST OF TABLES

Table 1 Distribution of ADRD risk by year of AD8 Survey and potential observation values. Data: Panel Study of Income Dynamics (PSID), years 2017-2023, unweighted. 28

Table 2 Unweighted descriptive statistics (n=2,627). Data: Panel Study of Income Dynamics (PSID) 1990-2023, Environmental Protection Agency Toxic Release Inventory (EPA TRI) 1990-2017, and Neighborhood Change Database (NCDB) 1990-2020. 41

Table 3 Descriptive statistics stratified by ADRD Risk (n=2,627). Unweighted chi-squared values are reported. Data: PSID 1990-2023, EPA TRI 1990-2017, and NCDB 1990-2020. Significance levels: $p < 0.05$ *, $p < 0.01$ **, $p < 0.001$ ***. 43

Table 4 Odds ratios from logistic regression models predicting ADRD risk. Reference categories and model fit statistics are shown. Significance levels: $p < 0.05$ *, $p < 0.01$ **, $p < 0.001$ ***. 46

Table 5 Approximate PSID observational coverage in U.S. states with known high concentrations of plastics/rubber facilities. 61

Table 6 Major phthalate esters (PAEs) and their metabolites. Full name, abbreviation, chemical formula, and corresponding de-protonated species mass. ... 72

Table 7 Depicts chemical classes, target analytes, and detection performance across different human biological matrices, adapted from Jagani et al., 2025. 85

Table 8 LC method parameters for the UPLC-MS of phthalates within stool samples. Mobile phase A: Water + 0.1% Formic Acid. Mobile phase B: Acetonitrile + 0.1% Formic Acid. 88

Table 9 Demographic and clinical characteristics of the MARS cohort (n = 315). Activity level is self-reported physical activity (5-point scale). Bristol Stool Scale reflects stool consistency at time of sample collection (7 point scale). 92

Table 10 Demographic and clinical characteristics of the MARS cohort (n = 315). Continuous variables are reported as mean ± standard deviation. 93

Table 11 Geo-social and cognitive biomarkers in ten fecal samples from the Microbiome in Alzheimer's Risk Study (MARS). 100

Table 12 Description of each sensor; PurpleAir ID, PurpleAir sensor name (shortened), available data timeframe, and the number of participants in our sample located nearest each sensor. 123

Table 13 Participant characteristics and environmental exposures (n = 1,066). 134

Table 14 Exposure measures and cognitive outcomes by PurpleAir sensor zone..... 137

Table 15 Comparison of socio-demographic and cognitive measures across six PurpleAir Sensor locations. 138

Table 16 Cognitive outcomes by socioeconomic status level among adults in Puente Piedra, Peru. SES categories reflect the Peruvian NSE classification system, ranging from NSE A (highest) to NSE E (lowest). (n = 1,066). 148

Table 17 Road type stratified sensitivity analyses: trunk, primary, secondary × dementia binary, RUDAS-PE, ACE. * $p < 0.10$, ** $p < 0.05$, *** $p < 0.01$. 150

LIST OF FIGURES

Figure 1 (A) LC chromatographic confirmation of (A) mono-n-butyl phthalate (mnBP) (B) mono(2-ethylhexyl) phthalate (MEHP) analytical standard. 84

Figure 2 PubChem 2D structural images of parent phthalates examined in this paper. From left to right: Di-ethyl phthalate, Di-n-butyl phthalate, Butylbenzyl phthalate, Di-(2-ethylhexyl) phthalate, Di-iso-nonyl phthalate. 84

Figure 3 Waters UPLC-MS. UCSB Materials Research Laboratory. Polymer Lab. 87

Figure 4 Gut microbiome enterotypes among WRAP participants (n = 315). Colors denote enterotypes based on dominant genera. Enterotype 1 = Orange, Enterotype 2 = Green. 94

Figure 5 Relative abundance of the top five bacterial species within each enterotype. 94

Figure 6 Detection of 19 phthalates in ten fecal samples from the Microbiome in Alzheimer's Risk Study (MARS (n = 10).. Green circles indicate strong signal, yellow circles indicate trace, and gray circles indicate non-detection. 103

Figure 7 Percent phthalate detected stratified by ADI score. Microbiome in Alzheimer's Risk Study (MARS) (n = 10). 104

Figure 8 Map of study area and participant locations, colored by cognitive status. RED = dementia, PINK = mild cognitive impairment, GREEN = healthy. Asterisk = sensor. Participants (n=1,066), Sensors (n = 6). 122

Figure 9 A-B Channel Agreement Heatmaps (PM2.5 and PM10) across six sensors, 2022-2026. Darker purple indicated lower disagreement (higher reliability); yellow-green indicates greater channel divergence. 126

Figure 10 PurpleAir Time Series (1st-99th percentile) PM2.5, PM10, temperature, and humidity across six sensors, post-QC. 127

Figure 11 Relationship between socio-economic status and dementia status (n = 1,066). NSE E = most socio-economically deprived. 142

Figure 12 Air quality exposures and cognitive outcomes (binary dementia, ACE younger adults, RUDAS-PE older adults). Exposures standardized per 1 SD. Cluster-robust SE at sector x "conglomerado" level. (n = 1,066). 145

Figure 13 Cognitive outcomes by distance to nearest major road (buffer zones: within 100m, 100-500m, 500-1km, beyond 1km). Unadjusted means for % cognitive impairment, mean RUDAS-PE, and mean ACE. 146

Figure 14 Road distance (log) and three cognitive outcomes (binary cognitive impairment, ACE, and RUDAS-PE) showing unadjusted, age and sex adjusted, and fully adjusted results (n = 1,066). 148

Figure 15 Predicted ACE scores from OLS regression adjusted for age and sex and with an interaction term between SES and roadway distance. NSE E = lowest category. Shaded bands reflect 95% CI. (n = 1,066). 151

INTRODUCTION

How do you identify toxicity, or simply harm, when something is so intertwined with habits and processes of daily life? The short answer is that it takes considerable time, determination, and collaboration. In recent years it has become abundantly clear that plastics pervade all aspects of our lives. Plastics break down into micro- and nano-plastics that can make their way into our bodies' organs and tissues, such as the placenta, the lungs, and the brain (Nihart et al., 2025). We are exposed across the life course, from in-utero to end of life. We can be exposed via direct contact through products we knowingly choose, yet many exposures come "second-hand" through the social and structural pathways that shape our exposures. With this in mind, in order to make meaningful improvements to public health, a collective, unified effort in the form of policy change and systemic-level interventions and investments is critical when approaching ubiquitous environmental exposures and health outcomes. This dissertation broadly asks how environmental and geo-social factors shape Alzheimer's disease and related dementia risk. We explore how environmental hazards become health inequities through geo-social differentiation. While exposure to plastics is ubiquitous in industrialized societies, geo-social factors create differential exposure patterns and vulnerabilities. Within this dissertation, we repeatedly observe the importance of socio-economic status and access to resources shaping dementia risk. Our work contributes to and reinforces the understanding that modifiable risk factors are present, are unequally impactful, and with concerted effort, can be minimized. A couple examples from public health allow us to elaborate on the challenges of identifying, managing, and mitigating systemic-level environmental hazards.

Silent epidemic: Lead

Since antiquity, lead has been known to cause harm, being associated by the ancient Romans with the “ghoulish” deity Saturn – the word “saturnine” was a term used to describe someone who had personality and behavior changes as a result of lead intoxication; they became irritable, anti-social, and impulsive (US EPA, n.d.) However, it was not until 1974 that concrete evidence for the harms of lead, at any level beyond zero, came to light. Dr. Needleman studied the deciduous (baby) teeth of children in a diverse group of elementary schools in Philadelphia, selected based on the socio-economic status of the students they served, and their proximity to known sources of lead (e.g., highways, smelting factories). Teeth can reflect a reliable estimate of body burden of lead because they permanently store lead. They provide a cumulative measure of lead exposure, even when other samples, like blood levels of lead, are low or zero (Strehlow, 1972). Dr. Needleman found that all levels of exposure to lead were detrimental to children' s cognitive development and socio-emotional skills, and that those at risk extend beyond the previously identified populations – low income, non-white race, living in deteriorating housing. While lead paint and leaded gas are primarily sources of lead exposure, this work highlighted the role of airborne lead settling in environments that children interact with, such as school yards and sand boxes, and by examining teeth, the authors were able to uncover that lead exposure is far more extensive than previously thought. These findings were contested by industrial giants that did not want limitations placed on using lead. Consequently, phasing out lead from products like gasoline, paint, and plumbing took place over decades, with some efforts continuing into the present day (*Lead and Children’s Health*, 2026).

Denial, then disparity

A similar story of adamant denial of the harms of something convenient, yet insidious can be found in smoking. Smoking was originally marketed as 'good for your nerves,' yet with the sharp rise in lung cancer, individuals, the medical community, and non-profit groups began to contest the safety of smoking. Leaders of these groups urged President Kennedy to commission a study to investigate the risks associated with smoking. It led to the 1964 landmark report *Smoking and Health: Report of the Advisory Committee to the Surgeon General of the Public Health Service (Selling Smoke: Tobacco Advertising and Anti-Smoking Campaigns, Yale University Library Online Exhibitions, n.d.).* The findings were conclusive, and anti-smoking efforts have been underway since the 1970s, including bans in public places, places of work, and within the home. However, bans frequently result in industry creating an alternative that is often equally harmful (e.g., BPA is banned, then replaced with BPS. Cigarettes replaced with vaping). Additionally, recent data show that although overall smoking rates have declined, smoking remains disproportionately prevalent among marginalized populations. Rates are estimated to be nearly three times higher among individuals with lower socioeconomic status (SES) or lower educational attainment, as well as among sexual and gender minorities and those with histories of unstable housing, mental health conditions, or substance use. These disparities underscore the need for targeted public health approaches. Relevant to our plastics work, smoking prevalence nearly doubles when *alternative* nicotine products such as e-cigarettes are included, increasing estimates from 9.9% to 18.8% of the U.S. population (Agaku, 2026).

Modern day public health crisis: Plastics

These examples highlight core challenges of researching population level environmental exposures and health outcomes – including determining how to measure the exposure, how to identify body burden, and how to communicate the findings to elicit population-level change. This dissertation investigates the potential harms of plastics. They are ubiquitous, under-researched, and largely unregulated. The mechanisms of how the chemicals in plastics impact health outcomes are still unclear. Echoing the nature of claims that lead and smoking were not overwhelmingly harmful, a recent NPR article states that the World Health Organization did not find evidence of health concerns from microplastics in drinking water (Neuman, 2019). However, upon close reading of the article, the researchers clarify that their report is based on incomplete information. They emphasize the urgent need to know more about the health impact of microplastics because of their omnipresence. The WHO director of public health paired this caution with a recommendation to develop new ways to remove microplastics from drinking water and to establish standard methods for measuring microplastics in water – clearly communicating that their report was no reason to sit back and enjoy the plastic-infused water.

Plastics present a third, and in some ways more complex, iteration of this same pattern seen in lead and smoking as a public health crisis. Microplastics are plastics that are less than 5mm, about the size of a pencil eraser tip. As they break down into their chemical components, whether that is due to time, heat exposure, or a contact interaction, they pose greater threat to the health of humans. Nanoplastics are those

that are less than 1 μm in size. They are unable to be seen with the naked eye, and they are small enough to enter the body's cells and tissues; nanoplastics have been found in human blood, lungs, gut, feces, and reproductive tissues like the placenta and testes.(Campanale et al., 2020; Y. Deng et al., 2017; Lim, n.d.) Plastic production has been increasing exponentially since the 1940s. Plastic manufacturing involves the use of additives, one major component being phthalates, a plasticizer. Phthalates are colorless, odorless, oily liquids. They're in shampoo bottles, medical equipment, food containers, vinyl flooring, children's toys—everywhere. Phthalates do not chemically bind to the material they are added to, which leads to them being readily absorbed into the human body; through leaching into food or water that has been stored in container made with phthalates, exposure to airborne phthalate particles when working with materials such as plastic piping or synthetic furniture, and our skin can absorb phthalates from certain lotion and cosmetics.(Zarus et al., 2021) Phthalates are rapidly metabolized in the body, roughly within 12 hours, however, due to constant re-exposure and the bio-availability of phthalates, more research is needed to determine what proportion is retained, and how they are excreted.

Geo-Social Determinants of Health and the Exposome

While exposure to plastics is ubiquitous in industrialized societies, geo-social factors create differential exposure patterns and vulnerabilities (Cox et al., 2019; Hale et al., 2020; Husted et al., 2024). Exposure to plastics, and the chemicals they are composed of, isn't random. Marginalized populations such as communities of color

and low-income neighborhoods face higher pollution levels (Braveman et al., 2011; Fricker, n.d.). They may live closer to plastic manufacturing plants and have fewer resources to reduce exposure. Choosing glass over plastic, whole foods over packaged goods — these are choices that are constrained by income and access. Geo-social factors don't just shape whose health deteriorates; they shape who gets exposed in the first place. Two theoretical frameworks unite this dissertation and help make sense of these patterns. Geo-social determinants of health refers to the upstream factors - those occurring prior to any clinical interventions - that shape health outcomes (Braveman et al., 2011; Diez Roux, 2022; Marmot, 2017; Sharkey & Faber, 2014). The key component is that individuals have constrained choices in where they are born, grow, live, work, and age (Marmot, 2015, 2017; *Status Syndrome - Marmot - 2004 - Significance - Wiley Online Library*, n.d.). These constraints are patterned by race, class, and place, and they create differential vulnerability to environmental exposures like phthalates. The second framework is the exposome — the sum of all environmental exposures across the life course, from air quality and diet to stress and housing (Karlsson et al., 2021; Rappaport, 2011; Wild, 2005). What's powerful about this concept is that it operationalizes how social inequalities literally get under the skin. It complements the genome; environmental factors can modulate epigenetic modifications, such as DNA methylation and histone modifications, thereby altering gene expression. The exposome reminds us that our biology is socially embedded, and that is good news, because it means it's potentially modifiable. Early life education access, midlife smoking and employment, later life social connection and proximity to healthcare are all entry points for ‘health’ interventions.

Phthalate-Gut-Brain Nexus

Chronic neuroinflammation is a direct contributor to Alzheimer's pathology, and many of the factors that drive it are social and environmental in origin. Phthalates are among the environmental factors suspected to drive this neuroinflammatory burden, though the mechanisms are still being explored (Agin et al., 2020; Z. Deng et al., 2024; Dutta et al., 2020; Jin et al., 2023). Dementia prevalence rises sharply with age, and is meaningfully higher among women across all age groups (*Dementia*, n.d.). By age 90+, nearly 39% of women globally carry a dementia diagnosis (*Dementia*, n.d.). The trajectory in the U.S. is stark. By 2050, it is expected that nearly 13 million Americans will be living with Alzheimer's, which is roughly double today's burden (*Alzheimer's Disease Facts and Figures*, n.d.). However, we know at a population level that social inequalities largely shape who gets dementia. The mechanisms, though, are still being worked out. We focus on pre-clinical biology and non-pharmacological entry points aimed at reducing ADRD risk. We leverage a variety of contextual data to investigate the relationship between phthalates and ADRD, including demographic, socio-economic, neighborhood deprivation, biomarker, industrial manufacturing, and air pollution data.

Examining deciduous teeth allowed researchers to understand the longitudinal impacts of low-level exposure to lead. A presidentially commissioned research effort decisively determined the harm of smoking. Both leading to assertive and enduring policy to protect public health. The methodological lessons from lead and tobacco research inform how this dissertation approaches plastics. While phthalate research has been around since the 70s, it has yet to achieve universal acceptance as a hazard

with across-the-board regulation implemented. Initially research focused on animal models and established the harms to endocrine and cardiovascular systems. Then the National Health and Nutrition Examination Survey (NHANES) began studying human urine levels of phthalates in 1999 and onward. However, there is growing evidence that a multi-modal approach is needed to gain the clearest picture of the effects of phthalates on humans.

Recent work by a group of scientists at Scripps studied over 2,300 seawater samples from various projects around the world, seeking to catalog traces of human-made chemicals. They used a non-targeted lab approach and reference libraries to tackle this project. One of their top pollutants identified were plasticizers. While this article was informative, simply through reporting on the contents of ocean pollution, a comment from one of the authors was particularly insightful and validating for this dissertation:

> *"The human footprint is in everything… What determines whether you find it is whether you look for it in your data"* (Fox, 2026). *–Lihini Aluwihare, a chemical oceanographer at Scripps and co-author of the study*

This dissertation directly looks for phthalates within a variety of data sources at different geographical and population scales, broadly asking how environmental and geo-social factors shape Alzheimer's Disease and Related Dementia (ADRD) risk. While many types of dementia fall under the ADRD umbrella, 60-80% of cases are estimated to be Alzheimer's Disease, and 40% of dementia cases worldwide are attributable to 12 modifiable risk factors (Alzheimer's Disease Facts and Figures, n.d.; Livingston et al., 2020). Different brain pathology and structural changes indicate underlying progressive neurodegenerative disease and help researchers

characterize an individual's disease. Specifically for Alzheimer's Disease, it's estimated that there can be a gap of ten to twenty years between when neuropathology begins and when memory loss and other symptoms arise, making early predictors of AD progression a critical research target. All three chapters are connected by the social determinants of health framework and the exposome paradigm, which together facilitate understanding how environmental hazards can become health inequities through geo-social differentiation.

Chapter 1 uses national data to examine how socio-demographic and geographic inequalities shape phthalate exposure and its links to cognitive impairment. Specifically, we examine how exposure to industrial pollution – measured as emissions intensity from the nearest plastics or rubber facility – affects ADRD risk over time. Socioeconomic status and neighborhood resources shape both where people live and their access to protective factors, and residential mobility can cause exposure to accumulate differently across the life course.

Chapter 2 zooms into the gut as a biological site of exposure to plastics using University of Wisconsin-Madison's Alzheimer's Disease Research Center clinical core and biomarker core data. The gut is central to this story: we have roughly 100 trillion microorganisms in the gut, producing hormones, modulating immunity and communicating bidirectionally with the brain (ELS, 2024; Heston et al., 2022, 2023). Research has shown that intestinal inflammation is associated with greater amyloid burden, and that specific microbial metabolites in cerebrospinal fluid track with faster neurodegeneration, yet no studies have examined fecal levels of

phthalates as they related to gut microbiome composition and brain biomarkers (Heston et al., 2022, 2023; Vogt et al., 2017). Because lab protocols for analysis of fecal samples for phthalates don't yet exist, this chapter is both a methodological and empirical contribution: a proof-of-concept project that opens up new measurement considerations and research questions.

Chapter 3 moves to Peru, examining chronic air pollution and dementia in a marginalized peri-urban community in Lima using secondary data from a door-to-door population-based study, along with publicly available PurpleAir monitoring data and OpenStreetMap data. While the environmental exposure focus shifts from phthalates to air pollution more broadly (which likely includes aggregated phthalates within particulate matter measurements), the primary goal is to explore health equity in data monitoring within low-to-middle-income countries. A critical barrier to understanding health inequities is the lack of adequate, fine-grained data, which leads to an underestimation of increased risk among lesser-resources populations. We specifically investigated how chronic air pollution exposure intersects with socio-demographic vulnerability to potentially affect dementia in Puente Piedra, Lima.

CHAPTER 1

Long-Term Environmental Exposure and Cognitive Impairment in Older U.S. Adults

Authors:

Gabrielle Eva Husted, M.A.[1], Susan L. Cassels, Ph.D.[1], Elizabeth S. Ackert, Ph.D.[1], Barbara B. Bendlin, Ph.D.[2]

[1]University of California-Santa Barbara Geography Department

[2]University of Wisconsin-Madison Division of Geriatrics and Gerontology within the Department of Medicine

Acknowledgments:

Some of the data used in this analysis are derived from Restricted Data Files of the PSID, obtained under special contractual arrangements designed to protect the anonymity of respondents. These data are not available from the authors. Persons interested in obtaining PSID Restricted Data Files should contact PSIDHelp@umich.edu.

Abstract:

Background: The demographic shift toward an older global population is contributing to the rising burden of Alzheimer's Disease and Related Dementias (ADRD), as increased life expectancy and declining fertility reshape population structure. While age remains the strongest risk factor, emerging evidence suggests that other determinants may also influence incidence trends. Environmental

toxicants, in particular, are increasingly recognized as contributors to cognitive decline, underscoring the need to examine their role in cognitive aging. **Objective:** To assess whether exposure to plastics/rubber industry emissions is associated with ADRD risk, and whether sociodemographic factors modify this relationship. **Methods:** We linked geocoded Environmental Protection Agency (EPA) Toxic Release Inventory (TRI) data with Panel Study of Income Dynamics (PSID) records and census data from the Neighborhood Change Database (NCDB). Using spatial statistical methods and neighborhood effects frameworks, we measured historical exposure to plastics/rubber emissions and time-varying sociodemographic characteristics from 1990–2017, leveraging PSID's longitudinal structure to capture residential mobility. ADRD outcomes were defined as any positive AD8 screen in 2017, 2019, 2021, or 2023. Logistic regression models estimated ADRD risk as a function of the average total pounds of chemicals (released into air, water, and land) from the TRI facility nearest to the centroid of each individual's census tract of residence. Models accounted for changes in residential location over time and adjusted for individual-level factors (sex, race, age, education, income, marital status, home ownership, number of moves) as well as neighborhood-level disadvantage. **Results:** Moderate average exposure to plastics/rubber TRI emissions was significantly associated with elevated ADRD risk (OR = 1.339), independent of income and neighborhood disadvantage. Other contextual effects, specifically neighborhood disadvantage, appeared to be highly predictive of elevated ADRD risk.

Introduction

Phthalates—chemicals widely used to soften plastics and stabilize plastic products—have become pervasive in daily life since the 1940s. They are found in flooring, food packaging, medical devices, cosmetics, and children's toys, entering the body via ingestion, inhalation, and dermal absorption. Exposure patterns are socially stratified, with low-income and marginalized populations facing higher burdens likely due to housing quality, occupational environments, and product usage patterns (Wang & Qian, 2021; Zarus et al., 2021). While traditionally classified as endocrine disruptors, phthalates are now recognized as neurotoxicants. Human and animal studies link higher phthalate metabolite levels to impaired memory, reduced processing speed, altered synaptic signaling, and neurodevelopmental disorders (Engel et al., 2021). Mechanistic work points to oxidative stress, mitochondrial dysfunction, acetylcholine disruption, and persistent neuroinflammation—processes closely aligned with ADRD. Despite these accumulating findings, regulatory oversight remains limited (Pletz, 2022; Sadeghzadeh, 2024), underscoring the need to examine phthalates as contributors to cognitive aging.

The social determinants of health framework recognizes that upstream, non-medical factors such as education, income, race, and neighborhood conditions shape both exposure and resilience. Life course experiences influence gut microbiome composition, which in turn may affect vulnerability to environmental toxicants (Subramanian, 2014; Rinninella et al., 2019). Plastic production itself reflects environmental inequities: the U.S. hosts 35 ethane cracker plants — concentrated in Texas and Louisiana — that convert fracked gas into ethylene for plastics.

Communities living near these facilities face greater phthalate exposure through polluted air and other pathways (EPA, 2017). In Louisiana's St. James Parish, "Cancer Alley" illustrates how historic racial and economic marginalization intersects with industrial siting to produce disproportionate burdens of cancer, respiratory disease, and adverse birth outcomes (Verdin, 2020; Terrell & Julien, 2021; Human Rights Watch, 2024).

Prior research has linked air pollution to dementia risk, but several important gaps remain. Most studies focus on broad categories of pollutants (e.g., PM2.5) rather than source-specific exposures, leaving the contribution of plastics/rubber manufacturing — a major emitter of phthalates and other neurotoxic chemicals — largely unexplored. Few analyses consider long-term exposures at fine spatial scales, and even fewer account for residential mobility or changing census tract boundaries. In addition, the environmental justice dimensions of dementia risk are understudied, despite evidence that disadvantaged communities and communities of color are disproportionately burdened by industrial facilities. Our study addresses these gaps by linking nearly three decades of geocoded TRI data on plastics/rubber facilities to cognitive outcomes, providing a novel test of source-specific toxic exposure in relation to ADRD symptoms. Establishing this connection would not only advance understanding of environmental contributions to dementia but also inform upstream, neighborhood-level, and policy interventions to promote healthier aging and reduce inequities in cognitive health (Farsetta, 2020).

The central focus of this paper is to examine whether exposure to plastics/rubber producing industries is associated with ADRD risk, and how socio-demographic context influences that relationship. This paper aims to identify the relationship between socio-demographic characteristics of individuals with ADRD risk and proximity to toxic chemical waste from the plastics/rubber sector.

Research questions & Hypotheses:

(1) **Primary association:** Is average yearly exposure intensity (total pounds of emissions released from the nearest plastics/rubber TRI facility) over the study timeframe (1990-2017) associated with ADRD risk?

Hypothesis: Individuals with higher yearly average exposure intensity—measured as greater total pounds of emissions released by their nearest plastics/rubber TRI facility over the study timeframe, 1990-2017—will exhibit higher ADRD risk, where ADRD is defined as reporting two or more cognitive difficulties on the PSID AD8 dementia screening tool.

(2) **Exposure accumulation:** Is living in a census tract with closer proximity to plastics and rubber polluting industries associated with increased likelihood of ADRD?

Hypothesis: Closer proximity (measured in km from census tract centroids to the nearest EPA TRI plastics/rubber facility) will be significantly associated with increased ADRD risk.

(3) **Effect modification:** Does household income (as a proxy for socioeconomic status) moderate the association between emissions from plastics/rubber polluting industries and ADRD risk?

Hypothesis: The association between emissions exposure and ADRD risk will vary by income level, as demonstrated by a statistically significant interaction term (exposure × income) in regression models.

Background

ADRD Burden and Risk Factors

Alzheimer's disease accounts for 60–80% of dementia cases (Alzheimer's Association, 2020; Alzheimer's Disease International, 2020; Alzheimer's Association, 2024) and is a progressive neurodegenerative disease defined by abnormal proteinopathies (amyloid plaques and neurofibrillary tangles), with a prolonged silent phase before eventual cognitive decline, behavioral changes, and physical challenges. The 2020 economic toll reached $305 billion (Wong, 2020; Milken Institute, 2022), though this doesn't capture broader societal repercussions or the loss of quality time with loved ones. Approximately 6.9 million Americans aged 65 and older have Alzheimer's dementia, with an additional 200,000 experiencing younger-onset dementia (Alzheimer's Association, 2024). Alzheimer's disease mortality has increased significantly, with deaths more than doubling between 2000 and 2021—a 141% rise. While demographic shifts toward longer lifespans contribute to rising ADRD rates, proper understanding and access to risk-minimizing behaviors could help plateau these trends.

ADRD pathology accumulates years before clinical diagnosis. While age and genetics are unmodifiable, twelve established modifiable risk factors—including low education, hypertension, hearing loss, obesity, smoking, and air pollution—account for about 40% of the global dementia burden (Livingston et al., 2020). Reduced environmental exposures are associated with reductions in neuropathological damage, supporting prevention efforts (Zetterberg & Bendlin, 2021).

Phthalates and Gut Microbiome Pathways

This study focuses specifically on pollutants released by plastics/rubber manufacturing industries, rather than general pollution exposure, due to their unique chemical composition and increasing environmental ubiquity. Unlike many airborne pollutants that dissipate quickly or face stricter regulation, phthalates persist environmentally and accumulate in human bodies. This targeted approach moves beyond broad environmental hazard measures to interrogate socially patterned exposure pathways especially relevant to ADRD.

One pathway through which phthalates may influence neurodegeneration is the gut microbiome. After absorption, phthalates can reach the gastrointestinal tract and alter microbial composition and metabolic function. Experimental evidence shows that exposure to diethylhexyl phthalate (DEHP) reduces *Clostridium sensu stricto* and increases *Lachnoclostridium*, leading to elevated p-cresol—a microbial metabolite associated with neurodevelopmental and inflammatory disorders (Lei et al., 2019).

Such dysbiosis is relevant because the gut–brain axis plays a critical role in regulating immune signaling, neurotransmitter production, and neuroinflammation. Perturbations in microbial composition can increase permeability of the gut and blood–brain barriers, triggering release of proinflammatory cytokines such as TNF-α (Jang et al., 2021). Although gut disruption can arise from diet, antibiotics, or chronic illness, environmental chemicals are increasingly recognized as key drivers (Goodrich et al., 2014; Vatanen et al., 2016). The EPA's emphasis on cumulative "chemical and non-chemical stressors" (Frey, 2022) further highlights the importance of considering how social inequities compound biological vulnerability along this pathway.

Geographic and Social Patterns of Exposure

Exposure patterns vary geographically from neighborhood blocks to entire regions, shaping cumulative risk. Place influences both environmental exposures and access to protective resources (Census Bureau, 2022). For older adults, the most relevant exposures may be local to home and immediate surroundings, yet their health outcomes reflect lifelong residence in inequitable environments (Marmot, 2015; Sharkey & Faber, 2014). Residential segregation, limited green space, and existing health vulnerabilities interact with chemical exposures to reinforce environmental injustice (Wilson et al., 2012). Phthalate exposure has been linked to developmental differences, allergic symptoms, and long-term brain effects (Bornehag et al., 2004), with risks persisting across the life course—particularly impacting communities facing multiple, compounding disadvantages.

Racial Stratification of Environmental Exposures over the Lifecourse

Social disadvantages, lack of environmental assets (i.e., green space, exposure to urban heat islands), and health vulnerabilities combine to produce racial stratification of disproportionate exposure to pollution through the environment. Historic redlining, zoning, urban planning and development, and industry regulation have varying impacts on individuals in relation to their socio-demographics (Wilson et al., 2012; Frey, 2022). For example, even amidst nationwide declines in pollution levels, on average, Blacks and Latinos are exposed to greater amounts of nitrogen dioxide (NO_2) and particulate matter, PM2.5 and PM10 (Kravitz-Wirtz et al., 2016). These inequities are not confined to single points in time but accumulate across the lifecourse, shaping long-term health trajectories and vulnerability to age-related conditions. This work lays the foundation for our exploration of how exposure to plastics/rubber producing industries follows a socio-demographic pattern—one that we expect to contribute to disproportionate risk for ADRD.

The lifecourse perspective underscores how exposures and social conditions experienced from the prenatal period through late life accumulate to shape health trajectories, particularly brain health. Phthalates, for example, cross the placenta, making exposure possible even before birth, and have been linked to allergic symptoms in children within the range of what is typically found indoors (Bornehag et al., 2004). Prenatal and early life exposures are especially consequential, as shown in a longitudinal study that measured phthalate metabolites in mothers at 16 weeks gestation and in mother–child pairs through age eight, finding inverse associations

with children's IQ (Li et al., 2019). Kawachi and co-authors (2002) describe three mechanisms by which such early exposures influence health inequalities across the lifecourse: latent effects, which carry forward from early environments into adulthood; pathway effects, which shape trajectories of health and opportunity; and cumulative effects, which reflect dose–response relationships with harmful environments over many years. These dynamics are highly relevant to ADRD, which develop decades before symptoms emerge, highlighting the importance of identifying modifiable exposures and protective factors long before clinical diagnosis. Given that Black and Native populations face heightened dementia risk not explained by genetics or cardiovascular disease (Farsetta, 2020), there is urgency to investigate socio-environmental determinants such as education, wealth, neighborhood conditions, and exposure to industrial pollutants across the lifecourse.

Current EPA Regulatory Status

The EPA is actively regulating phthalates through systematic risk evaluations under the Toxic Substances Control Act (TSCA), concerned about their toxicity and evidence of pervasive human and environmental exposure (US EPA, 2015a). The agency recently determined that Diisodecyl phthalate (DIDP) presents unreasonable risk to unprotected female workers of reproductive age using products containing DIDP in vehicle and construction applications (EPA, 2025; US EPA, 2015b).
EPA has released draft risk evaluations for dibutyl phthalate (DBP), di(2-ethylhexyl) phthalate (DEHP), diisononyl phthalate (DINP), dicyclohexyl phthalate (DCHP), and butyl benzyl phthalate (BBP). The Science Advisory Council on Chemicals is conducting peer reviews, and EPA is developing cumulative risk assessments

evaluating combined health risks from multiple phthalates simultaneously, recognizing that people typically face exposure to multiple chemicals rather than individual substances in isolation.

Data and Sample

Our research uses health and sociodemographic data from the Panel Study of Income Dynamics (PSID) and pairs it with data from the Environmental Protection Agency Toxic Release Inventory (EPA TRI) and the Neighborhood Change Database (NCDB). We investigate whether average annual exposure and proximity to emissions from toxic plastics/rubber industries are associated with cognitive health challenges among residents, using the PSID *Eight-item Informant Interview to Differentiate Aging and Dementia (AD8)* instrument to assess ADRD symptoms. Years 1990-2017 were selected as the exposure assessment period for measuring proximity to industrial emissions exposure, individual sociodemographic characteristics, and neighborhood variables. This 27-year window enables us to capture long-term patterns of industrial emissions, while accounting for demographic and socioeconomic characteristics that may influence both proximity to TRI facilities and ADRD risk. Although our models are not time-varying in structure, using longitudinal PSID data allows us to construct measures that reflect changes over time where relevant (e.g., residence, income) and to incorporate stable attributes where appropriate (e.g., education). Our outcome variable, ADRD risk, became available in 2017 when the PSID first administered the AD8 dementia screening survey. ADRD risk is measured as whether an individual ever fulfilled the criteria for ADRD risk (i.e., two or more memory challenges on the AD8) during any

of the available survey years: 2017, 2019, 2021, or 2023. Our analytic window begins in 1990. This was chosen because prior to 1990, census tract boundary definitions were not standardized nationally, making it difficult to align neighborhood-level data across time and space. Beginning our analyses with data from 1990 allows for harmonized linkage between the geocoded PSID, the NCDB, and the EPA TRI data. Year 2023 represents the most recent available wave of PSID data at the time of analysis. Fall 2025.

To construct our sample, we identified respondents ages 65 and over by the year 2023 (n = 3849). Of that sample, we restricted our analytic sample to participants aged 65 and over by year 2023 *and* having non-missing and valid AD8 responses in *any* of the AD8 survey years, 2017-2023 (n = 2627). A substantial number of cases were coded as "0" on the ADRD risk variable, which, according to the 2017 codebook (and similarly for 2019, 2021, and 2023), reflects inapplicable cases – the AD8 Survey was not asked for specific PSID sub-samples. These include respondents from the Immigrant recontact sample (ER30001=4700–4851) or Multiplicity sample (ER30001=4001–4462 and ER32052=2019); respondents from the Latino sample (ER30001=7001–9308); cases of main family nonresponse by 2017 or mover-out nonresponse by 2015 (ER34501=0); mover-out deceased individuals in 2017 (ER34502=81–89); or individuals younger than 65 years old or with age recorded as don't know/no answer (ER34581=5). These cases were excluded from analysis, which is appropriate given that they were *never* administered the AD8 instrument and therefore should not be conflated with individuals who were asked but did not screen positive for ADRD risk.

Datasets

1. Panel Study of Income Dynamics (PSID)

The Panel Study of Income Dynamics (PSID) is the longest running longitudinal household study in the world. It began in 1968 and has collected data annually from 1968-1997, and biennially 1997 onward (PSID, 2017). The panel began with data collection from 5,000 families and 18,000 individuals. However, through the PSID's combination of 'natural refreshment' design and purposeful refreshment of select subgroups, the sample has grown to roughly 25,000 individuals in 2023. We utilize geographic identifiers available under a restricted contract from the PSID in order to identify residential neighborhoods of respondents for each survey wave. The restricted PSID Geocode Match files contain the Census Tract data—standardized to 2020 tract boundaries in the 2023 release—for all survey years, allowing us to link data from the PSID annual family files to Census data by connecting the characteristics of the geographic area in which individuals and families live (e.g., the neighborhood) to the PSID individual via their family-level data.

We began with the 1990 to 2023 PSID public-use data download (https://psidonline.isr.umich.edu/), selecting relevant variables, along with the weighting and sample design variables automatically provided by PSID; this file was then imported to the PSID enclave, and the restricted use geo-coded files were merged to the family file for each survey wave. The main weighting variable is the 2023 longitudinal weight (ER35264). The PSID 2023 longitudinal weight accounts for the original sample design, differential attrition, and replenishment over the full

study period, ensuring estimates are representative of the U.S. population across all included waves. Throughout the analysis, we use unweighted results to maintain consistency with the multivariable models and because the AD8 subsample's representativeness is limited by the PSID's cohort-based design. The AD8 survey was only introduced in 2017 for adults 65+, and while the PSID maintains national representativeness for its original 1968 cohort and immigrant refreshes, the AD8 subsample is constrained to those birth cohorts present in these samples at that time; the weights are designed to represent these specific cohorts rather than the current U.S. population of older adults.

2. Environmental Protection Agency Toxic Release Inventory (EPA TRI)

Exposure to toxic industry data comes from the EPA TRI data. The EPA TRI was established by the 1986 Emergency Planning and Community Right-to-Know Act. It is a publicly available database that tracks chemical releases (into air, water, land) by industry; it has a measure of toxic plastics and rubber-emitting industries, identifying their geolocations and their chemical releases in pounds. The TRI enables communities, researchers, and policymakers to monitor environmental hazards, linking industrial activity to public health concerns. TRI began collecting data in 1987 and they publish new data each year in July. To align with our interest in environmental exposure to phthalates, we downloaded and merged EPA TRI data for plastics/rubber facilities in the years 1990–2017 and assigned provided facility geo-coordinates to census tracts based on 2020 boundaries. Both key predictor variables—chemical release amounts (lbs) and distance (km) to the nearest plastics/rubber facility—have right-skewed distributions. This means most

observations cluster at lower values, with a long tail of higher values. This pattern likely results from industrial facilities being concentrated in certain geographic areas rather than evenly distributed.

3. Neighborhood Change Database (NCDB)

The Neighborhood Change Database (NCDB) is a longitudinal census tract-level dataset developed by the Urban Institute and GeoLytics that provides standardized demographic, socioeconomic, and housing variables across multiple decennial censuses using consistent 2020 census tract boundaries (GeoLytics & Urban Institute, 2023). The database facilitates temporal analysis of neighborhood change by addressing census boundary changes over time, making it particularly valuable for studies examining how community characteristics evolve in relation to environmental exposures. We used NCDB harmonized to 2020 tract boundaries, which was the most widely available and validated source when this analysis began and aligned with our other geocoded datasets, EPA TRI and PSID.

We used NCDB data from the decennial censuses (1990, 2000, 2010, and 2020) to construct a census tract–level neighborhood disadvantage index (see Appendix 2). For intercensal years, we applied linear interpolation to estimate tract characteristics, assuming gradual change while recognizing this may not capture abrupt demographic or socioeconomic shifts. The index was built using eight tract-level variables selected for their data availability, temporal coverage, and conceptual alignment with the Area Deprivation Index framework (Kind & Buckingham, 2018), adapted to fit our study's constraints and PSID linkage. Constructing the index

before transforming the data from long to wide and before restricting the analytic sample ensured use of the full set of available tract data (1990–2017), maximizing coverage and stability of the principal components solution. This approach allowed us to derive a measure of neighborhood disadvantage independently of missingness in individual-level PSID data, maintaining comparability within our sample and preserving the hyper-local, structural neighborhood context relevant to our study population. Although our models are cross-sectional, this strategy yields a pseudo-longitudinal framework in which decades of census data characterize neighborhood conditions linked to individual outcomes.

Data Processing

We harmonize geographic and temporal identifiers across the three data sources, linking the geocoded PSID (1990–2023), EPA TRI (1990-2017), and NCDB data (1990-2020) by the census tract boundary for each year (harmonized to 2020 boundaries). Using restricted access data, we first identify each PSID respondent's census tract for every available PSID survey year (1990–2023) using tract geocodes standardized to 2020 boundaries. We then merge tract-level sociodemographic variables from the NCDB (1990–2020) to the PSID based on census tract and survey year, prior to constructing the neighborhood disadvantage index. Separately, we process TRI plastics/rubber facility data (1990–2017) to generate annual tract-level exposure metrics. These emissions measures and facility locations were then merged into the PSID by census tract and year, resulting in a spatially and temporally aligned person-year dataset that preserved the full PSID sample.

Analytic Strategy

Our outcome measure draws on repeated AD8 assessments from 2017–2023. To align the ADRD outcome, covariates, and exposure information, we collapse the dataset to the person-level, applying different summary statistics depending on the variable type; for time-varying variables, we use the mean across available years, while for demographic and outcome variables we retain the most recent non-missing observation.

Measures

1. Outcome Variable

ADRD Risk Indicator

We assess cognitive health risk using the AD8 Dementia Screening Interview, a brief, validated tool designed to detect early signs of dementia in community-based populations (Galvin et al., 2006). The AD8 focuses on functional changes such as difficulty with appointments, finances, or learning new tasks, making it particularly useful for identifying pre-clinical cognitive decline. In the PSID, the AD8 screener consists of eight questions about cognitive and functional problems (see Appendix Table A1 for the full list). The AD8 has demonstrated strong sensitivity and specificity when validated against clinical assessments like the Clinical Dementia Rating (CDR) and has been favorably compared to other screening tools such as the Mini-Mental State Examination (MMSE) and Montreal Cognitive Assessment (MoCA).

We construct an indicator of ADRD risk using the AD8 Dementia Screening Interview, administered in the PSID in 2017, 2019, 2021, and 2023. ADRD status is coded as "1" if a respondent endorsed two or more items on the AD8 screener (wtr2plus = 1). A person-level variable was then created to indicate whether an individual *ever* had a value of "1" on the AD8 screener in any of the four waves (2017-2023). Among those with valid data, 28.39% met this criterion at least once. Table 1 below depicts the distribution of participants aged 65 and older that are considered to have ADRD risk, that are not considered to have ADRD risk, and that identify as inapplicable to the AD8 survey for each of our outcome measure years, 2017-2023.

Table 1 Distribution of ADRD risk by year of AD8 Survey and potential observation values. Data: Panel Study of Income Dynamics (PSID), years 2017-2023, unweighted.

ADRD	2017, n (%)	2019, n (%)	2021, n (%)	2023, n (%)	2017-2023, n (%)
At Risk	475 (12.39%)	523 (13.64%)	501 (13.06%)	494 (12.83%)	672 (25.58%)
No Risk	1767 (46.08%)	1943 (50.68%)	2142 (55.82%)	2273 (59.05%)	1955 (74.42%)
0 [NA]	1593 (41.54%)	1368 (35.69%)	1194 (31.12%)	1082 (28.11%)	- - -
Total	3835	3834	3837	3849	2627

2. Key Predictor Variables: Plastics/Rubber Industry Variables

Exposure Variable Construction

Using 2020 TIGER/Line census tract shapefiles, we obtain tract centroids computed as the geometric center of each tract polygon using the largest polygon component to ensure a single representative point per tract. All spatial data were projected to the

Albers Equal Area Conic coordinate system (EPSG:5070 – NAD83/Conus Albers) to ensure accurate distance calculations across the continental United States.

We exclude (n = 3) individuals who lived in non-continental US locations (e.g., Alaska, Hawaii, US territories, and foreign county identifiers) during any observation year to ensure comparable geographic exposure assessment, as the density and distribution of manufacturing facilities differs substantially in these regions.

Using nearest neighbor analysis with the *sf* and *nngeo* packages in R, we identify the closest facility in any emission category to every census tract centroid and calculate the Euclidean distance in kilometers.

Although census tract centroids are spatially fixed, the set of nearby TRI facilities changes over time as facilities open, close, or vary in their annual reporting activity. Consequently, the nearest facility to a given tract centroid—and the corresponding distance and emission values—may differ across years. To capture this temporal variation, we calculate year-specific distances between each census tract centroid and the nearest active plastics/rubber TRI facility for each year from 1990 through 2017, using Euclidean distance (in kilometers). This approach allows exposure measures to reflect dynamic changes in the industrial landscape rather than assuming static proximity. Each person-year observation was assigned the distance and total chemical releases from the nearest facility to their census tract centroid in that year. We then average these annual values across all observation years to create person-level continuous variables representing mean distance (in km) and mean

exposure (in pounds) to the nearest plastics/rubber TRI facility over the study period (1990-2017).

The following example demonstrates our data processing approach for a single individual using simulated data. Due to the restricted nature of our geocoded PSID data, we present this illustration with fabricated values while maintaining methodological accuracy:

Longitudinal data for one person

Tract ID	Year	Nearest TRI ID	Distance (km)	Total Releases (lbs)
101	1990	TRI123	4.5	12,000
101	1991	TRI123	4.5	11,500
101	1995	TRI789	2.1	34,000
101	2000	TRI789	2.1	32,000
202	2003	TRI456	6.2	5,000

Summary data for one person

Tract IDs	Mean Distance (km)	Mean Total Releases (lbs)
101, 202	3.88	18,900

Given the right-skewed distribution of both our average annual values of emission exposure (pounds released by nearest plastics/rubber TRI and distance to nearest plastics/rubber TRI), with a concentration of observations at lower values (median distance = 16.31 km), median emissions = 0 lbs) and a long tail extending to higher values (maximum distance = 299.70 km, maximum emissions = 30,800,000 lbs), we categorize both measures of exposure into groups-based percentiles.

Person level average pounds of exposure from nearest plastics/rubber TRI across all years in which they are observed (1990-2017).

- 0 None, 0 lbs
- 1 Low, > 0-7,627 lbs (greater than zero up to 75th percentile)
- 2 Moderate, 7,627 lbs - 75,797 lbs (75th-90th percentile)
- 3 High, 75,797+ lbs (90th+ percentile)

Person level average distance to plastics/rubber TRI (regardless of emitter level) across available years (1990-2017) in kilometers. (minimum value is 0.53 km)

1. Near, 0.53-30.55 km (min up to 75th percentile)
2. Moderate, 30.55-50.59 km (75th-90th percentile)
3. Far, 50.59+ km (90th+ percentile)

This approach ensures adequate sample sizes for each exposure category while maintaining meaningful exposure contrasts. Models using alternative categorization,

in addition to log transformation, are reported in Appendix 4; results remain largely unchanged.

3. Additional Measures

Following the social determinants of health framework, we account for upstream factors — education, income, housing, and neighborhood characteristics — that may shape both exposure to TRI emissions and ADRD risk (Link et al., 2008; Diez Roux, A. V., & Mair, C., 2010; Majoka, M. A., & Schimming, C., 2021; CDC, 2022). Age is the greatest known risk factor for ADRD, with risk doubling every 5 years after age 65 (Alzheimer's Association, 2025); we categorize individual age at the 2023 interview as: 65-70 years, 71-80 years, 81-90 years, and 91+ years. Sex (male/female) is a well-documented non-modifiable risk factor, with increased risk for women attributed to biological and social factors (O'Neal M. A., 2024). Race and ethnicity contribute to ADRD risk through life experiences, socioeconomic indicators, and comorbidities (Adkins-Jackson et al., 2023; Alzheimer's Association, 2025; Lim, U. & Park, S. Y., 2022); participants were grouped into three categories based on their 2023 report of their race: white, Black, and all others (due to small sample sizes in other racial categories). Marital status (recorded based on response to the 2023 survey year) may influence ADRD risk, though findings remain mixed (Karakose et al., 2025); we categorize participants as ever married (including married, divorced, widowed, or separated) or never married. Number of residential moves (1990-2017) serves as a proxy for economic instability and residential precarity across the life course (Kushel et al., 2006; Alzheimer's Association, 2025). Home ownership (recorded based on the most recent available observation between

1990-2023) indicates wealth accumulation and neighborhood stability, which may influence dementia risk through access to resources and reduced housing-related stress (Hamoudi, A., & Dowd, J. B., 2014; Boehm, T., & Schlottmann, A., 2004). Education is a modifiable risk factor that may build cognitive reserve and enable access to resources supporting brain health (Barcellos et al., 2025; Alzheimer's Association, 2025; Yang et al., 2025). Highest education level was categorized as less than 12 years, 12-15 years, and 16+ years, based on years of education reported in survey year 2023. Income serves as a key proxy for socioeconomic status, with lower income increasing ADRD risk (Majoka, M. A., & Schimming, C., 2021). We calculate Average Income Percentile using inflation-adjusted total family income from PSID data years 1990-2017 (base year 2023, CPI: 304.7), ranking participants within each year using the formula: (rank-1)/(valid_count-1)×100, then averaging percentiles across all waves. An alternative coding of income was created for the interaction model; Binary Income uses the median of average income percentile as a cutoff, creating a 50/50 split identifying individuals whose Average Income Percentile value was in the bottom and top half of the distribution.

Mean Disadvantage Index (Standardized)

We include a measure of neighborhood quality – Census Tract Disadvantage – in order to capture potential structural determinants of health. Neighborhood features such as walkability, access to healthy food stores, and social cohesion are associated with lower ADRD risk (Yang et al., 2024). Our measure represents each participant's average neighborhood disadvantage exposure, calculated by taking the mean of their

standardized disadvantage index values (construct described in Appendix 2) across all years and residential locations in which they were observed in the study.

Methodological Approach

First, we use descriptive statistics to characterize the sample. Then we run simple chi-square tests to assess whether our key exposure measures, as well as other covariates, are independently associated with ADRD risk. Lastly, we examine whether TRI exposure factors, socio-demographics, and neighborhood characteristics are associated with ADRD risk by fitting a series of logistic regression models. Plastics exposure is operationalized in two ways: (1) emissions volume (pounds of toxic chemicals emitted by the nearest plastics/rubber TRI facility) and (2) geographic proximity (distance in kilometers from census tract centroid to the nearest plastics/rubber TRI facility). All regression models are estimated using both exposure measures. For brevity, the main text presents the set of results using the emissions measure (lbs), as this captures both the presence and intensity of industrial pollution. Parallel analyses using the distance measure (km) are reported in Appendix 3.

Confidence intervals are calculated at the 90% level, consistent with conventions in epidemiology and environmental health research where minimizing Type II error is prioritized, and to highlight the direction and magnitude of associations rather than strict significance testing. Statistical significance is regarded as $P < 0.10$. Analyses are limited to respondents with complete data on all analytic variables (n=2,627). All models are estimated in Stata using the *logit* command, with standard errors left

unclustered because the analytic dataset contains only one observation per census tract.

Descriptive statistics are unweighted to provide analytic sample estimates. Categorical variables are created based on analytic unweighted sample percentiles. Sensitivity analyses using survey-weighted percentiles show similar cutoff values (within 15%), suggesting minimal impact of the weighting on category definitions. Chi-squared tests and regression models are unweighted to examine associations within the analytic sample.

All analyses are conducted in Stata MP 17.0, with tract-level exposure data processed in R Version 2025.05.0 Mariposa Orchid.

Model development follows a theory-driven approach, informed by the socio-ecological model. Sensitivity checks are described in the limitations section. We fit five models to guide inference and evaluate robustness:

- **Model 1.** Binary ADRD risk was regressed on the categorical measure of Average Exposure to Nearest Plastics/Rubber TRI Emissions, lbs (1990-2017)
- **Model 2.** Model 1, plus individual and household covariates are added – sex, race, age, income, mobility, marital status, home ownership, education.
- **Model 3.** Model 2, plus neighborhood variable is added – mean neighborhood disadvantage index.
- **Model 4.** Model 3, plus interaction – distance exposure categories and individual binary income (top/bottom 50%).

- **Model 5.** Model 3, plus the categorical measure of Average Exposure to Nearest Plastics/Rubber TRI Emissions, lbs (1990-2017)

Results

Descriptive statistics for the analytic sample are shown in Table 2. A total of 74.42% of our sample is identified as never having risk of ADRD in 2017, 2019, 2021 or 2023 (see Table 2), whereas 25.58% of the sample is at risk of ADRD.

The mean pounds emitted from the nearest plastics/rubber TRI facility is 86,052 lbs, with a maximum of 30,800,000 lbs, minimum of 0.00 lbs, and median of 0.00 lbs (data not shown). In our sample, 58.81% of participants are in the None category (0 lbs), while 16.18% are in the Low category (>0–7,627 lbs; up to the 75th percentile). The Moderate category (7,627–75,797 lbs; 75th–90th percentile) contains 15.00% of our sample, and the High category (75,797+ lbs; 90th+ percentile) captures 10.01% of our sample.

The mean distance from residential locations to the nearest plastics/rubber TRI facility is 25.20 km, with a maximum of 299.70 km, minimum of 0.53 km, and median of 16.31 km (data not shown). A total of 74.99% of our sample is in the Near category (0.53–30.54 km; minimum up to the 75th percentile). The Moderate category (30.54–50.59 km; 75th–90th percentile) contains 14.96% of our sample, and 10.05% is in the Far category (50.59+ km; 90th+ percentile).

By design, our sample is aged 65 and older. Almost half of our sample is aged 65 to 70 years old (46.52%), with few 91+ year olds (2.21%). The vast majority of our sample has been, or currently is, married (94.63%), and has been, or currently is, a homeowner (93.60%). Our sample is skewed toward high educational attainment, with 56.22% of our sample having 12 to 16 years of education and only 9.14% having fewer than 12 years of education.

Participants in our sample reside in neighborhoods with below-average disadvantage relative to the reference population. The mean standardized neighborhood disadvantage index is -0.06 (SE = 0.017), indicating that individuals experience neighborhood environments slightly above average in terms of disadvantage during the observed timeframe. This composite index, derived from eight census tract-level socioeconomic indicators via principal component analysis, reflects lower poverty rates, reduced unemployment, higher educational attainment, greater homeownership, and fewer never-married residents compared to the average census tract in the PSID sample (1990-2017). Because the disadvantage index is calculated prior to collapsing to the person level, this measure represents each individual's average neighborhood disadvantage exposure across all years of observation (1990-2017), capturing both stable residence patterns and any residential mobility over the study period. Negative values on this standardized scale indicate relatively more advantaged neighborhood conditions, suggesting that our sample, on average, resides in socioeconomically favorable contexts.

In Table 3, we describe levels of ADRD risk by our key covariates, using unweighted chi-square tests to detect significant variation. Many variables show statistically significant differences between these two groups ($p < 0.05$). We see evidence of an association between exposure measured by average emissions (in pounds) from the nearest plastics/rubber TRI facility and ADRD risk prevalence. Individuals with moderate and high emissions exposure have the greatest ADRD risk prevalence (29.95% and 29.28% respectively). ADRD risk increases with increased exposure to emissions by the nearest plastics/rubber facility. Interestingly, the percentage of individuals with ADRD risk is highest among those with average far distance to a TRI facility (27.27%), compared to 24.68% among the moderate distance group and 25.53% among those in the near distance group. However, there is no statistically significant difference between the categories. As would be expected, rates of ADRD risk increase significantly with age, ranging from 17.51% among the youngest ages 65-70, to 70.69% among respondents 91 years and older. Black individuals have higher ADRD risk (29.12%) compared to whites (23.66%); individuals who never had married, and individuals with less education also have higher rates of ADRD risk. Rates of residential mobility are positively associated with ADRD risk, with more frequent movers exhibiting higher rates of risk. Among participants who never moved during the study period, 24.17% are at risk for ADRD, compared to 25.27% among those who moved three to five times and 44.44% among those who moved ten or more times. Never owning a home is significantly associated with ADRD risk (35.71%), compared to individuals who have or currently do own a home (24.89%). Significant differences are also observed in income categories, those that are in the

bottom 50th percentile of average household income are at higher risk of ADRD (33.56%).

Table 4 reports results of multi-variable logistic regression models predicting the association between plastics exposure (lbs emitted by nearest plastics/rubber TRI), neighborhood disadvantage, and other socio-demographic variables on ADRD risk. Odds ratios and p-values for all covariates, along with model fit statistics (AIC, BIC, log likelihood, and N) are reported. All models are also estimated using distance to the nearest plastics/rubber TRI facility (km) as the key exposure variable; these results are presented in Appendix 3.

The models indicate a positive and significant relationship between annual average exposure to emissions from the nearest TRI facility (measured in pounds) and ADRD risk. In model 1, before including additional covariates, we see that the odds of ADRD risk are 39% higher and 34% higher for individuals in the moderate and high risk exposure categories, compared to individuals with no exposure. Once covariates are added in, our results shift slightly. We continue to see a positive association between plastic exposure and ADRD risk, especially among individuals in the moderate-level exposure category. However, the coefficient for individuals in the highest exposure is no longer significant once controlling for additional covariates. This attenuation suggests that neighborhood conditions account for some of the observed variation in ADRD risk initially attributed to plastics/rubber emissions in Model 1. In Model 4, which includes individual, household, and neighborhood covariates plus an interaction term between income and emissions

exposure, the main effect of emissions exposure loses statistical significance. The non-significant interaction term indicates that the relationship between emissions and ADRD risk does not vary meaningfully by income level. Instead, the loss of significance for the emissions main effect suggests that the combination of sociodemographic factors (particularly income) and neighborhood conditions together explain the variance in ADRD risk that initially appeared attributable to emissions exposure alone. Model 5 captures the features of Model 3, while also controlling for distance to the nearest plastics/rubber TRI. Moderate levels of emissions exposure remain significantly associated with increased ADRD risk (OR = 1.343), meaning that when holding distance to the nearest TRI facility constant, moderate emissions exposure is independently associated with a 34% increase in odds of ADRD risk ($p < 0.05$), suggesting that toxic emissions from plastics/rubber manufacturing have effects beyond mere proximity to industrial sites.

Significantly, we see that people living in deprived areas over the course of their lives have higher odds of ADRD (OR = 1.171, model 3). As anticipated given the broader literature, our model suggests a strong positive association between age and ADRD risk, with older age increasing the odds of ADRD. Household average income is significantly associated with decreased odds of ADRD risk (OR = 0.98, model 3). Total residential moves across the survey years were significantly associated with increased odds at the high end of the range, 10+ moves (OR = 2.03, model 3). In model 4, having 16+ years or more of education is associated with a significantly decreased risk of ADRD (OR = 0.70), compared to the reference category of less than 12 years of education. Interestingly, sex, race, marital status/history, and home

ownership status/history are not significantly associated with ADRD risk, while holding other covariates constant. We do not observe a significant interaction between plastics/rubber TRI emissions exposure categories and income, contrary to our hypotheses (Model 4).

Table 2 Unweighted descriptive statistics (n=2,627). Data: Panel Study of Income Dynamics (PSID) 1990-2023, Environmental Protection Agency Toxic Release Inventory (EPA TRI) 1990-2017, and Neighborhood Change Database (NCDB) 1990-2020.

Variable	N	Percentage/Mean
ADRD Risk Indicator (2017-2023)		
No Risk	1955	74.42%
At Risk	672	25.58%
Average Distance to Nearest Plastics/Rubber TRI Facility, km (1990-2017) *continuous*	2,627	25.20 km
Average Distance to Nearest Plastics/Rubber TRI Facility, km (1990-2017) *categorical*		
1 Near, 0.53-30.54 km (min up to 75th percentile)	1970	74.99%
2 Moderate, 30.54-50.59 km (75th-90th percentile)	393	14.96%
3 Far, 50.59+ km (90th+ percentile)	264	10.05%
Average Exposure to Nearest Plastics/Rubber TRI Emissions, lbs (1990-2017) *continuous*	2627	86,052 lbs
Average Exposure to Nearest Plastics/Rubber TRI Emissions, lbs (1990-2017) *categorical*		
0 None, 0 lbs	1545	58.81%
1 Low, >0-7627.52 lbs (up to 75th percentile)	425	16.18%

2 Moderate, 7627.52 lbs - 75797.66 lbs (75th-90th percentile)	394	15.00%
3 High, 75797.66+ lbs (90th+ percentile)	263	10.01%
Age (2023)		
65-70 y.o.	1222	46.52%
71-80 y.o.	1088	41.42%
81-90 y.o.	259	9.86%
91+ y.o.	58	2.21%
Sex (2023)		
Male	1193	45.41%
Female	1434	54.59%
Race (2023)		
White	1754	66.77%
Black	728	27.71%
All other	145	5.52%
Wtr Ever Married (2023)		
Never married	141	5.37%
Current/previously married	2486	94.63%
Total Moves (1990-2017)		
0	695	26.46%
1-2	936	35.63%
3-5	637	24.25%
6-9	296	11.27%
10+	63	2.40%
Home Ownership (1990-2017)		
Never a homeowner	168	6.40%
Current or previous homeowner	2459	93.60%
Max Education Level (1990-2017)		

Less than 12 years	240	9.14%
12 years or more, less than 16 years	1477	56.22%
16 years or more	910	35%
Household Average Income Percentile (1990-2017)	2,627	54.085
Household Income Binary (recode of Household Average Income Percentile, 1990-2017)		
Bottom 50%	1314	50.05%
Top 50%	1313	49.98%
Mean Disadvantage Index, Standardized (1990-2017)	2,627	-0.06
Total Sample	2,627	

*Table 3 Descriptive statistics stratified by ADRD Risk (n=2,627). Unweighted chi-squared values are reported. Data: PSID 1990-2023, EPA TRI 1990-2017, and NCDB 1990-2020. Significance levels: $p < 0.05$ *, $p < 0.01$ **, $p < 0.001$ ***.*

Variable	No ADRD Risk (%) / mean (SE)	ADRD Risk (%) / mean (SE)	(un-weighted) χ^2
ADRD Risk Indicator (2017-2023)			--
No Risk	100%	--	
At Risk	--	100%	
Average Distance to Nearest Plastics/Rubber TRI Facility, km (1990-2017) *continuous*	25.06 km	25.60 km	0.669
Average Distance to Nearest Plastics/Rubber TRI Facility, km (1990-2017) *categorical*			0.753
1 Near, 0.53-30.54 km (min up to 75th percentile)	74.47%	25.53%	

2 Moderate, 30.54-50.59 km (75th-90th percentile)	75.32%	24.68%	
3 Far, 50.59+ km (90th+ percentile)	72.73%	27.27%	
Average Exposure to Nearest Plastics/Rubber TRI Emissions, lbs (1990-2017) *continuous*	95,536 (SE: 23,384)	58,461 (SE: 9933)	0.358
Average Exposure to Nearest Plastics/Rubber TRI Emissions, lbs (1990-2017) *categorical*			0.025**
0 None, 0 lbs	76.44%	23.56%	
1 Low, >0-7627.52 lbs (up to 75th percentile)	73.41%	26.59%	
2 Moderate, 7627.52 lbs - 75797.66 lbs (75th-90th percentile)	70.05%	29.95%	
3 High, 75797.66+ lbs (90th+ percentile)	70.72%	29.28%	
Age (2023)			< 0.001***
65-70 y.o.	82.49%	17.51%	
71-80 y.o.	72.74%	27.76%	
81-90 y.o.	55.60%	44.40%	
91+ y.o.	29.31%	70.69%	
Sex (2023)			0.642
Male	74.84%	25.15%	
Female	74.06%	25.94%	
Race (2023)			0.005**
White	76.34%	23.66	
Black	70.88%	29.12%	

All other	68.97%	31.03%	
Wtr Ever Married (2023)			0.018*
Never married	65.96%	34.04%	
Current/previously married	74.90%	25.10%	
Total Moves (1990-2017)			0.005**
0	75.83%	24.17%	
1-2	75.53%	24.47%	
3-5	74.73%	25.27%	
6-9	70.95%	29.05%	
10+	55.56%	44.44%	
Home Ownership (1990-2017)			0.002**
Never a homeowner	64.29%	35.71%	
Current or previous homeowner	75.11	24.89%	
Max Education Level (1990-2017)			< 0.001***
Less than 12 years	60.83%	39.17%	
12 years or more, less than 16 years	73.60%	26.40%	
16 years or more	79.34%	20.66%	
Household Average Income Percentile (1990-2017)	55.00 (SE: 0.523)	43.47 (SE: 0.874)	
Household Income Binary (recode of Household Average Income Percentile, 1990-2017)			< 0.001***
Bottom 50%	66.44%	33.56%	
Top 50%	82.41%	17.59%	

Mean Disadvantage Index, Standardized (1990-2017)	-0.116 (SE: 0.019)	0.089 (SE: 0.033)	
Total Sample %	71.61%	28.39%	

*Table 4 Odds ratios from logistic regression models predicting ADRD risk. Reference categories and model fit statistics are shown. Significance levels: $p < 0.05$ *, $p < 0.01$ **, $p < 0.001$ ***.*

Variable	Model 1	Model 2	Model 3	Model 4	Model 5
Average Exposure to Nearest Plastics/Rubber TRI Emissions, lbs (1990-2017) *categorical*					
Ref = 0 None, 0 lbs					
1 Low, >0-7627 lbs (up to 75th percentile)	1.175	1.14	1.135	1.110	1.141
2 Moderate, 7627 lbs - 75,797 lbs (75th-90th percentile)	1.387**	1.341*	1.339*	1.263	1.343*
3 High, 75,797+ lbs (90th+ percentile)	1.343*	1.2	1.203	1.134	1.202
Sex (2023)					
Ref = Male					
Female		0.900	0.904	0.927	0.904
Race (2023)					
Ref = White					
Black		1.062	0.936	0.997	0.924
All other		1.434	1.340	1.333	1.330
Age (2023)					
Ref = 65-70 y.o.					

71-80 y.o.		2.033***	2.066***	2.079***	2.073***
81-90 y.o.		3.881***	3.986***	4.231***	3.984***
91+ y.o.		11.638***	12.418***	13.302***	12.385***
Household Average Income Percentile (1990-2017)		0.982***	0.983***		0.983***
Total Moves (1990-2017)					
Ref = 0 moves					
1-2		1.188	1.193	1.190	1.194
3-5		1.186	1.175	1.202	1.172
6-9		1.378	1.355	1.417	1.354
10+		2.027*	2.026*	2.337**	2.024*
Wtr Ever Married (2023)					
Ref = Never married					
Current/previously married		0.885	0.874	0.751	0.874
Home Ownership (1990-2017)					
Ref = Never a homeowner					
Current or previous homeowner		1.096	1.158	1.013	1.168
Max Education Level (1990-2017)					
Ref = Less than 12 years					
12 years or more, less than 16 years		0.819	0.85	0.762	0.843
16 years or more		0.845	0.875	0.697*	0.869

Mean Disadvantage Index, Standardized (1990-2017)			1.171*	1.207*	1.168*
Household Income Binary (recode of Household Average Income Percentile, 1990-2017)					
Ref = Bottom 50%					
Top 50%				0.550***	
Binary Income*Exposure to Emissions					
*Ref = Bottom 50% income*None*					
Top 50% income*Low				1.076	
Top 50% income*Moderate				1.203	
Top 50% income*High				1.183	
Average Distance to Nearest Plastics/Rubber TRI Facility, km (1990-2017) *categorical*					
Ref = 1 Near, 0.53-30.54km (min up to 75th percentile)					
2 Moderate, 30.54-50.59 km (75th-90th percentile)					0.880
3 Far, 50.59+ km (90th+ percentile)					0.960
_cons	0.308***	0.485*	0.437**	0.345***	0.452*
	m1	**m2**	**m3**	**m4**	**m5**
n	2627	2627	2627	2627	2627
aic	2986.299	2755.262	2751.857	2772.724	2754.968

bic	3009.793	2866.860	2869.329	2907.817	2884.187
ll	-1489.149	-1358.631	-1355.929	-1363.362	-1355.484

Discussion

Before interpreting the broader implications of these findings, we systematically evaluate each research question and hypothesis to assess the extent to which the results provide empirical support.

The **first** research question examines if average yearly exposure intensity (total pounds of emissions released from the nearest plastics/rubber TRI facility) over the study timeframe (1990-2017) is associated with ADRD risk. The hypothesis predicts that individuals with higher average yearly exposure intensity—measured as greater total pounds of emissions released by their nearest plastics/rubber TRI facility over the study timeframe, 1990-2017— exhibit higher ADRD risk. The findings **partially support** this hypothesis. Individuals with moderate (OR=1.387**, Model 1) and high (OR=1.343*, Model 1) exposure demonstrated significantly elevated ADRD risk compared to those with no exposure. However, the significant association between high level exposure and ADRD risk is attenuated once accounting for additional socio-demographic and neighborhood variables (OR=1.203, Model 3); moderate level exposure and ADRD risk remains statistically significant (OR = 1.339*, Model 3).

The **second** question investigates whether living in a census tract with closer proximity to plastics/rubber polluting industries is associated with increased likelihood of ADRD. The hypothesis proposes that closer proximity (measured in km

from census tract centroids to the nearest EPA TRI plastics/rubber facility) will be significantly associated with increased ADRD risk, where ADRD is defined as reporting two or more cognitive difficulties on the PSID AD8 dementia screening tool. This hypothesis is **not supported,** given the results reported in Appendix 3. Proximity (measured in kilometers) to the nearest plastics/rubber TRI facility is not significantly associated with odds of ADRD risk (Appendix 3). Moderate distance compared to near distance to plastics/rubber TRI has slightly lower odds of ADRD risk (OR = 0.956), whereas further distance compared to near distance to plastics/rubber TRI has slightly higher odds of ADRD risk (OR = 1.094).

The **third** question explores whether household income (as a proxy for socioeconomic status) moderates the association between proximity to plastics/rubber polluting industries and ADRD risk. The hypothesis suggests the association between exposure and ADRD risk would vary by income level, as demonstrated by a statistically significant interaction term (exposure × income) in regression models. This hypothesis is also **not supported.** The interaction term between exposure and household income percentile is not statistically significant in either set of models (exposure measured in pounds and exposure measured in kilometers), indicating that income does not moderate the relationship between TRI facility exposure and ADRD risk. However, income demonstrates a significant main effect, with higher household income percentile associated with reduced odds of ADRD across all models in which it was included as a covariate (OR = 0.983, Model 3).

In this paper, we examine the association between exposure to polluting plastics/rubber industries and risk for ADRD. We find a statistically significant, yet nuanced, relationship between exposure to plastics, measured as pounds emitted by the nearest plastics/rubber TRI and residential location over the years 1990-2017. Notably, what emerges from our models is a strong and significant association between life-course exposure to neighborhood deprivation and ADRD risk—a finding that underscores the importance of social determinants in understanding dementia risk.

Our findings reveal elevated ADRD prevalence among individuals with any exposure to plastic/rubber TRI emissions compared to those with no exposure, though we do not observe the anticipated monotonic dose-response relationship. While the moderate exposure category shows increased odds of ADRD in adjusted models (ORs ranging from 1.339-1.343), the high exposure category paradoxically does not demonstrate the strongest association, and lost statistical significance in the adjusted models (models 2-5). Several interrelated factors likely contribute to this complex pattern and warrant careful interpretation.

The strong attenuation of effect estimates following adjustment for socioeconomic covariates—particularly in the high exposure category—suggests that residential selection bias and social determinants of health play important confounding roles. Neighborhoods surrounding high-emission facilities may not be uniformly disadvantaged; some may house individuals with greater socioeconomic resources who can buffer exposure impacts through better healthcare access, superior nutrition, lower cumulative stress, and reduced co-exposures to other environmental

hazards. This "healthy resident" effect could mask the true toxic impact of high-level exposures in observational data. Conversely, moderate-exposure neighborhoods may represent a particularly vulnerable configuration: enough emission levels to confer health risk, combined with population-level socioeconomic disadvantage that amplifies susceptibility and limits protective resources.

Additionally, residential mobility patterns may differ systematically across exposure categories. Individuals initially residing near high-emission facilities may be more likely to relocate (if resources permit), while those near moderate-emission facilities may be more residentially stable. Our person-level averaging approach would then underestimate peak exposures for mobile individuals while better capturing sustained exposure for stable residents, potentially flattening observed dose-response relationships.

Despite these important limitations, the consistent pattern of elevated ADRD prevalence across all exposure categories relative to no exposure suggests a plausible adverse association between plastics/rubber TRI emissions and cognitive health outcomes. The absence of a clear dose-response gradient should not be interpreted as evidence against a relationship, but rather as highlighting the methodological challenges inherent in observational environmental epidemiology. Residential selection bias, exposure misclassification, and unmeasured confounding likely obscure underlying biological relationships in analyses using administrative proximity-based exposure metrics.

Future research should employ more sophisticated exposure assessment methods. Atmospheric dispersion modeling could account for wind patterns, topography, and facility-specific emission profiles. Biomarker-based exposure measures would capture individual-level internal dose rather than relying on proximity alone. Studies with larger samples in high-exposure categories and more granular data on protective factors (e.g., healthcare utilization, diet quality, stress) would help clarify whether the observed pattern reflects true non-linearity or methodological artifact. Understanding these mechanisms is critical for informing environmental health policy and protecting vulnerable populations from neurotoxic exposures.

Another consideration relates to potential measurement limitations inherent in TRI reporting requirements. Facilities must report to the TRI if they exceed chemical quantity thresholds and meet facility criteria. Standard reporting thresholds are 25,000 pounds for manufacturing or processing and 10,000 pounds for otherwise using TRI-listed chemicals. However, Persistent, Bioaccumulative, and Toxic (PBT) chemicals, such as lead, certain plastics, and some PFAS, have much lower thresholds (e.g., 100 pounds). Beyond chemical thresholds, facilities must also have 10+ full-time equivalent employees and operate under a covered North American Industry Classification System (NAICS) industry code. Federal facilities are exempt from NAICS requirements. Facilities exceeding any applicable threshold must report. Additionally, facilities meeting reporting criteria must submit TRI reports even when reporting *zero* emissions, as the inventory tracks not only releases but also pollution prevention activities, recycling, energy recovery, and waste treatment practices. Thus, a facility may appear in TRI data with zero reported emissions while

still managing substantial quantities of TRI-listed chemicals through recycling or other waste management activities that prevent environmental release. These reporting thresholds and the inclusion of facilities with zero emissions may create systematic differences in exposure measurement across geographic areas, potentially contributing to the observed pattern where very low exposure areas may have incomplete capture of industrial activity while some facilities in our reference category (zero emissions) may actually be managing significant chemical quantities through pollution prevention measures. Future research should further differentiate types of industrial activity within the TRI, such as comparing proximity to plastics/rubber recycling facilities versus production facilities, to better understand how varying modes of chemical management relate to ADRD risk.

As expected, age emerges as a strong risk factor for ADRD in our sample, consistent with established literature. In contrast, sex is not significantly associated with ADRD risk, which diverges from much of the existing evidence. Sex is considered a non-modifiable risk factor for ADRD that is well documented yet not fully understood. Increased risk among women has been attributed to both biological and social factors, including the drop in estrogen at menopause, differences in brain glucose metabolism, higher prevalence of autoimmune conditions, historically lower levels of education, greater risk among ApoE-4 carriers, and longer average life expectancy (O'Neal M. A., 2024).

Our findings contribute to ongoing discussions about the variability of sex-based risk, suggesting that observed differences may depend on cohort composition,

measurement approach, or the influence of intersecting social and environmental factors. It is possible that evolving social conditions—such as improved access to education and healthcare among women—may be narrowing previously observed sex disparities in ADRD risk. Future research should further investigate these intersections to clarify the mechanisms driving sex differences in ADRD onset and progression across diverse populations.

Race, homeownership, and education show significant associations with ADRD risk in bivariate analyses (table 3) but become non-significant in the multivariable logistic regression model. This attenuation suggests these apparent associations may be confounded by other variables in the model, particularly income and neighborhood disadvantage, which are strongly correlated with race, homeownership, and education. The loss of significance likely reflects the complex interrelationships among socioeconomic position indicators rather than the absence of true associations. These variables may operate through shared pathways or serve as proxies for overlapping social determinants of health. Moreover, the protective effect of education on cognitive decline may diminish with advancing age, as the cognitive reserve built through early educational attainment becomes less influential relative to other biological and environmental factors that accumulate over the lifecourse.

Greater neighborhood disadvantage, measured using a composite index derived from Neighborhood Change Database census data corresponding to our analytic sample's geographic locations, is associated with higher odds of ADRD risk. This is

consistent with our hypothesis, bivariate findings, and the broader literature documenting the influence of social and structural determinants on cognitive aging. This association underscores how cumulative disadvantage, reflected in factors such as economic deprivation, limited access to health-promoting resources, and environmental burdens, can compound over the lifecourse to shape vulnerability to ADRD. These findings reinforce the importance of addressing place-based inequities as a modifiable pathway through which social context contributes to neurodegenerative risk.

In Model 4, the interaction between exposure and income was not statistically significant (exposure categories × binary income, $p > 0.10$), indicating that the effect of plastics/rubber TRI exposure on ADRD risk does not differ by income level. This finding contrasts with our hypothesis that household income would moderate the exposure-outcome relationship through protective resources such as residential air filtration, better healthcare access, superior nutrition, and greater residential mobility away from high-exposure areas.

Several factors may explain the absence of effect modification. First, neurotoxic exposures from plastics/rubber manufacturing may exert relatively uniform biological effects across socioeconomic strata, overwhelming the protective capacity of individual-level resources. Second, our binary income measure (above/below median) may lack sufficient granularity to detect effect modification, as protective resources may accrue non-linearly at higher income levels. The median split may obscure heterogeneity within both income categories, and our time-averaged measure may not capture peak earning years or economic shocks. Third, statistical

power limitations likely constrained our ability to detect true effect modification, as interaction terms require substantially larger sample sizes than main effects, particularly with only 263 individuals in our highest exposure category.

Despite the non-significant interaction, Model 4 demonstrated a strong main effect of income (OR=0.550, p<0.001), indicating that while income does not modify *how* exposure affects ADRD risk, it remains an important independent predictor. This pattern suggests an additive rather than synergistic relationship: both environmental exposures and socioeconomic disadvantage contribute to ADRD risk through potentially independent pathways. Upstream interventions targeting exposure reduction, through stronger emissions regulations and facility siting policies, can be effective measures to protect population health equitably.

Limitations

The main models we report on use emissions exposure measured in pounds by the nearest plastics/rubber TRI, and we categorize them based on meaningful percentiles (min value up to 75th percentile, 75th-90th percentile, 90th+ percentile). Model 5 also takes into account the distance to the nearest emitter (of any poundage amount), and these are categorized similarly.

Throughout this process, we explore various approaches to capture changes in residential location over time and link them to plastics/rubber industry data. We develop five sets of alternative models based on different exposure measures:

1. **Distance-based replication**: The same five models presented in this paper, but using kilometers to nearest plastics/rubber TRI facility (any emission level) rather than pounds emitted (Appendix 3)
2. **Pounds median/tail**: Pounds exposure categorized by median and tail distribution (Appendix 4, A)
3. **Distance median/tail**: Kilometers exposure categorized by median and tail distribution (Appendix 4, B)
4. **Log-transformed pounds**: Log-transformed pounds exposure divided into quartiles (Appendix 4, C)
5. **Log-transformed distance**: Log-transformed kilometers exposure divided into quartiles (Appendix 4, D)

Model output tables for all five alternative model sets are provided in the Appendices. Key findings:

Model Set 1 (Distance-based replication, Appendix 3): No exposure measures are significant. Age, total moves, average income percentile, and disadvantage index remain significant. Sex, race, marital status, homeownership, education, and the income×exposure interaction are not significant.

Model Set 2 (Pounds median/tail, Appendix 4 A): Similar pattern to our main model—mid-level exposure to emissions shows elevated OR for ADRD risk, with greater attenuation after adding covariates. Age, total moves, average income percentile, and disadvantage index remain significant. Sex, race, marital status,

homeownership, education, and the income×exposure interaction are not significant.

Model Set 3 (Distance median/tail, Appendix 4 B): Distance exposure (km) is significant in the base model and remains significant for mid-level exposure after adjusting for individual and household covariates. In fully adjusted models and models with the interaction term, the exposure effect is attenuated to non-significance. Age, total moves, average income percentile, and disadvantage index remain significant. Sex, race, marital status, homeownership, education, and the income×exposure interaction are not significant.

Model Set 4 (Log-transformed pounds, Appendix 4 C): Similar pattern to our main model, but the 4th quartile of exposure shows the highest (and statistically significant) OR for ADRD risk in models 1–3. In model 4, adding the interaction term attenuates the exposure effect to non-significance. Age, total moves, average income percentile, and disadvantage index remain significant. Sex, race, marital status, homeownership, and education are not significant.

The significant finding in the 4th quartile should be interpreted with caution. Log-transforming pounds before creating quartiles compresses high exposure values, meaning the 4th quartile encompasses an extremely wide range of original exposure levels. This broad categorization may mask important distinctions between moderately high and extremely high exposures and makes it difficult to determine whether the observed effect is driven by the full quartile or only the most extreme values within it.

Model Set 5 (Log-transformed distance, Appendix 4 D): No significant relationship between logged kilometer quartiles and ADRD risk. Age, total moves, average income percentile, and disadvantage index remain significant. Sex, race, marital status, homeownership, and education are not significant.

This study has several limitations related to data coverage, statistical power, and generalizability. We examined whether the PSID remained representative of the U.S. in our study, given our substantial restrictions we placed on the sample (i.e. 65+ years old and AD8 Survey Respondent). There are approximately 85,000 census tracts in the U.S. Our analytic sample, spanning 1990-2017, captures 6,595 unique census tracts (approximately 8% of all U.S. census tracts). While the PSID is designed to be geographically representative, the sample restrictions we applied to ensure relevance to ADRD research resulted in a study population that is not geographically representative of the U.S. The geographic diversity represented in our dataset is limited, which may constrain the generalizability of our findings and reduce our ability to detect spatial patterns in exposure and risk. Some states have low numbers of participants, in the single and double digits, such as Delaware, Hawaii, Montana, and Wyoming. Other states have high observations in the 1-2 thousands, such as California, Virginia, Texas, South Carolina, North Carolina, Pennsylvania, Michigan, and Florida. However, all lower 48 states and Washington, D.C. are represented in our sample.

To assess the geographic representativeness of the PSID sample relative to EPA TRI facility locations, we conducted a post hoc analysis of facility distribution across tracts with and without PSID participants. Results reveal that fewer than 1.44% of

TRI facilities fall within PSID-covered tracts, suggesting limited overlap between exposure areas and the sampling frame. To better understand coverage in publicly known industrial hotspots, we summarize approximate PSID observational density across states with a high concentration of plastics/rubber facilities (see Table 5). Results suggest underrepresentation in several key states, including parts of Appalachia and the Gulf South. This post hoc summary indicates whether participant observations are low, mid, or high within each state (vagueness is due to the restricted nature of the PSID geocoded data). Notably, coverage is low in several states with historically high plastics industry presence, including Louisiana and Alabama.

Table 5 Approximate PSID observational coverage in U.S. states with known high concentrations of plastics/rubber facilities.

Known High Concentrations of Plastics Industries (Appalachia and Gulf States)	**Available Observations (approximation, due to restricted geocoded data)**
Louisiana	low
Texas	high
Alabama	low
Mississippi	low
Florida	high
Indiana	mid
Illinois	mid
Ohio	high

The AD8 was only administered to individuals aged 65 and older, meaning this study does not capture potential early-onset ADRD or cognitive decline among younger adults. This age restriction reduces the window for detecting preclinical stages of

ADRD. Moreover, while our primary exposure window spans from 1990 to 2017, the average age of participants in 1990 was approximately 38 years. As a result, this study cannot assess exposure during earlier, potentially more sensitive developmental periods (i.e. childhood, puberty, etc.).

This analysis is limited in its ability to establish causal pathways or identify specific mechanisms through which environmental toxicants affect cognitive outcomes. While spatial patterns are consistent with an environmental contribution to cognitive decline, we cannot assess routes of exposure (e.g., inhalation, ingestion, dermal absorption), cumulative dose, or internal biomarkers of toxicant burden. Moreover, because the PSID does not include complete residential histories, we cannot determine the duration of residence within a given census tract or whether exposures were continuous or intermittent across the study period. Accordingly, our models capture associations between historical proximity—defined as any documented residence in a census tract containing plastics/rubber TRI facilities—and later-life ADRD risk, rather than causal effects of exposure.

Our exposure assessment approach—using person-level average emissions from the nearest plastics/rubber TRI facility over 1990-2017—introduces several sources of potential misclassification. This metric does not account for (1) spatial decay of pollutant concentrations with distance, (2) prevailing wind patterns and atmospheric dispersion, (3) contributions from multiple nearby facilities, or (4) differences in emission composition (air, land, water) across facilities. High-emission facilities may be geographically isolated in less densely populated areas, resulting in lower population-level exposure despite high facility-level emissions.

Conversely, moderate-emission facilities may cluster in urban or suburban areas with higher background pollution from traffic, industry, and other sources, creating a more toxic cumulative exposure environment. Our "nearest facility" approach captures proximity but not true inhalation exposure, potentially obscuring genuine dose-response relationships.

To ensure a comprehensive understanding of exposure to plastics/rubber TRI facilities, we examined total emissions (pounds) released by the *nearest* facility of *any* emission level—this is the primary exposure variable used in our main models. In addition, we explored exposure by emission intensity, categorizing plastics/rubber TRI facilities each year from 1990 to 2017 into tertiles of total annual releases: low (bottom third), medium (middle third), and high (top third) emitters. Among respondents living nearest low or medium emitters, approximately 24.81% had ADRD risk, compared to 26.34% among those living nearest high emitters. An unweighted chi-squared test ($p = 0.368 > 0.05$; data not shown) indicated no statistically significant difference in ADRD risk between these groups. Accordingly, our main models focused on ADRD risk in relation to proximity to the *nearest* plastics/rubber TRI facility, regardless of emission level.

Conclusion & Future Work

In this study, we examine the association between residential exposure to toxic-releasing plastics/rubber manufacturing facilities emissions (lbs) and ADRD risk among Panel Study of Income Dynamics (PSID) participants from 1990-2017. Using geocoded residential histories and EPA TRI emissions data, we find that individuals

with moderate average exposure to plastics/rubber TRI emissions from the nearest facility have significantly elevated ADRD risk (OR = 1.339) compared to those with no exposure, even after adjusting for age, income, residential mobility, and neighborhood disadvantage. However, we do not observe the anticipated monotonic dose-response relationship, as high exposure is not significantly associated with ADRD risk in adjusted models. Additionally, we find that neighborhood disadvantage is strongly associated with increased ADRD risk, underscoring the importance of social determinants in understanding dementia outcomes. Our findings suggest that environmental exposure to industrial pollutants contributes to cognitive decline, though the relationship is complex and likely influenced by residential selection patterns, exposure misclassification, and unmeasured confounding factors.

The results underscore the importance of environmental justice perspectives in ADRD research, demonstrating how environmental exposures and socioeconomic vulnerabilities compound to create differential cognitive health risks. Future work should investigate how average exposures and socio-structural vulnerabilities jointly shape cognitive aging across place and time, with particular attention to improving geographic coverage in heavily industrialized regions. These results highlight the complexity of ADRD etiology and the need for further research integrating environmental, biological, and social pathways while addressing measurement and sampling limitations that may obscure true exposure-outcome relationships.

This work represents a foundational step in a broader research agenda investigating preclinical pathways to ADRD, with primary focus on understanding how phthalate

exposure may influence ADRD risk through microbiome-mediated pathways. This biologically grounded approach will advance our understanding of environmental health disparities and the mechanisms linking chemical exposures, gut health, and cognitive decline. Our next study will draw on the Wisconsin Registry for Alzheimer's Prevention (WRAP) using lab-based measures, including fecal samples and microbiome sequencing. We hypothesize that protective neighborhood environments support greater microbiome resilience, which may buffer individuals from cognitive harms associated with phthalate exposure. This approach integrates environmental exposures, spatial data, socio-demographic context, and biological mechanisms to investigate the phthalate–gut–brain nexus as a potential contributor to ADRD disparities.

More broadly, this work highlights the pervasive presence of plastics in modern environments and the health risks posed by their chemical components. By linking environmental exposure to cognitive outcomes within a socio-ecological framework, we contribute evidence toward answering a central question spanning environmental science, public health, and neurology: *How do environmental exposures and geo-social determinants shape the development and distribution of Alzheimer's Disease and Related Dementias?*

CHAPTER 2

Quantifying Phthalate Exposure in Human Fecal Samples: Methods and Biomarker Characterization in the MARS Cohort

Authors:

Gabrielle Eva Husted[1], Rachel Behrens[2], Barbara Bendlin[3], Susan Cassels[1], Darby Peter[3], Sandra Harding[3], Ethan Grover[3], Elizabeth Ackert[1], Sterling Johnson[3], Sanjay Asthana[3], Federico Rey[4], Puja Agarwal[5], Henrik Zetterberg[3,6], Rachael Wilson[3,] Ramiro Rea Reyes[3]

[1] University of California-Santa Barbara, Geography Department

[2] University of California-Santa Barbara, Materials Research Laboratory

[3] University of Wisconsin-Madison, Geriatrics and Gerontology

[4] University of Wisconsin-Madison, Medical Microbiology & Immunology

[5] Rush University, Department of Internal Medicine

[6] University of Gothenburg, Department of Psychiatry and Neurochemistry

Acknowledgements:

The authors acknowledge the use of the Biological Nanostructures Laboratory within the California NanoSystems Institute, which is supported by the University of California, Santa Barbara and the University of California, Office of the President.

The MRL Shared Experimental Facilities are supported by the MRSEC Program of the NSF under Award No. DMR 2308708; a member of the NSF-funded Materials Research Facilities Network (www.mrfn.org)

The authors would like to acknowledge the clinical and neuropathology diagnostic support provided by the Wisconsin ADRC's Clinical, Neuropathology and Biomarkers Cores, and biostatistical support provided by the Data Management and Statistical Core. Wisconsin ADRC grant number: NIH-NIA P30-AG062715. Wisconsin Registry for Alzheimer's Prevention (WRAP) grant number NIH R01 AG027161. Thank you to all the participants who provided their samples for this research.

Abstract

Background: Phthalates are ubiquitous (e.g., plastics, cosmetics, food packaging), and re-exposure is continuous despite rapid elimination from the body. Phthalates are linked with adverse health outcomes, however their relationships with dementia risk are not known. This proof-of-concept study generated fecal phthalate metabolomics to examine gut microbiome ecology, geo-social determinants of health (area deprivation index or ADI), and brain biomarker outcomes. **Methods:** This study integrates participant and biospecimen-level data from the Microbiome in Alzheimer's Risk Study (MARS), drawn from the Wisconsin Registry for Alzheimer's Prevention (WRAP) and Alzheimer's Disease Research Center (ADRC) cohorts. Four aims guided this work: (1) method optimization of fecal phthalate analysis (n = 10); (2) quantification of 19 phthalates and metabolites; (3) characterization of gut microbiome composition via sequencing; and (4) description of relationships between phthalate prevalence, microbiome composition, geo-social factors, and brain health measures. Key outcomes include Alzheimer's diagnosis and plasma

biomarkers (GFAP, NfL, ptau-217). Key predictors include phthalate presence/absence, age, sex, race, education, Area Deprivation Index (ADI), Bristol score, BMI, MIND diet score, enterotype, Shannon index, and observed species count. **Results:** PERMANOVA confirmed significant differences in microbial community composition between the *Bacteroides* dominant enterotype and the *Prevotella* dominant enterotype ($R^2 = 0.04$, $F = 14.28$, $p = 0.001$); the modest effect size suggests enterotypes reflect shifts in relative abundance among shared taxa rather than discrete ecosystems. In this pilot cohort of ten cognitively unimpaired adults, ADI did not consistently predict within-sample phthalate burden — samples from both low- and high-deprivation areas spanned wide detection ranges. Butylbenzyl phthalate and DEHP were detected across nearly all samples regardless of socioeconomic context. **Conclusions:** This pilot study demonstrates that fecal phthalate measurement is analytically feasible. Measuring phthalate metabolites in feces, where gut microbes are directly present, provides the opportunity to examine direct phthalate effects on gut microbiome, compared to the more common use of urinary metabolites, which primarily reflect downstream metabolic and excretory processes. Consistent with the Brain Health *Synercome* framework (Baez et al., 2026), findings underscore the need to integrate structural and individual-level exposure characterization to understand plastic-associated risk for brain health.

Introduction

Phthalates are a group of synthetic compounds formed as diesters derived from phthalic acid (1,2-benzenedicarboxylic acid), with extensive industrial applications in manufacturing flexible plastics, consumer goods, and personal care items (Husøy

et al., 2019). Because phthalates lack covalent bonds with the plastics they're incorporated into, they can leach into surrounding environments and products. They easily dissolve in fats and oils, readily transferring from plastic containers (i.e., food wraps, bottles) into fatty foods such as oils, dairy, meat, and processed snacks. People are exposed throughout life by ingestion, inhalation, and dermal contact. Phthalate exposure varies substantially across geographic and demographic groups and is of particular concern for susceptible populations, including pregnant women, children, and adolescents, due to developmental sensitivity (Koch et al., 2009). Phthalates impact the gastrointestinal barrier, the microbial composition, and disrupt endocrine signaling (Claus et al., 2016; Kowalski and Mulak, 2019; Rinninella et al., 2019). They alter immune function pathways and endogenous hormone production. These effects are increasingly implicated in inflammation, metabolic dysfunction, and neurodegenerative risk across the life course. Older adults may represent a particularly vulnerable population, as age-related declines in metabolic and detoxification capacity, combined with the blood-brain barrier deterioration characteristic of dementia, could together create a more permissive environment for plastic uptake and accumulation.

This study is motivated by emerging evidence that suggests environmental toxicants, including phthalates, may influence neurocognitive health through pathways involving the gut–brain axis, inflammation, and microbial dysbiosis (Wang & Wang, 2016; Jang et al., 2021; Nihart et al., 2025). Feces capture intestinal-level exposure and metabolism, making them particularly relevant for studies linking phthalates to the gut microbiome and downstream neurological risk. Compared with urine, fecal

samples may reflect slower transit, microbial modification, and local exposure rather than rapid renal clearance. Measuring phthalate metabolites in fecal samples provides closer alignment with gastrointestinal exposure and gut microbial processes than urinary biomarkers alone, which primarily reflect short-term renal excretion. However, human fecal phthalate metabolites are poorly characterized, with very few studies explicitly measuring monoester metabolites in fecal samples (Jeong et al., 2020; Kato et al., 2006; Senta et al., 2020; Erben et al., 2021). In studies analyzing human fecal samples for microplastics using detection by micro-Raman spectrometer, microplastics were detected in all participants' feces (Yan et al., 2022). For some metabolites, excretion rates (via urine, feces, sweat) are still unknown, and while there are excretion rates known for many metabolites, they are still under-studied, have many uncertainties, and there are often conflicting results (Senta et al., 2020). In studies of dog feces, excretion rates were 3–36 times higher than the corresponding urinary excretion rates (Li and Kannan, 2024). Additionally, a laboratory study in rats found that less than 4% of an administered dose of parabens—while distinct from phthalates, both are linked to endocrine disruption—was excreted in feces following oral, topical, and subcutaneous exposure (Aubert et al., 2012). These findings highlight persistent uncertainties about how these compounds are metabolized and eliminated from the body.

This paper aims to address these gaps and move the needle on fecal phthalate analysis, as it relates to brain health. We focus on five major parent phthalic acid esters and their metabolites. We pair this descriptive data with socio-demographic data, geographic characteristics, and brain health biomarkers. Phthalate exposures

and the gut microbiome relationship is geographical in nature due to the effect both the natural and built environment has on behavior, aging, and accessibility of healthy living such as physical activity, quality food, education, health care. We examine phthalates as they relate to socio-demographic data, geographic characteristics, and brain health biomarkers in an effort to identify factors that work through biology to 'get under the skin' and affect aging, specifically ADRD risk. This targeted scope allows for method development and feasibility testing, while capturing biologically relevant exposure pathways at the gut level.

Research Questions

1. **Method optimization and phthalate detection:** Can fecal phthalate analysis methods be optimized to reliably detect phthalates (table 6) and their metabolites above methodological sensitivity thresholds, while minimizing contamination and storage-related bias? (n = 10)
2. **Gut microbiome characterization:** What are the gut microbiome profiles and microbial metabolite patterns — including genus-level community composition, alpha and beta diversity — among MARS participants undergoing sequencing analysis? (n = 315)
3. **Exposure–microbiome–brain health relationships:** Are fecal phthalate concentrations associated with gut microbiome composition, geo-social factors, and brain health measures within the pilot sample? (n = 10)

Table 6 Major phthalate esters (PAEs) and their metabolites. Full name, abbreviation, chemical formula, and corresponding de-protonated species mass.

Full name of PAE	Abbreviation	Chemical Formula	[M-H]-
Di-ethyl phthalate	DEP	C12H14O4	221.0814
Mono-ethyl phthalate	mEP	C10H10O4	193.0501
Di-n-butyl phthalate	DnBP	C16H22O4	277.1440
Mono-n-butyl phthalate	mnBP	C12H14O4	221.0814
OH-mono-n-butyl phthalate	OH-mBP	C12H15O5	238.0841
Mono-(3-carboxypropyl) phthalate	mCPP	C12H12O6	251.0556
Butylbenzyl phthalate	BBzP	C18H26O4	305.1752
Mono-benzyl phthalate	mBzP	C15H12O4	255.0657
Di-(2-ethylhexyl) phthalate	DEHP	C24H38O4	389.2691
Mono-(2-ethylhexyl) phthalate	mEHP	C16H22O4	277.144
Mono-(2-ethyl-5-hydroxy-hexyl) phthalate	mEHHP (5OH-mEHP)	C16H22O5	294.1467
Mono-(2-ethyl-5-oxo-hexyl) phthalate	mEOHP (5oxo-mEHP)	C16H20O5	291.1232
Mono-(2-ethyl-5-carboxy-pentyl) phthalate	mECPP (5cx-mEPP)	C16H20O6	307.1181
Mono-(2-carboxymethyl-hexyl) phthalate	mCMHP (2cx-mMHP)	C16H20O6	307.1181
Di-iso-nonyl phthalate	DiNP	C26H42O4	417.3005
Mono-isononyl phthalate	miNP	C17H24O4	291.1596
Mono-(hydroxy-iso-nonyl) phthalate	mHiNP (OH-miNP)	C17H24O5	307.1546
Mono-(oxo-iso-nonyl) phthalate	mOiNP (oxo-miNP)	C17H24O5	307.1546
Mono(carboxy-iso-octyl) phthalate	mCiNP (cx-miNP)	C17H22O6	321.1338

We hypothesize that higher phthalate concentrations will be associated with dysbiotic gut profiles, examined via alpha diversity and comparisons of key genera and species — including *Prevotella* (indicative of plant- and fiber-rich diets), *Akkermansia muciniphila* (a marker of healthy gut mucosal integrity and metabolic health), and butyrate-producing genera. Depletion of these taxa may reflect a gut environment with compromised barrier function and greater systemic inflammatory potential (Bauer, Huus, & Finlay, 2016). This hypothesis is grounded in evidence that phthalates can alter microbial community structure and that dysbiotic profiles characterized by reduced SCFA production and elevated lipopolysaccharide (LPS) translocation are associated with neuroinflammatory risk (Vogt et al., 2017; Heston et al., 2023). While research on the phthalate-gut-brain axis is sparse, some work

has found an association between urinary levels of di(2-ethylhexyl) phthalate (DEHP), monomethyl phthalate (MMP), and mono-n-butyl phthalate (MnBP) and dysbiosis characterized by altered gut bacteria, bile acids, SCFAs, and amino acid metabolism in patients with dementia with Lewy bodies (Deng et al., 2024). Additionally, recent work has established that socioeconomic status extends its impact even to the gut; SES is strongly associated with both composition and the diversity of the gut microbiome (Zuniga-Chaves et al., 2023; Kwak et al., 2024). Whether phthalate exposure shapes the microbiome, or whether certain enterotypes create conditions favorable to phthalate retention and absorption, remains a key open question this research seeks to address. Upon exposure to phthalates, how each individual's body systems processes, and potentially changes, the chemicals is still unknown; biomarkers within fecal samples are complex and can be a result of metabolism from gut microflora (Deda et al., 2015).

To our knowledge, this study is among the first to quantify fecal phthalates in humans, and to evaluate these measures in relation to gut microbiome composition and cognitive outcomes.

Background

Phthalate exposure is associated with inflammation, and developmental and reproductive toxicity (Heudorf et al., 2007; Zarus et al., 2021). We can detect metabolites in human matrices, which are the broken down parent phthalate, indicating active processing. These monoester metabolites are reliable biomarkers for exposure (Johns et al., 2015; Radke et al., 2018).

Most phthalates are quickly broken down and leave the body through urine, sweat, and feces, often within a day. The vast majority of human phthalate exposure biomonitoring studies have focused on urinary phthalate metabolites, which reflect recent systemic exposure and rapid renal excretion (Hasan et al., 2025). In parallel, environmental measurements of parent phthalates are well documented in food, indoor air, dust, soil, and on skin or hands, providing important information on exposure sources and pathways (Campanale et al., 2020). Yet, because phthalates are in so many products (plastics, cosmetics, food packaging), "re-exposure" is continuous, meaning they're always present, even if not stored long-term (Wang, Y., & Qian, H., 2021). Low molecular weight phthalates can accumulate, such as in the kidneys, liver, and brain (Nihart et al., 2025). In one study examining phthalates in sweat, Di(2-ethylhexyl)phthalate (DEHP) was found in all samples, even when absent from corresponding urine samples, indicating both some degree of bioaccumulation and retention, and that perspiration might be an effective method to eliminate toxic phthalates (Genuis et al., 2012).

There is a small body of literature examining wastewater to assess exposure and excretion of plasticizers such as phthalates. “Wastewater based epidemiology” has been previously used to monitor illicit drugs and viruses such as COVID-19 and polio (Larsen et al., 2024). Wastewater provides more accessible spatial and temporal monitoring, compared to individual biomarker sampling, and can serve to motivate public health interventions, or closer biomonitoring endeavors (Been et al., 2018). However, ambient environmental monitoring identifies external sources of phthalate exposure, whereas individual human biomonitoring more accurately captures

internal dose and biologically relevant exposure (Koch et al., 2009). Biomonitoring evidence demonstrates that phthalates can induce biological effects at low, environmentally relevant concentrations, presenting analytical challenges such as ubiquitous background contamination ("the phthalate blank problem"), which has been mitigated by focusing on specific hydrolytic and oxidative metabolites less prone to contamination (Koch et al., 2009).

Recent research has investigated the interconnections between urinary phthalate metabolite concentrations, gut microbiome dysbiosis, and metabolic profiles in patients with Dementia with Lewy Bodies (Deng et al., 2024). The investigation incorporated human fecal microbiota transplantation experiments into mice, which served to elucidate the mechanistic role of phthalate metabolites in gut dysbiosis, phthalate exposure, and disease-relevant outcomes.

A central question in this area concerns the route by which environmental plastics translate into internal biological burden. Emerging evidence suggests that dietary fat absorption represents a key gateway (Nihart et al., 2025). Lipid digestion involves a highly organized sequence: pancreatic enzymes break down and emulsify dietary fats, epithelial cells of the gut absorb the resulting fatty acids and repackage them into chylomicrons, and these lipid-rich particles are then transported into systemic circulation. Critically, this distribution is not random — chylomicrons are directed toward tissues with high lipid demand, including the brain, which is extensively composed of lipids and myelin. Microplastics may exploit this pathway by associating with dietary lipids and effectively “hitchhiking” through the same absorptive machinery the body uses for nutrient uptake (Nihart et al., 2025). Under

this "hijacking hypothesis," gut and brain vasculature function less as protective barriers and more as inadvertent gateways for plastic translocation — though this framework remains under active investigation.

Postmortem human brain tissue provides some of the most striking evidence of central nervous system accumulation to date. Nihart et al. (2025) found microplastic concentrations in brain tissue to be 5-8 times higher in individuals with dementia compared to those without, with plastics clustering in and around the arteriolar walls of affected brains. High concentrations were also identified in and around inflamed regions associated with immune cell infiltration, raising the question of whether plastics are driving neuroinflammation or whether sites of existing disease represent preferential destinations for plastic deposition; this directionality remains unresolved (Nihart et al., 2025; Somarelli et al., 2026). Some research additionally suggests that nanoplastics may promote the aggregation of pathological proteins including tau, beta-amyloid, and alpha-synuclein, potentially through surface chemistry interactions (West et al., 2026). This evidence requires cautious interpretation and replication.

Our paper contributes to this growing body of knowledge by presenting a proof-of-concept study assessing whether fecal phthalate metabolites can be reliably measured, an important step toward better characterizing plastic-associated exposures relevant to brain health. We contribute to filling the gap by providing a guide to detecting phthalate metabolites using a targeted and non-targeted screening approach for human fecal biomonitoring (Guo et al., 2019).

Data & Methods

This study integrates participant visit- and fecal biospecimen-level data from the Microbiome in Alzheimer's Risk Study (MARS. It is an on-going study that began in 2016 and includes participants from the Wisconsin Registry for Alzheimer's Prevention (WRAP) and Alzheimer's Disease Research Center (ADRC) cohorts. Sequencing metadata derived from fecal samples was processed at University of Wisconsin-Madison. While some participants in MARS are also participants in WRAP and ADRC cohorts, the MARS dataset was designated as the authoritative source for participant demographics, clinical diagnoses, and cognitive and biomarker measures. We established a Materials Transfer Agreement and Biological Use Authorization plan in order to gain access to this restricted data, available upon application to the UW-Madison ADRC.

I begin by describing the two groups we create from our MARS cohort (n = 315). Then I explain the measures we use to characterize them, including the Area Deprivation Index (ADI), the MIND diet scores, and gut microbiome analysis (shotgun metagenomics data, PERMANOVA, Principle Coordinate Analysis (PCoA), alpha diversity, and beta diversity). Next, I outline the fecal sample preparation, analytical workflow for phthalate detection, including chemical structure of phthalates and mass spectrometry (Group 2, n = 10). Finally, I report our plasma brain biomarker variables available for Group 2.

We have two subsets of participants that we worked with for this paper. Group 1 included 315 unique participants, all who have fecal samples that underwent

metagenomic sequencing and had this raw data available to be shared via Globus, a secure, cloud-based platform for transferring, sharing, and managing large datasets between institutions. We have the diagnosis and sparse plasma biomarkers for this group. Group 2 included 10 unique participants within Group 1 that were selected based on known levels of socio-economic deprivation as measured by the Area Deprivation Index, and we have complete plasma biomarker data for this group.

The Area Deprivation Index (ADI), obtained from the Neighborhood Atlas, was merged into the MARS cohort dataset and was available for all participants. The ADI is a validated measure of neighborhood-level socioeconomic disadvantage and is commonly used to capture aspects of the adverse social exposome—the broader social and environmental conditions that shape health across populations (Kind & Buckingham, 2018; Figueroa et al., 2020; Kind et al., 2020). Calculated at the census block group level, the ADI combines multiple socioeconomic indicators, including income and poverty levels, educational attainment, employment, housing quality, transportation access, prevalence of single-parent households, and the proportion of older adults living alone. These indicators are integrated using a factor analysis model to generate a standardized score ranging from 1 to 10, with higher scores indicating greater neighborhood deprivation relative to other areas nationally or within a state. For this pilot study, ADI values were used to intentionally select ten eligible participants, including five residing in neighborhoods with low deprivation and five residing in neighborhoods with high deprivation.

The diet of each participant is assessed via their MIND diet score. The Mediterranean-DASH Intervention for Neurodegenerative Delay, known as the MIND diet, is a dietary pattern that has demonstrated protective benefits against cognitive decline (Barnes et al., 2023). The MIND diet focuses on consuming plant-based foods, with an emphasis on green leafy vegetables, nuts, berries, fish, and olive oil. It encourages limiting foods with high levels of saturated fat and sugar, which may include processed meat, butter, margarine, sweets, and fried foods. A MIND diet 14-item questionnaire developed by Martha Clare Morris at Rush University was used as an abbreviated approach to assess adherence to these guidelines; scores range from 0 to 14, with lower scores indicating a less adequate diet with respect to brain health (Barnes et al., 2023).

Gut microbiome composition for participants in Group 1—including the subset of 10 participants in Group 2—was characterized using shotgun metagenomic sequencing of fecal samples (Quince et al., 2017). Shotgun metagenomic sequencing of human gut microbiome fecal samples involves extracting all microbial DNA present in a stool sample and sequencing it without targeting a specific gene. The resulting DNA fragments are computationally assembled and compared to a reference database or *library* to identify the microorganisms present and the genes they carry. This approach allows researchers to characterize both the taxonomic composition and functional potential of the gut microbiome at high resolution.

We analyze and summarize the gut microbiome data using *R* (version 4.5.2; 2025-10-31), leveraging the “vegan” package for ordination and community-level

statistical analysis (Oksanen et al., 2024). To provide structure to the inherently high-dimensional data, we apply enterotyping, which groups microbiomes based on the dominant bacterial genus (Arumugam et al., 2011). Although microbial community structure exists along a continuum rather than as discrete categories, enterotypes offer a useful framework for high-level interpretation.

Enterotypes are identified using PAM (Partitioning Around Medoids) clustering, implemented via the "cluster" package in R (Kaufman & Rousseeuw, 1990; Maechler et al., 2024). PAM operates by selecting k actual data points, called medoids, that best represent the center of each cluster, then assigning all remaining samples to the nearest medoid based on a dissimilarity metric. Unlike k-means, which uses abstract centroids, PAM anchors each cluster to a real observation making it more robust to outliers and more interpretable in the context of microbial community profiles. To determine the optimal number of clusters, we evaluate average silhouette width across candidate values of k (Rousseeuw, 1987). For each sample, the silhouette width measures how similar it is to its own cluster relative to the next-nearest cluster, ranging from -1 (misclassified) to +1 (well-matched); averaging these values across all samples produces a summary score for a given k. The value of k that maximizes average silhouette width is selected, balancing cluster cohesion and separation. This approach avoids arbitrarily imposing a fixed number of enterotypes and instead allows the structure of the data to guide the grouping.

We formally test differences in microbial composition across enterotypes using PERMANOVA (Permutational Multivariate Analysis of Variance), a statistical test

used to determine whether the overall composition of microbial communities differs significantly between groups (Anderson, 2001). Briefly, the method first computes a distance matrix between all pairs of samples using a beta-diversity metric, then calculates a pseudo-F statistic — the ratio of between-group variance to within-group variance in that distance space. Group labels are then permuted thousands of times, with the pseudo-F recalculated at each iteration to build a null distribution; a p-value is derived by asking how often a random permutation produces an F statistic as large as the observed one. To visualize this, we use Principal Coordinate Analysis (PCoA) to depict similarities and differences between samples, reducing complex microbial profiles into lower-dimensional space and enabling interpretation of patterns in community composition using ordination based on Euclidean distances (Gower, 1966).

Because PCoA typically captures only a portion of total variation, often within the first two or three components, we interpret these results alongside additional metrics, particularly alpha diversity and other explanatory variables, to ensure a more complete and robust characterization of microbiome structure.

Alpha diversity refers to the diversity of species *within* a sample. The Shannon index is a commonly used metric that assesses diversity by measuring both species richness and evenness within a community (Shannon, 1948). Values generally fall between 1.5 and 3.5 with higher values indicating greater diversity. Beta diversity refers to the compositional difference between any two samples. Bray Curtis dissimilarity index is a commonly used metric to assess beta diversity (Bray & Curtis,

1957). A value of 0 indicates that the samples are identical, while a value of 1 indicates that they have no overlap.

Laboratory Protocol

Within Group 1, 10 fecal samples, selected based on their ADI and availability of plasma ADRD biomarkers, were shipped to UC-Santa Barbara to undergo phthalate analysis. Fecal samples were analyzed for multiple phthalate monoester metabolites.

Frozen human fecal samples were stored at −80 °C until processing. Samples were thawed on ice and weighed (1.42–2.04 g wet weight). Exact mass was recorded for normalization. Standardized sample preparation practices for human fecal analyses were informed by Hosseinkhani et al. (2021). Fecal samples were extracted using a monophasic methanol protocol adapted from Kelly et al. (2022), suitable for UPLC-MS analysis of small molecule metabolites. Methanol is indicated for extraction of less polar compounds, such as phthalates (Deda et al., 2015). Methanol (UPLC–MS grade, pre-chilled to 4 °C) was added at a ratio of 10 mL per gram of feces (30 mL per 3 g target mass). Samples were vortexed for 30 s and agitated on an orbital shaker (125 rpm) for 30 min at 4 °C to facilitate extraction. Samples were centrifuged at 4,000 × g for 15 min at 4 °C to pellet particulate material. The supernatant was transferred to clean tubes and centrifuged again at 10,000 × g for 10 min at 4 °C to ensure complete clarification. Clarified extracts were transferred to amber glass vials and stored at −80 °C until analysis. All materials in contact with samples were glass whenever possible to minimize background phthalate contamination. Prior to UPLC–MS analysis, extracts were transferred to autosampler vials for injection. The samples did not undergo dilution.

Detection of analytes used LC-MS/MS methods similar to those developed by CDC for phthalate metabolites, incorporating labeled internal standards to correct for instrument variability (CDC, 2017-2018). We purchased two phthalate standards: mono(2-ethylhexyl) phthalate (MEHP) and mono-n-butyl phthalate (mnBP), which correspond to the parent compounds Di(2-ethylhexyl)phthalate (DEHP) and Di-n-butyl phthalate (DBP). The standards allow us to confirm their presence and retention times. Detection was performed in negative ionization mode. The mnBP standard produced a single, well-resolved peak at approximately 2.28 minutes with a mass-to-charge ratio (m/z) of 221.08, consistent with the expected $[M-H]^-$ ion. The MEHP standard eluted later at approximately 5.03 minutes, consistent with its greater hydrophobicity, and produced a characteristic ion at m/z 277.14. These standards established reference retention times and mass signatures used to identify target metabolites in subsequent sample analyses.

> DEHP (di-2-ethylhexyl phthalate) is a high–molecular weight plasticizer commonly used in PVC products (e.g., medical tubing, flooring, and food packaging), and it was measured via its primary metabolite, **mono-2-ethylhexyl phthalate** (MEHP).
>
> DBP (dibutyl phthalate), a low–molecular weight phthalate used in personal care products, adhesives, and coatings, was assessed using **mono-n-butyl phthalate** (MnBP).

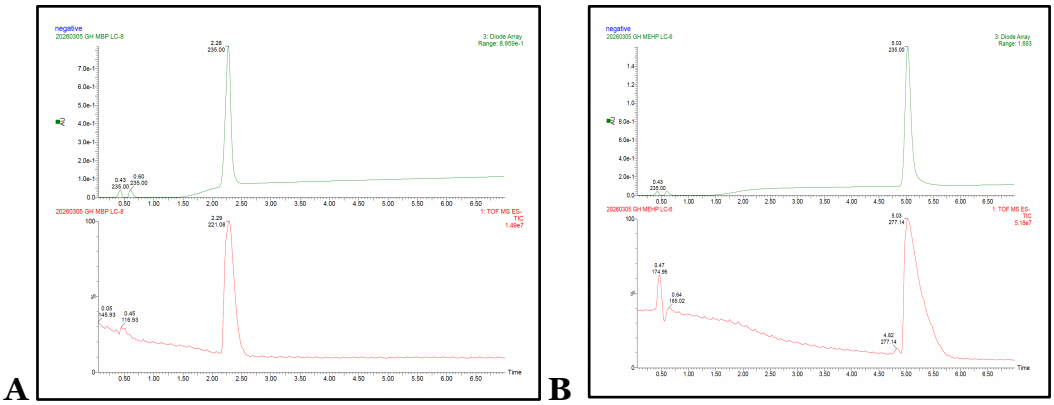

Figure 1 (A) LC chromatographic confirmation of (A) mono-n-butyl phthalate (mnBP) (B) mono(2-ethylhexyl) phthalate (MEHP) analytical standard.

In addition to these standards, we also screened the data for other prominent phthalates based on their expected mass-to-charge ratios. While we can learn about retention times of phthalates from the literature that examines them in human urine, for example, we cannot glean the retention times and exact mass spectral characteristics from the literature because our exact conditions are a critical factor in determining the phthalate signature in our laboratory. The corresponding standards are needed to definitively determine their retention times and confirm identities on our column.

Chemical Structure of Parent Phthalates of Interest

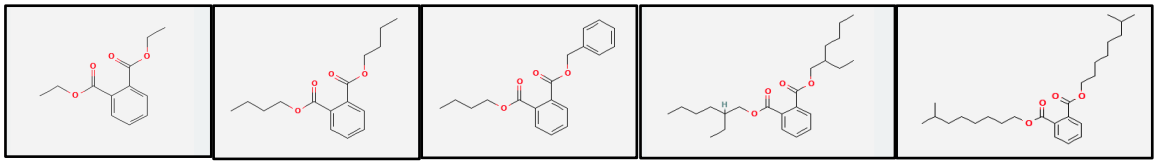

Figure 2 PubChem 2D structural images of parent phthalates examined in this paper. From left to right: Di-ethyl phthalate, Di-n-butyl phthalate, Butylbenzyl phthalate, Di-(2-ethylhexyl) phthalate, Di-iso-nonyl phthalate.

The analytical workflow is optimized for low-level detection. Metrics for detecting phthalates in human feces do not exist. We draw on the findings from Jagani and

colleagues (2025), which reviews quantification of exposome measures to ground our work among other established results analyses of phthalates in human biological matrices. Our study does not expect to directly replicate urinary biomonitoring metrics, but rather to complement them by capturing fecal-level toxicant presence relevant to gut microbial ecology. Phthalate monoester metabolites are known to be present at substantially lower concentrations in feces than in urine, reflecting differences in absorption, metabolism, and excretion pathways. Experimental animal studies suggest that only a small fraction of phthalate metabolites are eliminated via feces, with the majority excreted in urine (EPA, 2017). As a result, fecal concentrations are expected to be lower, more variable, and more sensitive to measurement error. Table 7 provides a brief overview of studies that have examined phthalates, and their laboratory performance.

Table 7 Depicts chemical classes, target analytes, and detection performance across different human biological matrices, adapted from Jagani et al., 2025.

Chemical Class	*Analytes*	*Matrix*	*LOD Range (ng/mL)*	*LOQ Range (ng/mL)*	*Detection Frequency (%)*	*Recovery Range (%)*	*Study*
Phthalates	MMP, MEHP, MIBP	Human urine	0.01-1.0	Not specified	≥ 20%	Not specified	Lee et al., 2022
Phthalates	MEHP, MBP, DEHP metabolites	Urine	0.078-0.425	0.236-1.289	0-100%, Majority ≥ 90%	85-114%	Oh et al., 2025
Phthalates	DEHP metabolites, DiNP metabolites	Urine	0.004-0.53	Not specified	6-100%	70-129%	Kunde et al., 2025

Quality control (negative controls) procedures were implemented throughout the analytical workflow. Procedural blanks consisting of methanol only (solvent without sample) were processed in parallel with samples to assess background contamination (Hitha et al., 2023). Extraction blanks were also carried through the full workflow to identify potential contamination introduced during sample handling.

To evaluate whether sample storage conditions could influence our phthalate retention, we conducted a brief experiment on a fresh fecal sample. We divided it into two aliquots, and a known quantity of mnBP phthalate was added to each. One aliquot was processed immediately through the full laboratory workflow— extraction and analysis—on the same day the sample was produced. The second aliquot was stored at −80 °C for three days prior to undergoing the same laboratory procedures. Chromatograms from the two samples were then compared. The results indicate that both samples have matching m/z peaks and retention times, and are of similar intensity levels. Although this short experiment cannot fully replicate the long-term storage conditions of samples kept frozen, some for up to five years, it provides preliminary evidence that mnBP and likely phthalates in general, remain detectable in fecal samples following freezing at −80 °C and do not appear to degrade over short-term storage.

Mass spectrometry

To determine whether the samples in our study contain phthalates, we utilize the Waters Acquity H-class Ultra High Pressure Liquid Chromatography (UPLC) system

coupled with a Waters Xevo G2-XS Time-of-Flight Mass Spectrometer with high resolution (10 ppm or less). With an electrospray ionization (ESI) source, the Time-of-flight mass spectrometry (ToF-MS) can provide mass data up to 100,000 m/z either operating with the UPLC or independently, and signals can be optimized by operating in resolution or sensitivity mode. We are able to resolve the parent ion and its fragments, using increased collision energy, providing quantitative and qualitative results.

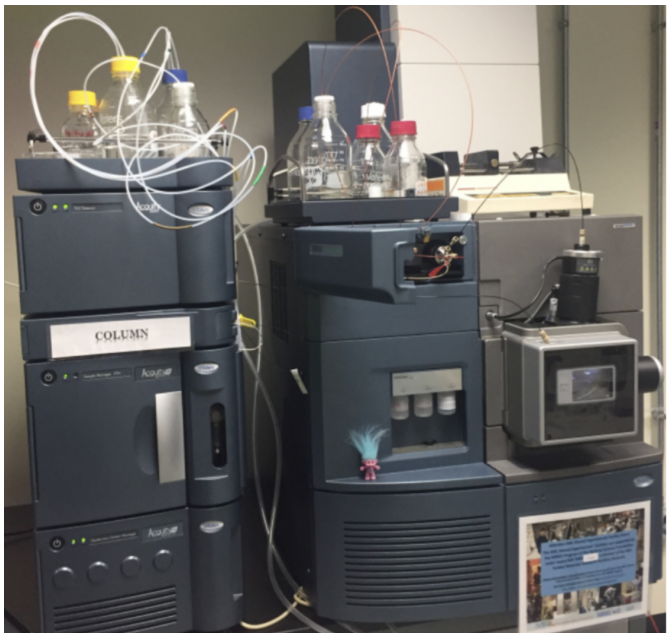

Figure 3 Waters UPLC-MS. UCSB Materials Research Laboratory. Polymer Lab.

During mass spectrometric analysis, analytes were ionized in negative electrospray ionization (ESI–) mode, which is well-suited for detecting compounds that readily form deprotonated species. “Species” refers to the distinct ionic forms of molecules that are detected by the instrument; different charged versions or fragments of a compound. In this process, molecules typically gain a negative charge through the loss of a proton, producing $[M–H]^-$ ions that are detected based on their mass-to-

charge (m/z) ratios. The resulting mass spectrum contains peaks corresponding to molecular ions and fragment ions, which can be used to infer the chemical composition and structure of the analytes. The most abundant and stable ion in the spectrum, referred to as the base peak, is assigned a relative intensity of 100%, and all other peaks are scaled proportionally. Analysis of the m/z values and fragmentation patterns enables the identification and confirmation of phthalate metabolites.

Table 8 LC method parameters for the UPLC-MS of phthalates within stool samples. Mobile phase A: Water + 0.1% Formic Acid. Mobile phase B: Acetonitrile + 0.1% Formic Acid.

Time (min)	Flow Rate (mL/min)	% A	% B	% C	% D	Curve Initial
initial	0.300	70.0	30.0			Initial
0.20	0.300	70.0	30.0			6
0.75	0.300	52.0	48.0			6
7.00	0.300	42.0	58.0			6
7.10	0.300	0.0	100.0			6
8.30	0.300	0.0	100.0			6
8.40	0.300	70.0	30.0			6
11.00	0.300	70.0	30.0			6

Fecal phthalate metabolites were analyzed using ultra-performance liquid chromatography coupled with mass spectrometry (UPLC-MS). Chromatographic separation was achieved using a reversed-phase C18 (octadecylsilane) column, in which a non-polar stationary phase facilitates retention of hydrophobic compounds such as phthalates. A traditional LC gradient was utilized for separation with water and acetonitrile mobile phases, both containing 0.1% formic acid, enabling efficient elution and ionization (see Table 8). As in traditional column chromatography,

separation is driven by differential interactions between analytes, the stationary phase, and the mobile phase; compounds partition based on their polarity and chemical properties, resulting in distinct retention times. Compared to conventional column chromatography, UPLC provides enhanced sensitivity, resolution, and the ability to analyze small sample volumes, making it well-suited for detecting phthalate metabolites. Analytes were identified and quantified based on their retention times and mass spectral characteristics across the chromatographic run. A signal rising above 3x the background noise was considered present. Any signal below $1e^3$ was recorded as trace to absent.

Plasma Brain Biomarkers

Three plasma biomarkers were examined to assess neuroinflammatory and neurodegenerative burden among Group 2: glial fibrillary acidic protein (GFAP), neurofilament light chain (NfL), and phosphorylated tau 217 (ptau-217). These markers index glial activation, neurodegeneration, and AD pathology respectively.

Plasma GFAP and NfL levels were measured using the Simoa Neurology 4-Plex E assay at the University of Wisconsin ADRC Biomarker Lab, utilizing the Quanterix HD-X platform. Plasma pTau217 levels were measured using the ALZpath p-Tau 217 Advantage PLUS assay at the University of Wisconsin ADRC Biomarker Lab, utilizing the Quanterix HD-X platform. All concentrations are reported in pg/mL. Cut-off values identifying thresholds warranting further clinical attention Identifying are developed for each assay, and are not standardized across assays and research sites. This is an ongoing challenge for the field of AD biomarkers, and efforts are

underway to determine more universal ways to communicate AD biomarkers across clinics despite varying laboratories, methodology, and patient populations; ratios between biomarkers (e.g., p-tau217/p-tau181 and Aβ42/Aβ40 ratio) (Mayo Foundation for Medical Education and Research, 2022; Khasanov, Tolibov, & Daminova, 2026).

Plasma GFAP is a structural protein released by astrocytes in response to injury or neuroinflammation, and while this marker is not specific to one neurodegenerative disease, its elevated concentrations have been associated with increased likelihood of underlying amyloid pathology. Plasma NfL, a marker of axonal damage and neuronal injury more broadly, reflects the degree of active neurodegeneration regardless of its etiology. Elevations signal ongoing or cumulative neuronal loss, which may be present across a range of neurodegenerative conditions (Simrén et al., 2022). Plasma ptau-217 is the most Alzheimer's Disease-specific of the three, with elevated concentrations directly associated with amyloid plaque pathology characteristic of Alzheimer's disease. However, a positive result alone is insufficient for an Alzheimer’s disease dementia diagnosis and must be interpreted alongside other patient-specific clinical information (ARUP Laboratories, 2025).

In this study, we used GFAP as a marker of glial reactivity and early amyloid-associated astrocytic response, NfL was used to capture neuronal injury; and ptau-217 was used to capture pathology central to AD pathophysiology. While only working with a small N, the pilot project explored the feasibility of testing the extent

to which phthalates may be associated with pathology as indexed by these biomarkers.

Results

Participant characteristics are summarized in Table 9 and 10. The cohort was predominantly female (64.4%) and White (88.3%), with a mean age of 67.1 ± 7.1 years. The cohort has a mean of 16.2 ± 2.8 years of education, reflecting a relatively well-educated sample. Many participants (88.9%) were cognitively unimpaired at the time of fecal sample collection, while 11.1% carried a diagnosis of Alzheimer's-related cognitive impairment — including Dementia-AD (7.0%) and MCI-AD (2.5%). The sample also reflected impaired-other (1.3%), and non-AD MCI (0.3%). Most participants reported moderate levels of physical activity, with 73.9% exercising more than once per week. The cohort has a mean BMI of 29.1 ± 6.1, indicating overweight status. Stool consistency as measured by the Bristol Stool Scale was concentrated in the normal range, with Types 3 and 4 accounting for approximately 59.2% of the sample. Gut microbiome alpha diversity was moderate, with a mean Shannon diversity index of 3.9 ± 0.3 and 168.1 ± 41.9 observed species, consistent with typical diversity levels reported in older adult cohorts. Neighborhood-level socioeconomic disadvantage, assessed via ADI state rank, was distributed across all deciles, with the largest proportion of participants residing in the least deprived areas (Deciles 1–3, 42.2% combined).

Table 9 Demographic and clinical characteristics of the MARS cohort (n = 315). Activity level is self-reported physical activity (5-point scale). Bristol Stool Scale reflects stool consistency at time of sample collection (7 point scale).

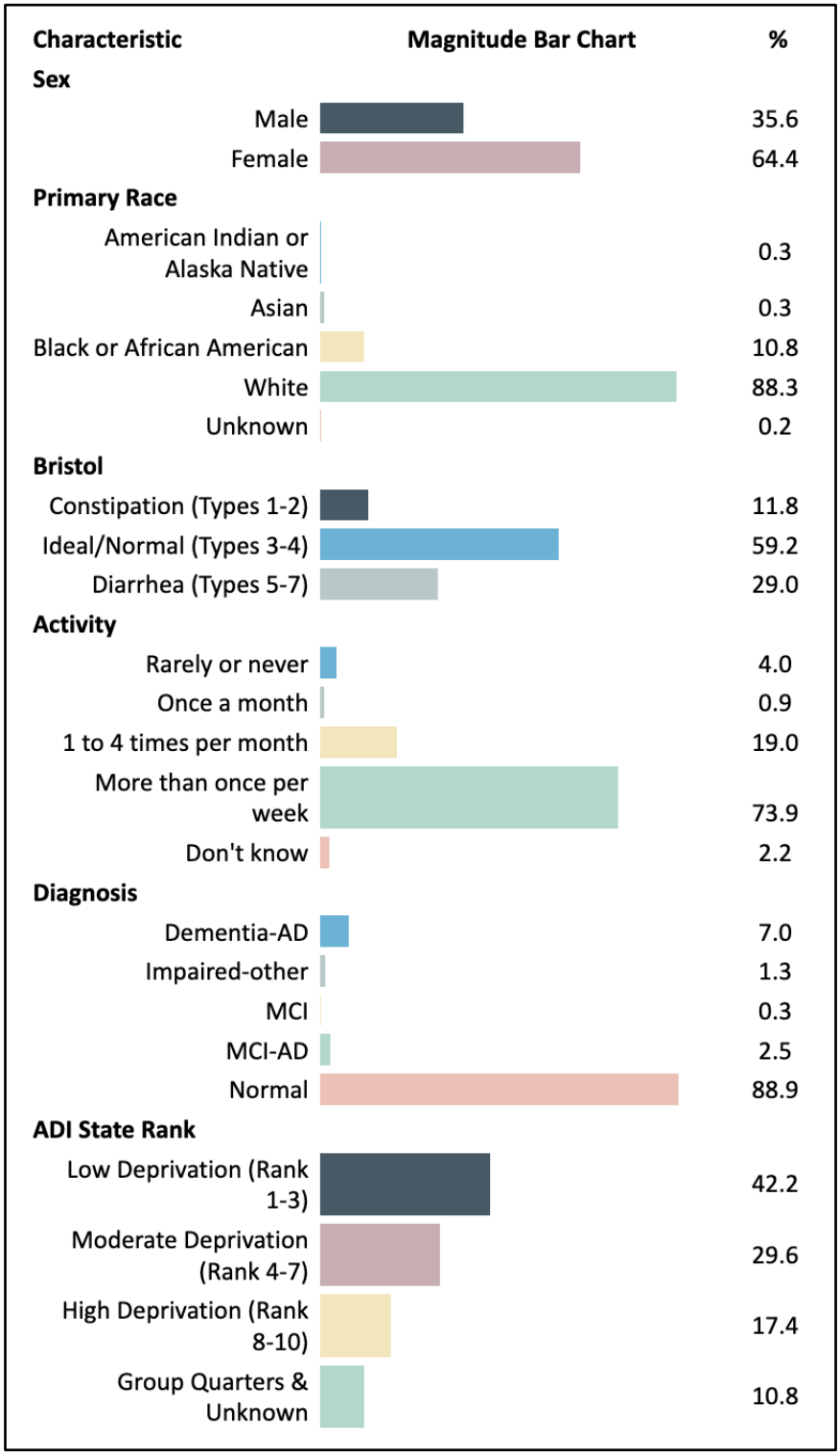

Table 10 Demographic and clinical characteristics of the MARS cohort (n = 315). Continuous variables are reported as mean ± standard deviation.

Characteristic	Mean ± SD
Age	67.1 ± 7.1
BMI	29.1 ± 6.1
Education	16.2 ± 2.8
APOE NP Score	0.7 ± 1.1
Shannon Diversity	3.9 ± 0.3
Observed Species	168.1 ± 41.9

Group 1 Analysis

Gut microbial community composition varied across participants, as visualized in Figure 4. This is a principal coordinate analysis map of gut microbial community composition across all participants, colored by the two enterotypes that emerged from the data. Each point is one individual's microbiome; proximity between points reflects compositional similarity as determined by the Bray-Curtis Dissimilarity Index. Samples that clustered more closely together exhibited greater similarity in overall microbial composition, while separation along the first two principal coordinates reflected broader compositional differences.

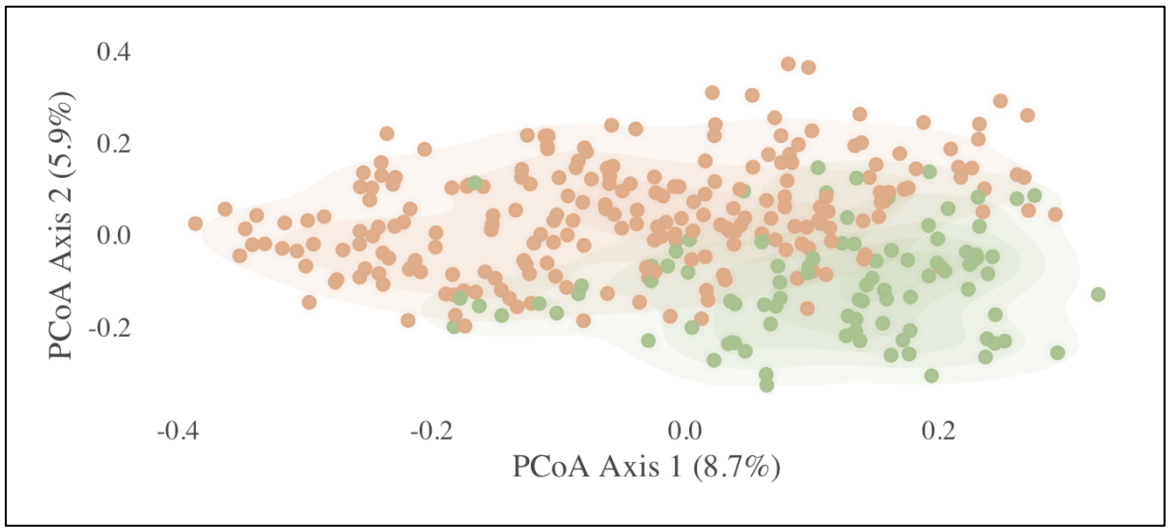

Figure 4 Gut microbiome enterotypes among Microbiome in Alzheimer's Risk Study (MARS) participants (n = 315). Colors denote enterotypes based on dominant genera. Enterotype 1 = Orange, Enterotype 2 = Green.

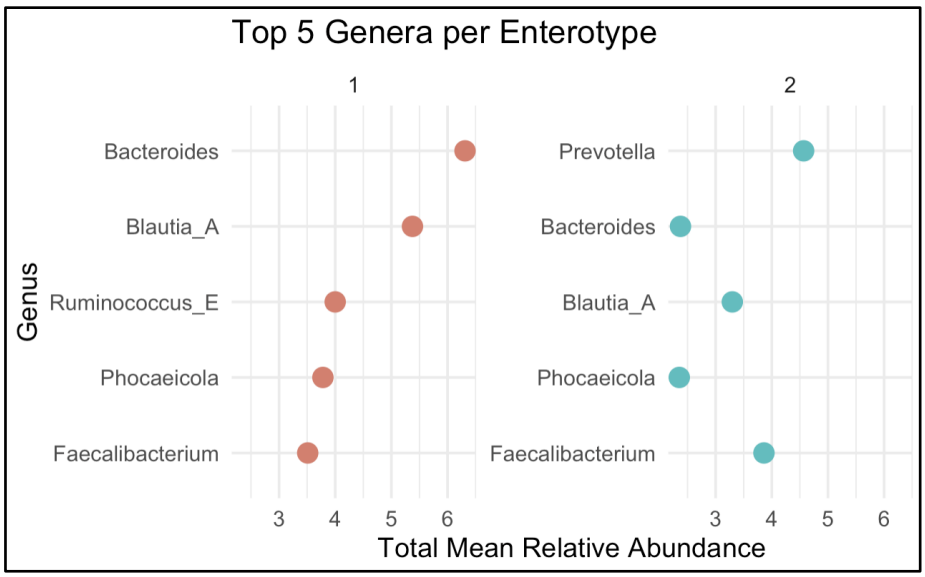

Figure 5 Relative abundance of the top five bacterial species within each enterotype.

Distinct dominant taxa characterize each enterotype, highlighting differences in community structure between groups (Figure 5). Enterotype 1 was characterized by a predominance of *Bacteroides* (total abundance = 6.31), followed by *Blautia* (5.38), *Ruminococcus* (4.00), *Phocaeicola* (3.78), and *Faecalibacterium* (3.51). In contrast, Enterotype 2 was driven primarily by *Prevotella* (4.57), with *Faecalibacterium*

(3.86), *Blautia* (3.30), *Bacteroides* (2.37), and *Phocaeicola* (2.35) also contributing to overall abundance. While several genera were present across both enterotypes, their relative contributions differed, with higher *Bacteroides* abundance distinguishing Enterotype 1 and greater *Prevotella* abundance distinguishing Enterotype 2.

Enterotype 1 was defined by a dominant *Bacteroides* signature, consistent with a Western dietary pattern high in animal protein and fat. *Bacteroides* occupies a foundational ecological role in the gut: it metabolizes polysaccharides and oligosaccharides, providing nutrition and vitamins to the host and supporting other microbial residents, effectively sustaining what has been described as the "microbial food web" of the gut (Zafar & Saier, 2012). Beyond nutrition, *Bacteroides* interactions with the gut mucus layer are considered pivotal for microbiota assembly and stability. A species of particular focus in the literature is *B. thetaiotaomicron*. It has been shown to influence butyrate production by *Eubacterium ramulus* and modulate flavonoid degradation dynamics, with downstream implications for gut immune signaling (Zafar & Saier, 2012). Despite these beneficial roles, *Bacteroides* species are opportunistic pathogens capable of causing extraintestinal infections; following entry into the bloodstream, they may access the central nervous system via penetration of the blood-brain barrier through olfactory and trigeminal cranial nerves (Zafar & Saier, 2012). This duality, whereby the same microbial taxa can sustain host health under conditions of balance yet promote pathology when that balance is disrupted, is not unique to *Bacteroides*, but is often observed in host-microbiome relationships. The gut microbiome functions less like a passive

bystander and more like a dynamic regulatory organ: through metabolic, immune, and neuroendocrine signaling, it can exert an influence far beyond the intestines. When microbial equilibrium is maintained, these signals support barrier integrity, immune tolerance, and metabolic homeostasis. When dysbiosis arises, the same pathways can become vectors for systemic harm, implicated across a spectrum ranging from chronic inflammatory and metabolic conditions such as obesity, type 2 diabetes, and cardiovascular disease, to acute trajectories including infection susceptibility and sepsis (MahmoudianDehkordi et al., 2019; Chen et al., 2024; Liang et al., 2026 preprint). In this sense, the gut microbiome reach is systemic, and its disruption can carry consequences beyond itself.

Also prominent in Enterotype 1 were *Blautia*, *Ruminococcus*, *Phocaeicola*, and *Faecalibacterium* — a consortium of taxa collectively enriched in carbohydrate fermentation and short-chain fatty acid (SCFA) production. *Blautia*, one of the top ten most detected genera in the healthy human gut (representing 2–8% of the microbiome), plays a key role in indigestible carbohydrate degradation and produces acetate, which contributes to gut barrier integrity (Arumugam et al., 2011; Eren et al., 2015; Maturana & Cárdenas, 2021; Sheridan et al., 2016). Its abundance has been positively associated with whole grain consumption (Martínez et al., 2013), suggesting dietary responsiveness. *Ruminococcus* contributes particularly to butyrate production and possesses a complex repertoire of genes involved in cellulose hydrolysis, reflecting adaptation to plant-rich diets; notably, within the literature, *R. bovis* and *R. champanellensis* have been linked to non-Western lifestyle patterns (Valentino et al., 2024). *Phocaeicola*, though variable in its effects,

can beneficially degrade complex polysaccharides into SCFAs and has been implicated in immune regulation, including anti-atherosclerotic effects, though it retains opportunistic pathogenic potential outside the gut (Nakashima et al., 2025). *Faecalibacterium*, a keystone taxon typically comprising 5–15% of the total microbiota in healthy individuals, is among the most significant butyrate producers in the gut; through this mechanism it fuels colonocyte energy metabolism, reinforces the gut epithelial barrier, and exerts anti-inflammatory effects (Zou et al., 2025).

Enterotype 2 was distinguished by elevated *Prevotella*, characteristic of agrarian, high-fiber, plant-heavy dietary patterns and more prevalent in non-Western populations (Yeoh et al., 2022). While *Prevotella* is a beneficial commensal adapted to fiber-rich substrates, its overrepresentation has been associated with rheumatoid arthritis, gut inflammation, and cardiovascular complications, again illustrating the fine line between commensalism and pathogenicity within the microbiome. Several taxa shared across both enterotypes — *Faecalibacterium*, *Blautia*, *Bacteroides*, and *Phocaeicola* — suggest a core functional microbiota that persists regardless of enterotype, with community-level differences likely reflecting proportional shifts rather than wholesale compositional divergence. These findings reinforce that enterotype classification can detect meaningful variation in the gut bacteriome even within a relatively homogenous sample like ours, and potentially capture ecologically and functionally variation in the gut bacteriome.

Alpha diversity differed significantly between enterotypes. Enterotype 2 demonstrated greater species richness and diversity than Enterotype 1, with a higher

mean number of observed species (190.15 ± 36.18 vs. 159.13 ± 40.84; $W = 5691$, $p < 0.001$) and a higher mean Shannon diversity index (3.97 ± 0.35 vs. 3.83 ± 0.31; $W = 7007$, $p < 0.001$). These differences suggest that the *Prevotella*-dominant gut community characteristic of Enterotype 2 supports a more diverse microbial ecosystem, consistent with its association with high-fiber, plant-rich dietary patterns that are known to promote microbial richness. These findings should be interpreted in the context of the unequal distribution between groups, with Enterotype 1 comprising approximately 71% of the sample ($n = 224$ vs. $n = 91$), which may affect the precision of estimates for Enterotype 2.

PERMANOVA analysis confirmed that overall microbial composition differed significantly between the two enterotypes ($R^2 = 0.04$, $F = 14.28$, $p = 0.001$). Although statistically significant, the effect size was modest, indicating that the enterotypes reflect shifts in relative abundance among shared taxa rather than completely distinct microbial ecosystems.

Group 2 Analysis

From the 315 participants with metagenomic sequencing data described earlier, we selected a subset of ten fecal samples for phthalate analysis. Five samples were drawn from individuals residing in neighborhoods with low Area Deprivation Index (ADI) scores and five from high-ADI neighborhoods. This proof-of-concept design allows us to evaluate and refine our analytical procedures for fecal phthalate detection before scaling to the full sample. Piloting the method on a small,

strategically selected subset optimizes laboratory protocols and analytical workflows, improving efficiency and cost-effectiveness as the study expands.

Detailed demographic and clinical characteristics of the ten selected participants are presented in Table 11. All samples are labeled with anonymized identifiers to preserve participant confidentiality. The mean age is 67.25 years. Seven participants are female and three are male. Eight participants identify as White and two as Black or African American. Mean years of education is 14.9. Consistent with the sampling design, five participants reside in low-ADI neighborhoods (ADI = 1) and five in high-ADI neighborhoods (ADI = 9 or 10). All participants are from Wisconsin.

Table 11 Geo-social and cognitive biomarkers in ten fecal samples from the Microbiome in Alzheimer's Risk Study (MARS).

	Sample 1	Sample 2	Sample 3	Sample 4	Sample 5	Sample 6	Sample 7	Sample 8	Sample 9	Sample 10
Sociodemographics										
Age	65.84	53.45	76.02	72.05	76.55	63.83	66.44	66.67	69.82	61.87
Sex	female	male	female	female	male	female	female	male	female	female
Race	white	white	black or AA	white	white	black or AA	white	white	white	white
Education	13	16	10	16	15	15	15	19	14	16
Geography										
ADI	1	9	10	9	1	1	10	1	1	9
State	WI	WI	WI	WI	WI	WI	WI	WI	WI	WI
Gut										
Bristol	5	4	4	4	4	3	3	4	3	4
BMI	28.33	34.67	41.79	32.15	26.39	44.72	26.57	23.11	27.89	33.81
MIND	7	4.5	5	9	10	8.5	10	7.5	10.5	6
MIND minus wine	6.5	4.5	5	9	9	8.5	10	7	10.5	6
Enterotype	1	2	1	2	2	1	1	1	1	2
Shannon Index	4.04	3.76	3.54	3.63	4.46	3.62	4.03	4.13	3.87	3.89
Observed Species	175	165	89	142	238	102	176	207	135	198
Brain										
Diagnosis	cog. normal	cog. normal	cog. normal	cog. normal	cog. normal	cog. normal	cog. normal	cog. normal	cog. normal	cog. normal
Plasma GFAP mean conc.	61.03	72.00	158.02	68.93	156.51	78.23	125.82	78.69	82.06	187.44
Plasma Nfl	13.11	5.03	9.63	13.14	25.82	15.08	18.47	12.13	11.12	14.91
Plasma ptau 217	0.20	0.21	0.18	0.34	0.23	0.23	0.23	0.50	0.20	0.95

Nine of ten participants have a Bristol Stool Form Scale classification within the ideal or normal range; one participant has a Bristol type 5 classification, which is slightly outside the typical range. The mean BMI is 31.94, indicating mild obesity on average. Dietary quality, assessed using the MIND diet score, averaged 7.8 (7.6 when wine intake is excluded). The total MIND diet score ranges from 0 to 15 and represents the sum of 15 component dietary indicators, with higher scores reflecting greater adherence to the MIND dietary pattern.

Based on enterotyping conducted on the full set of 315 samples, six participants in this subset are classified as Enterotype 1 and four as Enterotype 2. The mean Shannon diversity index is 3.90, and the average number of observed microbial species is 162.7. All participants were cognitively normal at the time of sample collection. Plasma biomarkers of neurodegeneration were also assessed: mean plasma glial fibrillary acidic protein (GFAP) was 106.87 pg/mL, mean plasma neurofilament light chain (NfL) was 13.84 pg/mL, and mean plasma phosphorylated tau 217 (p-tau217) was 0.33 pg/mL. Together, these measures provide a baseline characterization of neurodegenerative biomarker burden within this exploratory subset.

Phthalate analyses were conducted across all ten samples, with results summarized in Figure 6. Green circles indicate strong signal detection (i.e., base peak 3x background noise), yellow circles indicate trace detection (clear signal yet not necessarily 3x background noise), and gray circles indicate non-detection (far below E3). Prevalence within samples reflects the proportion of phthalates detected per

sample; prevalence across samples reflects the proportion of samples in which each phthalate was detected. Of the 19 phthalates screened, 14 were detected in at least one sample. The remaining five — diethyl phthalate, di-n-butyl phthalate, mono-n-butyl phthalate, mono-(2-ethylhexyl) phthalate, and mono-(2-ethyl-5-hydroxy-hexyl) phthalate — were not detected in any sample. Butylbenzyl phthalate was ubiquitous, present in all ten samples (100%), and di-(2-ethylhexyl) phthalate was nearly as prevalent, identified in 90% of samples.

Two samples warrant particular attention from a brain health standpoint. Sample 10 presented with the highest plasma GFAP concentration (187.44 pg/mL), the highest p-tau217 value (0.95 pg/mL), an ADI of 9, Enterotype 2 classification, and a within-sample phthalate prevalence of 47% — the second highest in the cohort. This convergence of adverse exposures and biomarker burden makes Sample 10 the most concerning profile in the pilot study. Sample 8, by contrast, resides in a low-deprivation area (ADI = 1), yet presents the second-highest p-tau217 at 0.50 pg/mL, illustrating that socioeconomic advantage does not confer straightforward protection from neurodegenerative pathology. Together, these two cases reinforce that no single geo-social variable cleanly predicts brain biomarker burden in this cohort, and raises the possibility that microbiome composition influences phthalate metabolism, neuroinflammatory signaling, or both.

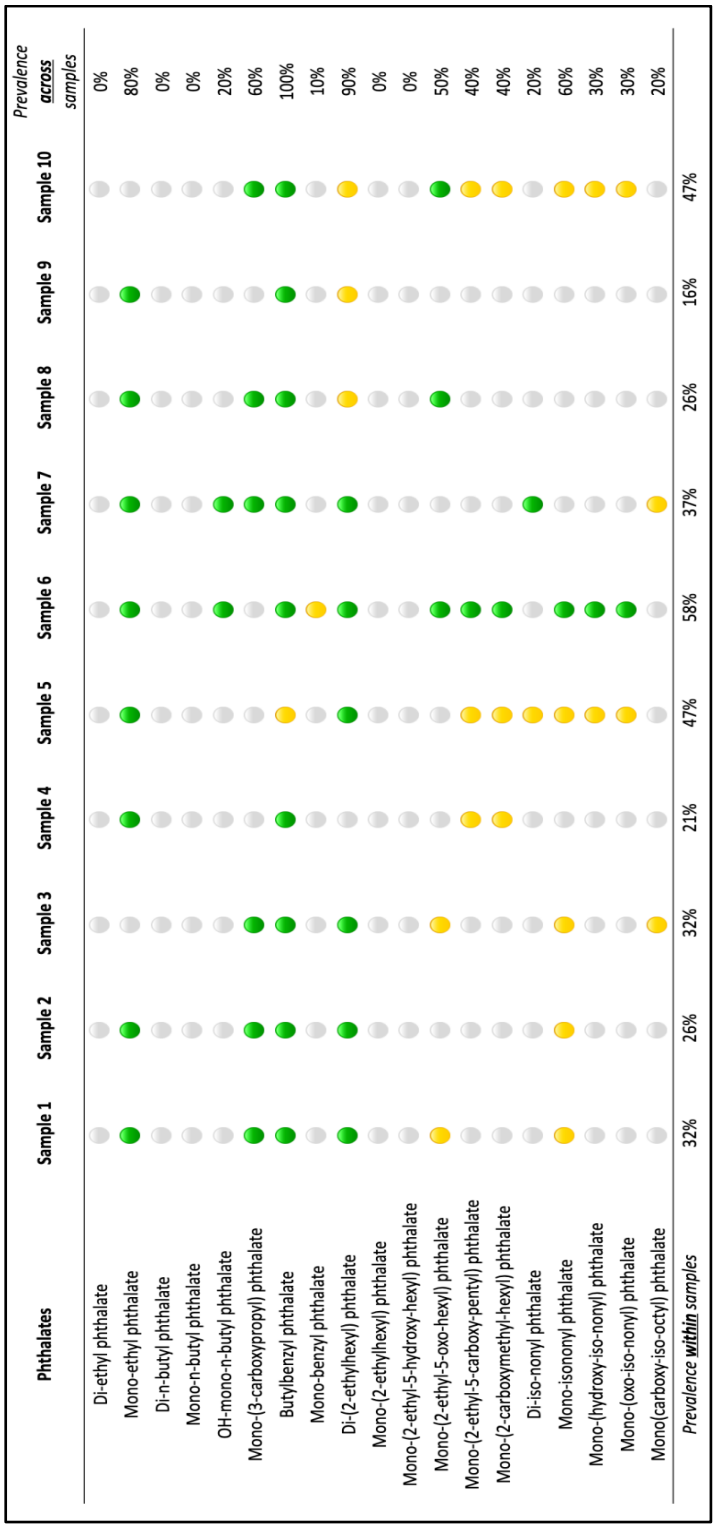

Figure 6 Detection of 19 phthalates in ten fecal samples from the Microbiome in Alzheimer's Risk Study (MARS (n = 10).. Green circles indicate strong signal, yellow circles indicate trace, and gray circles indicate non-detection.

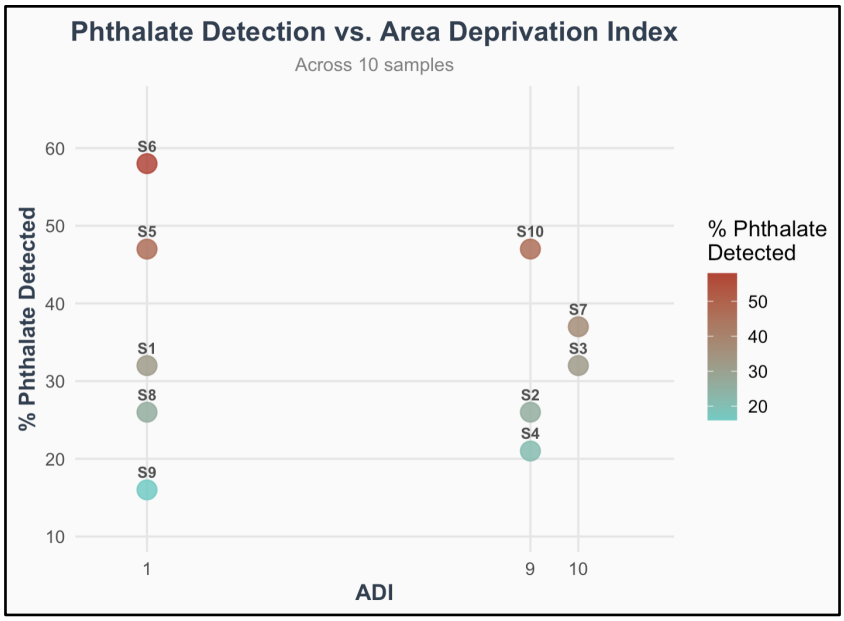

Figure 7 Percent phthalate detected stratified by ADI score. Microbiome in Alzheimer's Risk Study (MARS) (n = 10).

A notable pattern in this subset is that ADI level tracks with enterotype: participants in high-deprivation neighborhoods (ADI = 9 or 10) cluster into Enterotype 2, while low-deprivation participants (ADI = 1) are predominantly Enterotype 1. However, no corresponding gradient is apparent between ADI and phthalate prevalence (Figure 7). Low-ADI participants ranged from 16% to 58% in within-sample phthalate prevalence, while high-ADI participants ranged from 21% to 47%. While the N was quite small, the initial findings regarding the lack of a clean gradient may challenge the assumption that socioeconomic disadvantage is a primary driver of chemical exposure in this context, and suggests that future work should incorporate more granular exposure data including occupation and household product inventories and more measures that can address ways the body may build resilience, such as exercise, sleep, and stress levels.

Discussion

The gut microbiome is not a static entity; its composition is shaped by intrinsic and extrinsic forces including host physiology, genetics, health status, antibiotic exposure, and diet (Voreades, Kozil, & Weir, 2014; Pope et al., 2025). Most species within this ecosystem have the capacity to exert both beneficial and detrimental effects on the host, underscoring the context-dependent nature of host-microbiome relationships. The findings reported here address our three scientific questions concerning method optimization, gut microbiome characterization, and the relationships among phthalate exposure, microbiome composition, and brain health.

Method optimization and phthalate detection. The first research question asked whether fecal phthalate analysis methods could be optimized to reliably detect phthalates and their metabolites at concentrations exceeding methodological sensitivity thresholds, while minimizing contamination and storage-related bias. The analytical procedures successfully detected phthalates while addressing challenges related to storage conditions, environmental contamination, and signal validity, supporting the hypothesis that optimized methods can produce reliable fecal phthalate measurements. Two parent compounds — butylbenzyl phthalate (100% prevalence) and di-(2-ethylhexyl) phthalate (90% prevalence) — were detected across nearly all samples regardless of diet quality, microbiome enterotype, or neighborhood deprivation status. Their near-universal presence is consistent with their widespread use in food packaging, flooring materials, and personal care products, and suggests a shared environmental baseline exposure across this

Wisconsin population that ADI alone cannot capture. Within-sample prevalence ranged from 16% to 58%, with Sample 6 (ADI = 1, female, Black or African American) carrying the highest burden despite residing in a low-deprivation area — a pattern pointing toward exposure pathways, potentially occupational, dietary, or related to housing materials, that intersect in ways standard deprivation indices do not fully index.

An important interpretive question arising from this work is whether elevated fecal phthalate detection reflects greater exposure burden, more efficient elimination, or some combination of the two. While the ideal circumstance is no exposure and therefore no excretion, this is practically unattainable in an industrialized society. From an intervention standpoint, it may be most productive to focus on enhancing excretion and on fostering gut conditions that limit systemic absorption during intestinal transit — questions that larger follow-up studies should address directly.

Gut microbiome characterization. The second research question asked what gut microbiome profiles and microbial metabolite patterns characterize participants undergoing sequencing analysis. Distinct enterotype profiles emerged across the full cohort (n = 315): Enterotype 1 is characterized by *Bacteroides* dominance and Enterotype 2 by elevated *Prevotella* abundance, a distinction that mirrors well-documented dietary and lifestyle gradients in the literature. Notably, Enterotype 2 also demonstrated significantly greater alpha diversity and species richness compared to Enterotype 1. In the pilot subset, ADI tracked with enterotype, with high-deprivation participants clustering into Enterotype 2 and low-deprivation

participants predominantly classified as Enterotype 1. Together, these patterns support the hypothesis that meaningful variation in gut microbiome composition exists within the cohort, and position enterotype as a potential moderating variable for both phthalate metabolism and downstream brain health effects.

Exposure–microbiome–brain health relationships. The third research question asked whether fecal phthalate concentrations are associated with gut microbiome composition, geo-social factors, and brain health measures. The evidence partially supports the hypothesis that such associations exist, though the pilot sample size limits the strength of inference that can be drawn. Enterotype 2 samples tended toward higher p-tau217 values relative to Enterotype 1 samples, raising the possibility that microbiome composition influences phthalate metabolism, neuroinflammatory signaling, or both. Sample 10 in particular — combining Enterotype 2 membership with high phthalate burden, high ADI, and the most adverse brain biomarker profile in the cohort — may represent a convergence of gut-brain-environmental risk factors. While no causal inference can be drawn from a sample of ten, this pattern is consistent with emerging literature on the gut-brain axis and warrants longitudinal investigation. Shannon diversity and observed species counts did not show a clear gradient with phthalate burden or biomarker severity, though the sample size precludes ruling out such a relationship. MIND diet scores did not vary dramatically enough in this small sample to support firm conclusions; the relationship between dietary quality and phthalate metabolite burden nonetheless remains a compelling avenue for larger study.

Future directions. Taken together, the three research questions converge on a picture in which no single geo-social variable cleanly predicts brain biomarker burden, yet signs of convergent risk are apparent — a signal consistent with the gut-brain axis literature. These preliminary findings support a multi-factorial model of phthalate-related neurotoxic risk in which geographic deprivation, gut microbiome composition, sex, diet quality, and specific compound exposure each contribute in ways not reducible to any single variable. That the most concerning profile in this cohort — high ADI, high phthalate burden, Enterotype 2, and the highest plasma amyloid and neurodegeneration biomarker values — occurred in a cognitively normal individual underscores the value of early biomarker surveillance. Larger, longitudinal studies with more granular exposure characterization, including occupational history, household product inventories, and measures of biological resilience such as sleep, physical activity, and stress, will be essential to disentangle the directionality and relative contribution of these intersecting geo-social and biological factors.

Limitations & Conclusion

Social exposome, and the greater Brain Health Synercome (Baez et al., 2026), calls for a framework that captures whole-body health, addressing the social and physical exposome. Increasingly, research agendas are called to focus on structural and environmental influences, rather than single exposures. Identifying adversities across the life course helps provide context and direction for preventative efforts. Exposome research has the potential to inform both vulnerability and resilience approaches to cultivate greater, more equitable brain health (Baez et al., 2026).

Given that exposome research studies the dynamic interactions between body systems, social and physical exposures, and brain health measures, it is a behemoth of a research program. This paper is the tip of the iceberg for fecal phthalate analysis as it relates to brain health. Several limitations of this study warrant consideration. The first is that phthalate analysis was conducted on only 10 of the 315 participants in the MARS cohort for whom gut metagenomic sequencing data are available, to serve as a proof of concept for future studies. While this pilot subset was sufficient to evaluate analytical feasibility and generate preliminary observations, the sample size precludes any inferential statistical analysis, and no findings should be interpreted as generalizable beyond this group. Replication in the full cohort — or a substantially larger subset — is necessary before conclusions about exposure patterns, microbiome relationships, or brain biomarker associations can be drawn with confidence.

A central methodological challenge in this work is the near-absence of standardized protocols for measuring phthalate metabolites in human fecal material. Established analytical methods have been developed primarily for urine, and this study required adaptation of those urine-based protocols to a chemically and physically distinct and complex matrix, i.e., stool (Deda et al., 2015). The performance characteristics of these adapted methods — including extraction efficiency, metabolite recovery, and signal clarity — require additional evaluation, and some uncertainty remains regarding how well fecal phthalate measurements capture true exposure relative to urinary biomarkers. This limitation also reflects a broader gap in the field, and the

work presented here contributes directly to addressing it. More research is needed to better understand how body systems interact with and process phthalate chemicals, the possibility that some storage and elimination pathways may be more favored, and the acknowledgement of the variety of responses possible between individuals with the same exposures (Deda et al., 2015). We observed that when a parent compound was detected, the corresponding metabolite typically was not, and vice versa, which has implications for interpreting fecal versus urinary measures.

DEHP exposure estimation can illustrate these concerns. Di-(2-ethylhexyl) phthalate is a high-molecular-weight phthalate whose primary *urinary* metabolite, MEHP, represents only approximately 10% of the original DEHP dose (Heudorf et al., 2007). The oxidative metabolites, including MEOHP, MEHHP, and particularly 5cx-MEPP, provide substantially more accurate estimates of total DEHP exposure and offer the advantage of longer elimination half-lives, making them less sensitive to the rapid intestinal transit that can obscure time-weighted exposures (Koch et al., 2006). A priority for future work could be to simultaneously estimate parent phthalates and their metabolites in urine, feces, and sweat, capturing multiple matrices and allowing for comparison of quantification of the phthalates, giving insight into the different pathways they take within the body.

The ubiquity of phthalates in the environment introduced a persistent contamination risk throughout sample collection, processing, and analysis. To mitigate this, rigorous quality control procedures were employed, including procedural blanks, spiked samples, and controls distributed throughout the

analytical workflow. Nonetheless, the possibility of low-level contamination cannot be entirely excluded, and results should be interpreted with this in mind. Related to this, phthalate solubility is restricted to a narrow set of organic solvents, water is not among them, which affects extraction efficiency and may contribute to variability in chromatographic signal intensity across samples.

The fecal samples analyzed here were drawn from a biobank in which specimens have been stored frozen for variable durations, in some cases exceeding five years. Freeze-thaw history and storage duration may influence metabolite stability and the integrity of the fecal matrix, introduce additional uncertainty when comparing values across samples. The degree to which long-term frozen storage affects fecal phthalate metabolite recovery is not yet well characterized in the literature and represents a meaningful source of unmeasured variability. We carried out a brief experiment to determine if freezing the samples exerted an effect on the sample durability, as explained in the Data & Methods section. Our results showed that freezing samples did not reduce phthalate retention, but this was done in a controlled environment and stored for only a short time.

This pilot study demonstrates that measurement of phthalate metabolites in human fecal samples is analytically feasible and that fecal phthalate profiling holds meaningful promise as a complement to traditional urinary biomonitoring. By measuring metabolites directly in feces, this approach achieves closer temporal and biological alignment with gut microbiome composition than urinary analyses alone can offer. The ability to pair fecal phthalate data with existing metagenomic

sequencing data from the broader MARS cohort positions this work as a foundation for future investigation into the gut as both a site of phthalate metabolism and a potential mediator of downstream biological effects.

Preliminary observations in this pilot subset suggest that the relationship between geo-social factors and phthalate exposure is not straightforward. Area Deprivation Index did not predict within-sample phthalate burden in any consistent direction — samples from both low- and high-deprivation areas spanned a wide range of detected metabolites. Certain compounds, particularly butylbenzyl phthalate and di-(2-ethylhexyl) phthalate, were detected across nearly all samples regardless of socioeconomic context, reflecting the pervasive presence of these chemicals in shared consumer and food environments. These patterns suggest that exposure is shaped by a complex interplay of individual-level factors — including diet, lifestyle materials (housing, clothing, containers), occupation, and personal care product use — that standard deprivation indices do not adequately capture. Future analyses should incorporate more granular exposure characterization alongside structural geo-social measures.

At the individual level, the sample with the highest phthalate burden in this pilot also presented with the most elevated plasma GFAP, NfL, and ptau-217 values, as well as high area-level deprivation and Enterotype 2 gut microbiome classification. While no causal inference can be drawn from a pilot of this scale, this convergence is consistent with a hypothesis in which phthalate exposure, gut microbiome

composition, and geo-social stressors interact over time to contribute to neurobiological burden.

Borrowing from van der Kolk's observation that *the body keeps score,* we might extend this framing to suggest that the **brain**, too, keeps score — accumulating the biological consequences of environmental chemical exposures and structural inequalities across the life course. Testing this hypothesis rigorously will require longitudinal data, larger sample sizes, and integrative models that treat these exposures as co-occurring rather than independent.

In sum, this feasibility study establishes the groundwork for a novel research program linking fecal phthalate metabolomics, gut microbiome ecology, geo-social determinants, and brain health biomarkers in an aging cohort. The analytical challenges encountered and addressed here — matrix adaptation, contamination control, metabolite completeness — contribute practical knowledge to a field where standardized fecal methods are still nascent. Future work extending these analyses to the full MARS cohort (and other, more diverse cohorts), incorporating oxidative DEHP metabolites, and integrating urinary alongside fecal biomarkers will be essential to advancing understanding of how phthalate exposure shapes brain aging across diverse socioeconomic contexts.

CHAPTER 3

Environmental and Social Determinants of Cognitive Health in Puente Piedra, Peru

Authors:

Gabrielle Eva Husted[1], Eder Herrera Perez[3,4,5], Alexandra Chang Tamayo[7], Nilton Custodio[4,6], Elizabeth Ackert[1], Barbara Bendlin[9], Susan Cassels[1], Serggio Lanata[8], Monica Diaz[2]

[1] Department of Geography, University of California, Santa Barbara

[2] Department of Neurology, University of North Carolina at Chapel Hill School of Medicine

[3] Universidad San Ignacio de Loyola, Lima, Perú

[4] Unidad de Investigación, Instituto Peruano de Neurociencias, Lima, Perú

[5] Centro de Excelencia en Biotecnología e Investigación Traslacional, Lima, Perú

[6] Escuela Profesional de Medicina Humana, Universidad Privada San Juan Bautista, Lima, Perú

[7] Facultad de Ciencias de la Salud, Universidad Peruana de Ciencias Aplicadas, Lima, Perú

[8] Department of Neurology, Memory and Aging Center, University of California, San Francisco, San Francisco, CA

[9] Department of Geriatrics and Gerontology, University of Wisconsin, Madison

Highlights:

(max 85 characters/bullet point)

- Air pollution monitoring in Puente Piedra remains limited despite its dense population.
- Mixed micro- and macro-level data reveal unexpected cognitive health patterns.
- PM2.5 and PM10 show no significant association with cognitive function.
- Further proximity to major roads is significantly associated with poorer cognitive function.
- Cognitive impairment prevalence increased steadily as SES levels decreased.
- Findings highlight the need for improved pollution monitoring in disadvantaged areas.

Abstract

INTRODUCTION: In 2021, more than 60% of the 57 million people living with dementia worldwide resided in low- and middle-income countries (LMICs), a proportion expected to increase substantially as global populations age. Pollution has been identified as one of 12 modifiable risk factors for Alzheimer's disease and related dementias (ADRD) (Livingston et al., 2020), yet the environmental, social, and structural determinants of ADRD remain underexplored in LMICs. This study examines how pollution exposures, particularly air quality, and individual-level factors interact to influence cognitive impairment in Puente Piedra, a growing district in Lima, Peru with poor health indicators. **METHODS:** We analyzed secondary data from a door-to-door population-based study (n = 1,066) and publicly available atmospheric data from six PurpleAir sensors. Roadway data is accessed via QGIS, obtained through OpenStreetMap. The analytic sample included adults aged

30 years and older with measures of cognitive function and geolocated residence. Exposure variables included particulate matter (PM2.5 and PM10), temperature, humidity, and proximity to roads (log-transformed). Cognitive outcomes were assessed using the Peruvian version of the Rowland Universal Dementia Assessment Scale (RUDAS-PE) and Addenbrooke's Cognitive Examination (ACE), analyzed individually and as a combined indicator of cognitive impairment with or without functional impairment, assessed by the Pfeffer Functional Activities Questionnaire (PFAQ). Descriptive analyses, spatial buffer analysis, and logistic regression modeling were conducted to evaluate associations between environmental exposures and cognitive outcomes. **RESULTS:** No significant associations were observed between particulate matter (PM2.5 or PM10) and cognitive outcomes. However, proximity to roads was significantly associated with cognitive function, with the strongest relationship observed for ACE scores. Descriptive patterns indicated a counterintuitive gradient in which individuals living closer to roads had slightly better cognitive scores and lower rates of cognitive impairment. **DISCUSSION:** The null PM2.5 and PM10 findings likely reflect limited exposure contrast across only six sensor zones and possibly residual ecological confounding by unmeasured neighborhood-level factors not captured by individual SES adjustment. Proximity to roads showed a counterintuitive protective pattern consistent with urban access advantages in this peri-urban context, rather than traffic-related harm. Improved air quality monitoring and more detailed environmental data are needed to disentangle these dynamics to effectively inform public health interventions in rapidly urbanizing, resource-constrained settings.

Research in Context

Systematic Review: We searched PubMed and GoogleScholar using the terms (air pollution OR PM2.5 OR PM10 or particulate matter) AND (cognitive impairment OR dementia OR neurocognitive) AND (Latin America OR Peru OR low-and-middle-income countries) and focused on work from 2020 - 2026. We identified a limited but growing literature linking ambient particulate matter to cognitive outcomes. We did not find any studies using publicly available sensor-based exposure characterization linked to validated cognitive assessments in the northern Lima metropolitan area, nor Peru at large. **Interpretation**: This study found no statistically significant association between sensor-assigned PM2.5 or PM10 and cognitive impairment in a cross sectional survey population in Puente Piedra, Peru. The absence of an exposure gradient across six sensor zones – rather than a true null mechanistic biological effect – may explain this null result. Proximity to major roads was significantly associated with Addenbrooke's Cognitive Examination (ACE) scores in adults aged 30 - 59 (β -0.92, $p = 0.004$, age and sex adjusted), with the counterintuitive direction likely reflecting urban access advantages rather than pollution burden in this peri-urban context. **Future Directions**: Future studies in the urban periphery of Lima should deploy denser sensor networks or personal exposure monitors to generate individual-level exposure estimates based on activity spaces. Disentangling pollution from socio-economic access gradients requires simultaneous fine-grained measurement of both environmental exposures and social determinants of health. Indoor air quality monitoring and wearable mobility data would further improve exposure characterization in settings where time spent indoors and commuting patterns substantially modify true exposure.

Introduction

Dementia represents one of the most urgent global health challenges of the twenty-first century. The World Health Organization estimates that 55 million people are currently living with dementia worldwide, with approximately 60% residing in low- and middle-income countries (LMICs) (World Health Organization, 2021a). If current trajectories continue without intervention, this figure is expected to rise to 71% of cases living in LMICs. Diagnosis and service gaps are substantially more severe in LMICs than high-income countries (HICs): some estimates suggest that up to 90% of dementia cases in LMICs go undiagnosed, compared to 20-50% in HICs (*Dementia Statistics*, 2021). Community-based dementia services are more than 19% more prevalent in HICs than in LMICs, and up to 51% more prevalent than in rural LMIC settings (*Dementia Statistics*, 2021).

Particulate matter (PM) refers to tiny solid particles and liquid droplets suspended in the air; they are classified by size in micrometers ($\mu g/m^3$). PM10 includes particles 10 micrometers or smaller, often originating from dust, construction, agriculture, pollen, and mining waste. PM2.5 includes finer particles sized 2.5 micrometers or smaller, which is about 30 times thinner than a human hair. Typical sources of PM2.5 are combustion sources like vehicles, wildfires, power plants, and industrial activity. A key difference between the two are the pathways in which they can negatively impact health; PM10 particles can be inhaled through the nose and throat and irritate the respiratory tract, however, the body's natural defense systems can often filter them out effectively. In contrast, PM2.5 is far more dangerous because it can penetrate the alveoli of lungs, the bloodstream, and even the integrity of the

blood brain barrier (Arias-Pérez et al., 2020; Butler et al., 2025; Gimeno-Ferrer et al., 2026; B. Zhang, Weuve, et al., 2023). A substantial epidemiological literature from North America, Europe, and East Asia examine pollution exposure as it relates to health outcomes, emphasizing the role of pollution in cardiac, respiratory, immune, and neurological health (D. Chen et al., 2025; B. Zhang, Langa, et al., 2023; B. Zhang, Weuve, et al., 2023; Zheng et al., 2025). Increasingly, research is linking exposure to PM2.5 and PM10 in Latin America with accelerated cognitive aging, mild cognitive impairment, and dementia (Carrasco-Escobar et al., 2020; Moguilner et al., 2024; Parra et al., 2021; Porta et al., 2018; Steenland et al., 2022; Tapia et al., 2020; Warren et al., 2021; Zegarra-Valdivia et al., 2025). However, this research is underexplored, and LMIC, including Latin American countries (LAC), are under-represented. A 2022 systematic review found that pooled all-cause dementia prevalence in the LAC region was 10.7%, with higher rates among women, rural residents, and those without formal education (Ribeiro et al., 2022). To help fill this gap, this paper examines ambient air pollution and particulate matter (PM) as a potentially modifiable risk factor for cognitive impairment and dementia in an under-represented, peri-urban community outside of Lima — one with both a documented higher-than-expected rate of neurocognitive disorders and a large proportion of residents without formal education (Herrera-Perez et al., 2023).

Peru's capital, Lima, is one of the most polluted cities in Latin America, with pollution driven primarily by traffic and industrial activity (*Air Quality Database*, n.d.; *Informe Nacional de La Calidad Del Aire 2013 - 2014*, n.d.). Within Lima's 43 districts, Puente Piedra, which is in the northern metropolitan cone, is among the

most socially and economically vulnerable (Herrera-Perez et al., 2023). The district sits at approximately 237 meters elevation in a peri-urban zone characterized by rapid population growth, limited regulatory air quality monitoring, and high concentrations of informal economic activity including brick kilns and heavy vehicle traffic along the Panamericana Norte (Herrera-Perez et al., 2023). A geospatial analysis of Lima's pollution landscape designated Puente Piedra as a high-risk area, with estimated PM2.5 concentrations of 30 $\mu g/m^3$ (5 $\mu g/m^3$ annual mean is the WHO target) and PM10 concentrations of 60 $\mu g/m^3$ (15 $\mu g/m^3$ annual mean is the WHO target) and exposure of approximately 100,000 vulnerable residents (Romero-Baylón et al., 2024).

Two critical research gaps converge in Puente Piedra: (1) air pollution-cognition research has focused mostly on high-income populations with regulatory-grade monitoring, and (2) environmental exposures as determinants of dementia in Latin America remain understudied. This paper addresses both simultaneously. We use a network of publicly available low-cost PurpleAir citizen-science sensors independently deployed across and around the district, linking them to validated cognitive assessments in a community-based sample of 1,066 adults. We address three research questions: (RQ1) whether ambient PM2.5, PM10, temperature, and humidity are associated with cognitive impairment among adults in Puente Piedra; (RQ2) whether residential proximity to major roads is independently associated with cognitive impairment; and (RQ3) whether socioeconomic status confounds or modifies the relationship between environmental exposures and cognitive outcomes. We hypothesize that higher PM2.5 and PM10 concentrations, along with adverse meteorological conditions, will be associated with increased cognitive impairment

and lower scores on the RUDAS-PE and ACE-III (H1); that closer residential proximity to major roads will similarly predict poorer cognitive outcomes, reflecting greater traffic-related exposure burden (H2); and that these associations will vary by socioeconomic status, with individuals of lower SES experiencing greater cognitive vulnerability to environmental exposures (H3). Beyond their local implications, our findings speak to the methodological challenges of conducting environmental epidemiology in under-resourced settings and to the urgent need for more granular, equitably distributed atmospheric monitoring in the communities that bear the greatest pollution burden.

Methods

Study Site and Participants

This analysis uses data from a 2022 cross-sectional, door-to-door neuroepidemiological study conducted in Puente Piedra, Lima, Peru, using two-stage household cluster sampling, described in detail elsewhere (Herrera-Perez et al., 2023). Participants were adults aged 30 years or older residing in sampled "conglomerados" (similar to census tracts or block groups) across the district. The final analytical sample comprised 1,066 participants: 313 older adults aged 60-95 years (mean age: 69 ± 7) assessed with the Peruvian Version of the Rowland Universal Dementia Scale (RUDAS-PE), and 753 younger adults aged 30-59 years (mean age: 43± 9) assessed with the Addenbrooke's Cognitive Examination-III (ACE-III). Full sociodemographic and health data were collected during in-person household interviews.

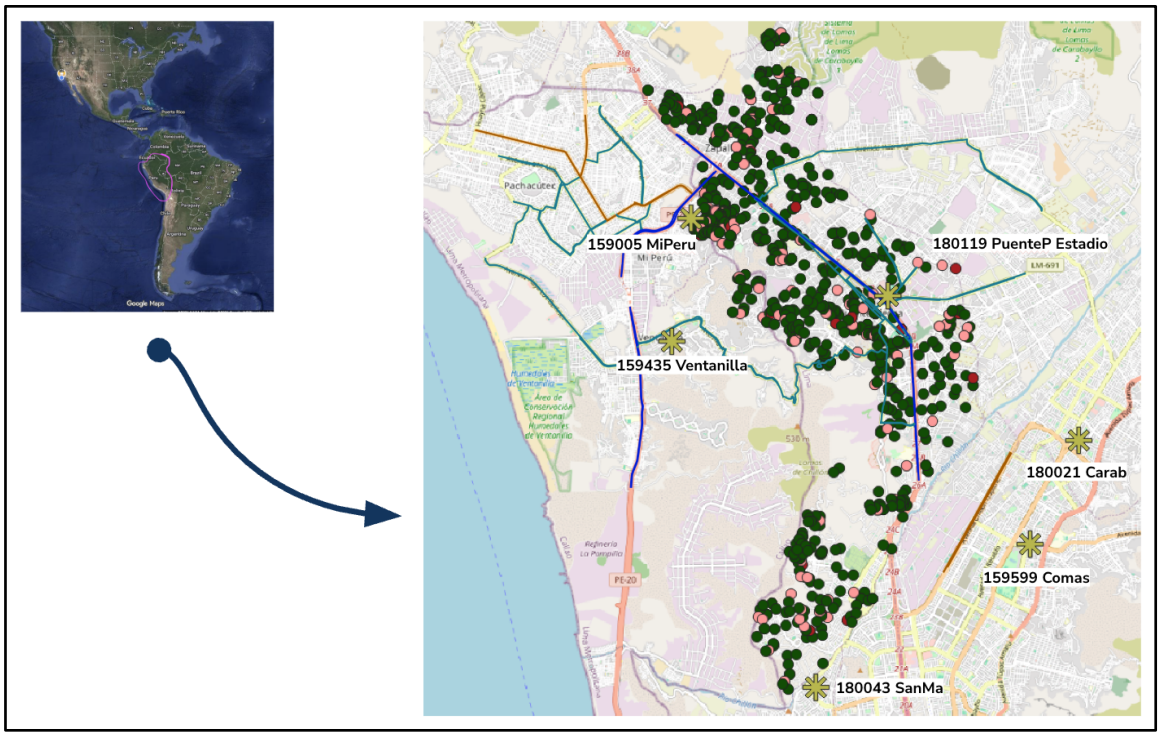

Figure 8 Map of study area and participant locations, colored by cognitive status. RED = dementia, PINK = mild cognitive impairment, GREEN = healthy. Asterisk = sensor. Participants (n=1,066), Sensors (n = 6).

PurpleAir Sensor Network and Exposure Characterization

Ambient air quality data were obtained from a network of six PurpleAir low-cost optical particle sensors (sensor IDs: 159005, 159435, 159599, 180021, 180043, 180119) deployed in the vicinity of the study area (*PurpleAir in Research*, n.d.). Figure 8 depicts a Google map locating Peru within South America and QGIS map of the study area, Puente Piedra in Lima, Peru. The map indicates locations of participants and their cognitive status. Red represents participants with cognitive impairment with functional compromise (dementia), pink represents participants with cognitive impairment *without* functional compromise (mild cognitive impairment), and green represents participants that are cognitively healthy. The green asterisk marks the locations of the sensors. PurpleAir sensors use laser light scattering to measure airborne particle concentrations, generating PM2.5 and PM10

readings from two independent internal channels (A and B). The exact range of each sensor depends on local weather and wind patterns, but the estimated coverage is about 50-100 meters. Previous research using PurpleAir sensors has demonstrated their potential to enhance air quality monitoring by complementing regulatory networks, supporting Sustainable Development Goals related to reducing air pollution, reliably capturing particulate matter variation in urban environments, and empowering local communities to address environmental health concerns (Stavroulas et al., 2020; Keyes et al., 2023; Wallace and Zhao, 2023; Lassalle, 2024). All data were downloaded via the PurpleAir Historical Data Download Tool for the period January 2022 through January 2026 using 43,200-minute (30-day) averaging intervals (Table 12). Due to sparse coverage of air quality data for our survey timeframe, we have gathered average levels of air pollution over multiple years, allowing our exposure measures to serve as a proxy for typical exposure within the district, based on six sensors present for any period of time from 2022 (when the cross-sectional study data was collected) to 2025 (when we began this paper).

Table 12 Description of each sensor; PurpleAir ID, PurpleAir sensor name (shortened), available data timeframe, and the number of participants in our sample located nearest each sensor.

Nearest Sensor ID	**Nearest Sensor Name**	**Coverage**	**n**
180119	PuenteP Estadio	Jul 2023-Dec 2025	361
159005	MiPeru	Mid 2024-Dec 2025	501
180043	SanMa	2024-Dec 2025	127
159599	Comas	2024-Dec 2025	54
159435	Ventanilla	Mid 2024-Dec 2025	19
180021	Carab	Mid 2024-Dec 2025	4

Before linking sensor data to participants, we validated sensor performance using internal A/B channel agreement. PurpleAir sensors contain two independent laser counters (channels A and B) that measure simultaneously, and agreement between them serves as a quality control indicator. The Environmental Protection Agency (EPA) recommends flagging sensors when the absolute PM2.5 difference exceeds 5 μg/m³ or the percent difference exceeds ~70%, though at the mean concentrations observed in this study (~30–40 μg/m³), a 5 μg/m³ discrepancy represents only ~13–17%, suggesting large absolute differences are more detrimental to interpretation at lower concentration ranges. Observations were excluded when absolute disagreement between channels exceeded 5 μg/m³ or relative disagreement exceeded 70%. Our monthly mean values from channels A and B were compared for each sensor (see Figure 9). Sensor 159005 (MiPeru) showed the greatest temporal variability in A-B channel agreement across the monitoring period, which may reflect sensor maintenance issues or environmental contamination given its location in a historically informal settlement. Sensitivity analyses using alternative thresholds (2-20 μg/m³ absolute; 25-100% relative) produced similar exposure estimates, confirming robustness of our approach.

Post-QC sensor means were computed across the full monitoring period for each sensor: PM2.5, PM10, temperature, and humidity. Sensor geographic coordinates were obtained via the PurpleAir API, as coordinates are not included in the historical data download. Each participant was assigned the mean average exposure values of the sensor nearest their location (unique composite ID derived from sector +

"conglomerado"), determined by a nearest-feature spatial join using projected coordinates (UTM Zone 18S, EPSG:32718). Every participant was assigned a sensor based on which one of the six available were closest to them; no cutoffs were employed. All four sensor-derived variables — PM2.5, PM10, temperature, and humidity — were examined as exposures, each modeled separately given high collinearity across sensor-zone-assigned variables. Sensor coverage across the 1,066 participants sample was uneven: the two primary sensors (MiPeru and PuenteP Estadio) covered 501 and 361 participants respectively, with the remaining four sensors covering between 4 and 127 participants.

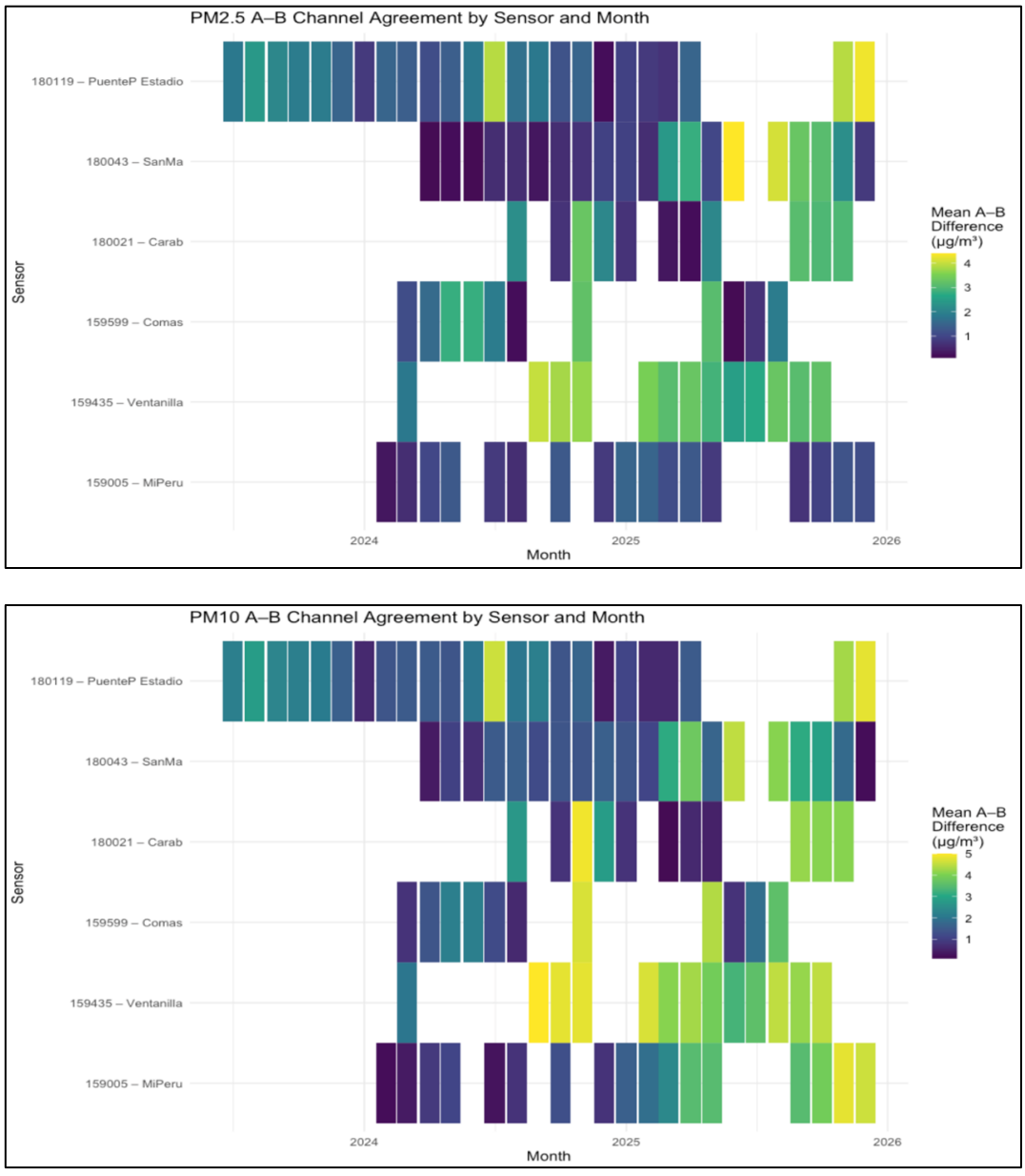

Figure 9 A-B Channel Agreement Heatmaps (PM2.5 and PM10) across six sensors, 2022-2026. Darker purple indicated lower disagreement (higher reliability); yellow-green indicates greater channel divergence.

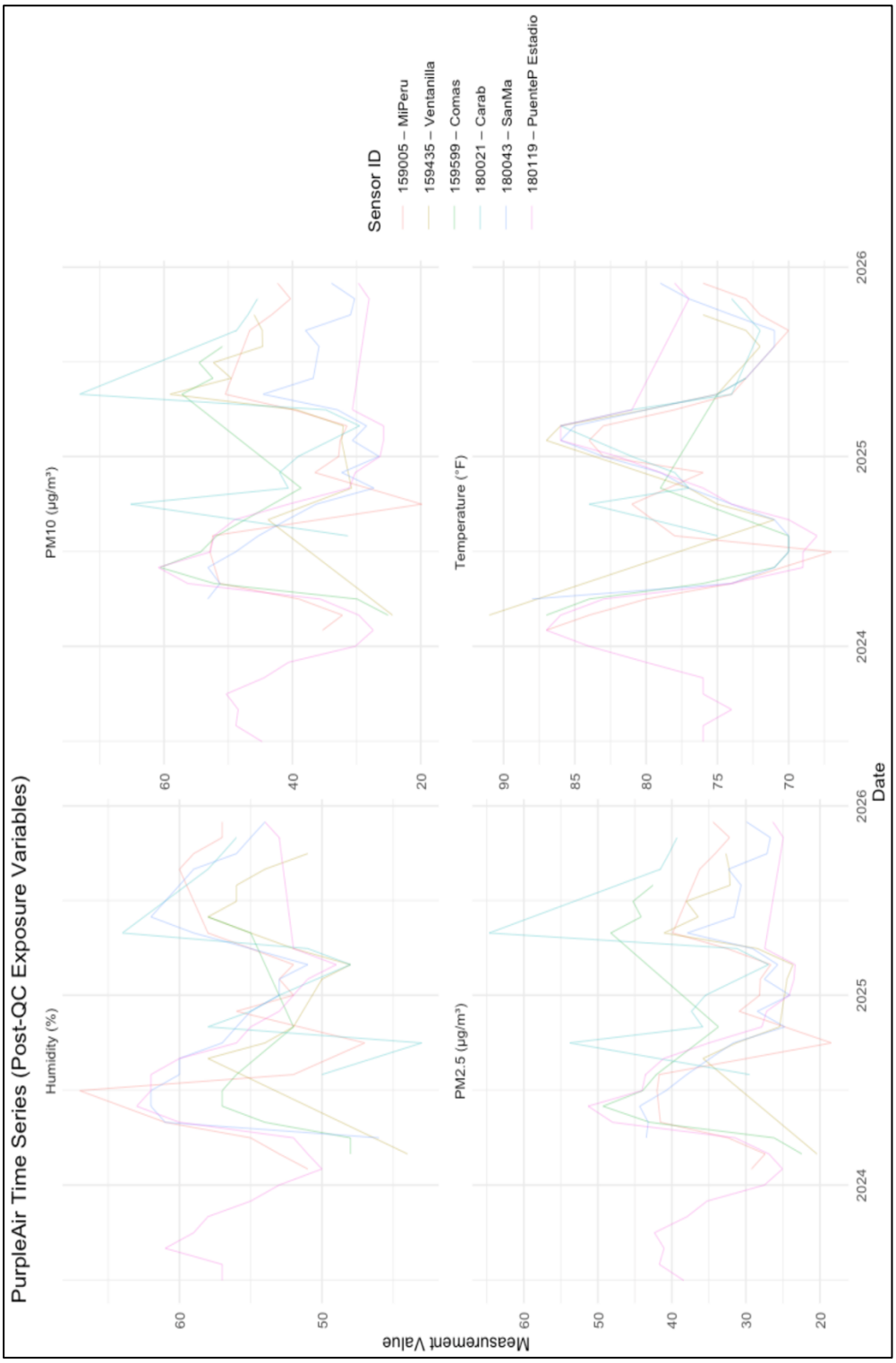

Figure 10 PurpleAir Time Series (1st-99th percentile) PM2.5, PM10, temperature, and humidity across six sensors, post-QC.

Mean PM2.5 across sensors ranged from 30.9 to 40.1 μg/m³, a difference of approximately 9 μg/m³. To contextualize this, the WHO 2021 annual mean guideline for PM2.5 is 5 μg/m³, with interim targets (IT) set at 35 μg/m³ (IT1) and 25 μg/m³ (IT2) for settings where the guideline is not yet achievable. All sensors in our study area fell beyond the IT1 and IT2 thresholds, indicating uniformly elevated exposure across participants. The PurpleAir Time Series plot presenting PM2.5, PM 10, temperature, and humidity across the six PurpleAir sensors is in Figure 10. Sensor 180021 had the highest mean PM2.5 (39.6 μg/m³), but contributed only 4 participants to the analytic sample and therefore had negligible influence on model estimates. The two sensors covering the majority of participants (n=501, mean 32.7 μg/m³; n=361, mean 34.0 μg/m³) differed by only 1.3 μg/m³. Temperature and humidity were similarly compressed, ranging 75.7–77.8°F and 52.9–56.8% respectively. However, this apparent spatial homogeneity likely reflects a limitation of the sensor network rather than the true pollution environment. Within the literature, Puente Piedra is identified as among the highest-variability districts in metropolitan Lima, with PM concentrations fluctuating substantially by time of day, season, and local meteorological conditions (Warren et al., 2021). Annual mean sensor averages, as used here, smooth over this within-zone temporal variability, potentially obscuring meaningful exposure contrasts that finer-grained temporal or individual spatial monitoring would capture.

Road Proximity

OpenStreetMap road data for the study area were exported from QGIS as a geopackage. Road features classified as trunk, primary, or secondary were retained

(n=345 features: trunk = 83, primary = 22, secondary = 240), representing the major road network. Euclidean distance from each participant's conglomerate centroid to the nearest major road feature was computed using the *sf* package in R after reprojection to UTM Zone 18S. The resulting distance variable ranged from 9 meters to 4.5 km (median 674m, mean 1,001m), with a right-skewed distribution indicating the need for log-transformation. Road exposure was operationalized using log(distance + 1) to the nearest road of any classification, with additional binary indicators for proximity within 100m and 500m.

Socioeconomic Status

Socioeconomic status (SES) was operationalized using the Nivel Socioeconómico (NSE) classification, a composite index developed by Ipsos and administered by the Peruvian Association of Market Intelligence Companies (APEIM). The NSE assigns households to one of five levels — A (highest) through E (lowest) — based on a weighted scoring system that draws on multiple structural and household variables, including the education level of the head of household, asset ownership, access to services such as private health insurance, and housing characteristics. Because each household receives a total score that determines its classification, the levels are mutually exclusive but not defined by any single criterion. The NSE is primarily a structural and material classification, distinct from the monetary poverty measure tracked by INEI; a household's level reflects its assets and access to services rather than its income or expenditure directly. The approximate asset profiles associated with each level are:

- NSE A = household head has higher education; owns a car for personal use; has private health insurance
- NSE B = owns a computer/laptop and has home internet access
- NSE C = owns a refrigerator or washing machine
- NSE D = has a bathroom connected to public sewage
- NSE E = unable to cover monthly cost of basic food and necessities

Cognitive Outcomes

Three cognitive outcomes were operationalized. The primary outcome was a binary variable derived from the dementia classification variable for the full sample coded "0" for no cognitive impairment (cognitively healthy) and "1" for cognitive impairment both with or without functional impairment. Cognitive impairment without functional impairment is considered mild cognitive impairment (MCI) and cognitive impairment with functional impairment is considered dementia Alzheimer's Foundation of America, n.d.). Functional impairment was assessed with the Pfeffer Functional Activities Questionnaire (PFAQ) instrument (Pfeffer et al., 1982). For older adults (60+), the RUDAS-PE score was used as a continuous outcome (scored 0-30; lower scores indicate greater impairment). For younger adults (30-59), the ACE-III total score was used as a continuous outcome (scored 0-100). Classification cutoffs were: in younger adults, ACE-III <70 indicated cognitive decline; in older adults RUDAS-PE scores of ≤ 23 and ≤ 19 distinguished possible mild cognitive impairment and possible major neurocognitive disorder (dementia) respectively (Herrera-Perez et al., 2023).

RUDAS-PE is a multiculturally valid cognitive assessment tool designed to be less influenced by education or language (Custodio et al., 2021). It has a total score of 30 and a score of 22 or less suggests cognitive impairment. It assesses memory, body orientation, praxis (planning/coordination), drawing, judgement, and language (Vara et al., 2022).

ACE-III is a comprehensive and widely used screening tool for detecting dementia and early cognitive impairment. It is scored out of 100, with higher scores indicating better cognitive functioning. It captures five domains: attention/orientation, memory, fluency, language, and visuospatial function. It takes about 20 minutes to administer (Bruno & Schurmann Vignaga, 2019).

The Pfeffer Functional Activities Questionnaire (PFAQ) is an instrument completed by the patient's caregiver or family member to assess competency with tasks like managing finances, shopping, transportation, and remembering appointments(Pfeffer et al., 1982). It takes about ten minutes to administer. Total scores range from 0 to 30, with higher scores indicating higher levels of impairment.

Statistical Analysis

Descriptive statistics were computed for all participant characteristics, exposure variables, and cognitive outcomes, stratified by sensor zone and SES level. For the primary binary outcome, logistic regression models were fit using the full analytic sample. For continuous outcomes, linear regression models were fit separately for older adults (RUDAS-PE) and younger adults (ACE).

All four sensor-derived environmental variables – PM2.5, PM10, temperature, humidity – were examined as exposures alongside log-distance to nearest road, with each entered separately as the primary predictor given high collinearity across sensor-zone-assigned variables (variance inflation factors (VIF) exceeded 5 for humidity and 10 for PM10 in a fully adjusted model; common convention is to keep VIF below 5). Exposures were standardized (mean = 0, SD = 1) to facilitate comparison in forest plots. Models were fit in three stages: unadjusted, adjusted for age and sex, and fully adjusted for age, sex, SES, BMI, education, civil status, occupation, hypertension, glucose level, and chronic disease status – all selected a priori based on established confounders in cognitive epidemiology and availability within our sample (Livingston et al., 2020).

To account for the nested structure of the data — participants clustered within "conglomerados" nested within sectors — a unique composite cluster ID was derived from sector and "conglomerado" identifiers, and cluster-robust standard errors were applied to all models. To assess potential spatial confounding, sociodemographic and health characteristics were tested across sensor zones using chi-square and Kruskal-Wallis tests (categorical variables, with Monte Carlo p values due to small expected cell counts in some zones); no significant differences were observed (all $p > 0.10$; Supplementary Table 1), indicating that the zones were comparable in baseline characteristics..

Spearman correlations between road distance and all sociodemographic variables were additionally computed to assess the strength of associations between road proximity and measured covariates. Road proximity findings were examined in sensitivity analyses stratified by road classification (trunk, primary, secondary) and an interaction term between road proximity and SES was tested to assess effect modification.

All analyses were conducted in R (Version 2026.01.1+403).

Results

Sample Characteristics

The analytic sample includes 1,066 participants across five sectors of Puente Piedra. Overall, 14.9% of the sample met criteria for cognitive impairment (including both with and without functional impairment). The older adult subsample (ages 60-95 years; mean age 69 ± 7) included 328 individuals assessed with RUDAS-PE, and the younger adult subsample (ages 30-59 years; mean age 43 ± 9) included 753 individuals assessed with ACE-III. The sample was predominantly female (69.9%), with a mean age of 50.8 years and mean BMI of 28.8. Approximately 25.7% had hypertension, and 37.4% reported a chronic disease. The majority (57.1%) were enrolled in Seguro Integral de Salud (SIS), Peru's government-subsidized public health insurance program. In terms of socioeconomic status, the largest proportion were classified as level of B (45.7%, e.g., owning a laptop/PC or microwave), followed

by NSE C (31.8% e.g., owning a refrigerator or washing machine). Full descriptive statistics are presented in Table 13.

Table 13 Participant characteristics and environmental exposures (n = 1,066).

Panel A: Sociodemographic and Health Characteristics		
Variable	**% or Mean (SD)**	**n**
Age, mean (SD)	50.8	1,066
Sex		
Male	30.1	321
Female	69.9	745
Education		
None	5.1	54
Primary	27.9	297
Secondary or higher	67.1	715
Civil Status		
Partnered	63.3	675
Single	20.4	217
Separated/Widowed	16.2	173
Occupation		
Employed	43.5	464
Homemaker	33.6	358
Not employed	22.8	243
BMI, mean (SD)	28.8	
Hypertension		
Yes	25.7	274
No	74.2	791
Native language		
Castellano	79.5	848
Quechua o Aimara	20.5	218

Health Insurance		
SIS	57.1	609
Essalud	21.0	224
Uninsured	14.4	154
Other	7.4	79
Chronic Disease		
Yes	37.4	399
No	62.6	667
Socio-economic Status Level		
NSE A (highest)	7.3	78
NSE B	45.7	487
NSE C	31.8	339
NSE D	8.7	93
NSE E (lowest)	5.6	60
Panel B: Environmental Exposures and Cognitive Outcomes		
Variable	**Mean (SD)**	**n**
Environmental Exposures		
PM 2.5 μg/m³	33.5 (1.7)	1,066
PM 10 μg/m³	39.9 (2.0)	1,066
Temperature, °F	77.4 (0.6)	1,066
Humidity, %	55.6 (0.7)	1,066
Distance to nearest road, m	1,001 (674)	1,066
Cognitive Outcomes		
Dementia		
Yes	14.9	159
No	85.1	907

ACE score, mean (SD)*	78.8 (11.3)	753
RUDAS-PE score, mean (SD)*	23.8 (3.3)	328**
ACE administered to adults aged 30–59 (n=753);* RUDAS-PE *administered to adults aged 60+ (n=313)* * Some younger adults (30-59) also have* RUDAS-PE *scores, however, our later models will correctly use 313 (i.e., adults aged 60+ as the denominator for our* RUDAS-PE *models*		

Sensor Zone Characteristics

Exposure assignment was dominated by two sensors: MiPeru (n = 501, PM2.5 = 32.7 μg/m^3) and PuenteP Estadio (n = 361, PM2.5 = 34.0 μg/m^3) together covered 862 of 1,066 participants (81%). The remaining four sensors each covered between 4 and 127 participants, with Carab (n = 4) and Ventanilla (n = 19) having sample sizes too small for meaningful inference. Sensor-averaged PM2.5 across the monitoring period ranged from 30.9 to 40.1 μg/m^3 across the six sensor zones, all exceeding the WHO 2021 annual PM2.5 guideline (World Health Organization, 2021b) of 5 μg/m^3, and most fall within the “Moderate” to “Unhealthy for Sensitive Groups” range of U.S. Environmental Protection Agency (EPA) Air Quality Index (AQI). Full exposure and cognitive outcome distributions by sensor zone are presented in Table 2. Full descriptive exposure and cognitive outcomes by PurpleAir sensor zone are presented in Table 14. % CI = percentage of participants meeting criteria for cognitive impairment. RUDAS-PE score (max 30) was administered to adults aged 60 and older; ACE score (max 100) to adults aged 30–59.

Table 14 Exposure measures and cognitive outcomes by PurpleAir sensor zone.

Panel A: Main Exposure Measures

Sensor ID	Sensor Name	n	PM 2.5 (µg/m³)	PM 10 (µg/m³)	Temperature (µg/m³)	Humidity (µg/m³)
180021	Carab	4	39.6	45.2	77.7	53.9
159005	MiPeru	501	32.7	39.9	77.6	55.6
180119	Puente P Estadio	361	34	39.2	77.8	55.6
180043	SanMa	127	32.6	37.9	76.4	56.8
159435	Ventanilla	19	30.9	41.3	77.7	53
159599	Comas	54	40.1	48	75.7	53.8

Panel B: Road Exposure Measures

Sensor ID	Sensor Name	n	Mean Distance to Any Road (m)	Trunk Roads (m)	Primary Roads (m)	Secondary Roads (m)
180021	Carab	4	1161	1161	1602	1332
159005	MiPeru	501	888	1059	1887	1029
180119	Puente P Estadio	361	408	851	3705	431
180043	SanMa	127	3200	3681	3291	4287
159435	Ventanilla	19	1112	1999	3102	1112
159599	Comas	54	796	807	1792	1760

Sensor ID	Sensor Name	n	% Cognitive Impairment	Mean (SD) RUDAS-PE	Mean (SD) ACE	
180021	Carab	4	25	NA	73.0 (8.7)	
159005	MiPeru	501	15.4	24.1 (3.3)	78.6 (11.2)	
180119	Puente P Estadio	361	14.7	23.6 (3.3)	79.5 (11.5)	
180043	SanMa	127	15.7	23.2 (3.7)	78.1 (11.9)	
159435	Ventanilla	19	15.8	24.5 (3.5)	78.6 (10.4)	
159599	Comas	54	9.3	24.5 (2.9)	79.2 (10.7)	

Note: A participant is noted as cognitively impaired if they meet criteria for dementia or mild cognitive impairment. (RUDAS-PE score (max 30) was administered to adults aged 60 and older;

ACE score (max 100) to adults aged 30–59.

Average covariate characteristics across sensor zones were broadly comparable. No significant differences were observed across any sociodemographic or health characteristic (all p > 0.10; Table 15) supporting the assumption that exposure was not systematically associated with participant characteristics.

Table 15 Comparison of socio-demographic and cognitive measures across six PurpleAir Sensor locations.

Characteristic	N	Carab N = 4	Comas N = 54	MiPeru N = 501	PuenteP Estadio N = 361	SanMa N = 127	Ventanilla N = 19	P Value
Age	1,066	55.0 (14.9)	52.2 (14.8)	50.6 (14.8)	51.5 (14.0)	49.8 (14.4)	46.5 (13.8)	0.5
Sex	1,066							0.4
Females		3 (75%)	40 (74%)	351 (70%)	241 (67%)	94 (74%)	16 (84%)	
Males		1 (25%)	14 (26%)	150 (30%)	120 (33%)	33 (26%)	3 (16%)	
ACE score		73.0 (8.7)	79.2 (10.7)	78.6 (11.2)	79.5 (11.5)	78.1 (11.9)	78.6 (10.4)	0.6
RUDAS		NA (NA)	24.5 (2.9)	24.1 (3.3)	23.6 (3.3)	23.2 (3.7)	24.5 (3.5)	0.5
Education	1,066							0.2
None		0 (0%)	5 (9.3%)	26 (5.2%)	13 (3.6%)	10 (7.9%)	0 (0%)	
Primary		1 (25%)	18 (33%)	148 (30%)	98 (27%)	25 (20%)	7 (37%)	
Secondary or higher		3 (75%)	31 (57%)	327 (65%)	250 (69%)	92 (72%)	12 (63%)	
Civil Status	1,065							0.5
Partnered		3 (75%)	30 (56%)	320 (64%)	225 (63%)	88 (69%)	9 (47%)	
Single		0 (0%)	15 (28%)	103 (21%)	74 (21%)	19 (15%)	6 (32%)	
Separated or widowed		1 (25%)	9 (17%)	78 (16%)	61 (17%)	20 (16%)	4 (21%)	
BMI	1,061	26.3 (2.2)	28.1 (4.8)	29.0 (5.1)	28.7 (4.9)	28.7 (4.5)	30.8 (6.1)	0.2
Hypertension	1,065							0.5

None		4 (100%)	44 (81%)	367 (73%)	261 (72%)	100 (79%)	15 (79%)	
Hypertension		0 (0%)	10 (19%)	133 (27%)	100 (28%)	27 (21%)	4 (21%)	
Native Lanugage	1,066							0.4
Castellano		4 (100%)	41 (76%)	407 (81%)	288 (80%)	95 (75%)	13 (68%)	
Quechua o Aimara		0 (0%)	13 (24%)	94 (19%)	73 (20%)	32 (25%)	6 (32%)	
Health Insurance	1,066							0.2
SIS		1 (25%)	37 (69%)	293 (58%)	188 (52%)	79 (62%)	11 (58%)	
Essalud		3 (75%)	8 (15%)	102 (20%)	89 (25%)	18 (14%)	4 (21%)	
Uninsured		0 (0%)	6 (11%)	68 (14%)	55 (15%)	23 (18%)	2 (11%)	
Other		0 (0%)	3 (5.6%)	38 (7.6%)	29 (8.0%)	7 (5.5%)	2 (11%)	
Occupation	1,065							0.14
Employed		1 (25%)	22 (41%)	235 (47%)	150 (42%)	50 (39%)	6 (32%)	
Homemaker		2 (50%)	15 (28%)	156 (31%)	121 (34%)	54 (43%)	10 (53%)	
Not employed		1 (25%)	17 (31%)	109 (22%)	90 (25%)	23 (18%)	3 (16%)	
Chronic Disease	1,066							0.7
No		2 (50%)	39 (72%)	315 (63%)	219 (61%)	80 (63%)	12 (63%)	
Yes		2 (50%)	15 (28%)	186 (37%)	142 (39%)	47 (37%)	7 (37%)	
SES Level	1,057							0.4
NSE E		0 (0%)	4 (7.5%)	32 (6.4%)	14 (3.9%)	7 (5.6%)	3 (16%)	
NSE D		0 (0%)	1 (1.9%)	53 (11%)	30 (8.4%)	9 (7.2%)	0 (0%)	
NSE C		1 (25%)	14 (26%)	161 (32%)	112 (31%)	43 (34%)	8 (42%)	
NSE B		3 (75%)	31 (58%)	218 (44%)	169 (47%)	59 (47%)	7 (37%)	
NSE A		0 (0%)	3 (5.7%)	36 (7.2%)	31 (8.7%)	7 (5.6%)	1 (5.3%)	

Mean (SD); n (%)

Kruskal-Wallis rank sum test; Fisher's Exact Test for Count Data with simulated p-value (based on 2000 replicates)

Carab

Carab is the zone with the smallest coverage by far and descriptively an outlier on several characteristics, though none should be interpreted as meaningful given the sample size (n = 4). Participants here were the oldest on average (mean 55.0 years), all spoke Castellano, none had no formal education, and none had hypertension — but again, these figures reflect 4 people, not a population pattern. It is entirely composed of socio-economic status level B and C participants, with no representation from lower SES categories.

Comas

Comas (n = 54) stands out as the zone with the highest proportion of participants with no formal education (9.3%) and the lowest rate of partnered civil status (56%). It has the highest SIS health insurance coverage (69%) and the second highest rate of unemployment/not employed (31%), suggesting a lower-resource profile. It is more socioeconomically heterogeneous, with visible representation across socio-economic status levels B, C, D, and E, including one of the higher shares of level E. Its covariate profile reflects a lower-resource zone. It captures a broader SES spectrum than most other areas.

MiPeru

MiPeru is the largest zone (n = 501) and in many ways the most representative of the full sample. It skews toward employed participants (47%), has moderate education distribution (65% secondary or higher), and the highest rate of uninsured

participants (14%) alongside relatively high hypertension (27%). It has the second highest proportion of Quechua or Aimara speakers (19%), suggesting meaningful indigenous-language representation.

PuenteP Estadio

PuenteP Estadio is the second largest zone (n = 361) and closely resembles MiPeru across most characteristics. It has the lowest proportion of female participants (67%), the highest hypertension rate (28%), and the highest chronic disease burden (39%). It also has the highest proportion of uninsured participants alongside MiPeru (~15%), and a relatively low proportion with no education (3.6%).

MiPeru and PuenteP Estadio zones together comprise the majority of the sample, and they show very similar SES distributions: both are heavily concentrated in SES level B and level C, with modest representation from level D and minimal level E. This similarity is important, as it indicates that the two largest analytic zones are broadly comparable in socioeconomic composition.

SanMa

SanMa (n = 127) has the highest proportion of partnered participants (69%) and the second highest rate of secondary or higher education (72%). It has the highest proportion of Quechua or Aimara speakers among the mid-sized zones (25%) and a relatively high homemaker rate (43%), which paired with its female skew (74%) likely reflects gendered occupational patterns. Chronic disease prevalence is

moderate (37%). SanMa has a relatively even spread across SES levels, with modest representation at both ends. It most closely resembles the full-sample distribution.

Ventanilla

Ventanilla has the highest proportion of young participants by a notable margin (mean 46.5 years, roughly 4–8 years younger than most other zones) and is the most female-skewed (84%). It has the highest BMI (mean 30.8), the highest homemaker rate (53%), and the highest proportion of Quechua or Aimara speakers (32%), suggesting a more recently migrated or indigenous-heritage population. It has 63% participants with secondary or higher education. This zone stands out for having a relatively higher share of SES level C and level E compared to some other zones. This could reflect a population of younger, recently migrated residents who are educated but economically precarious, though its small sample size limits interpretation.

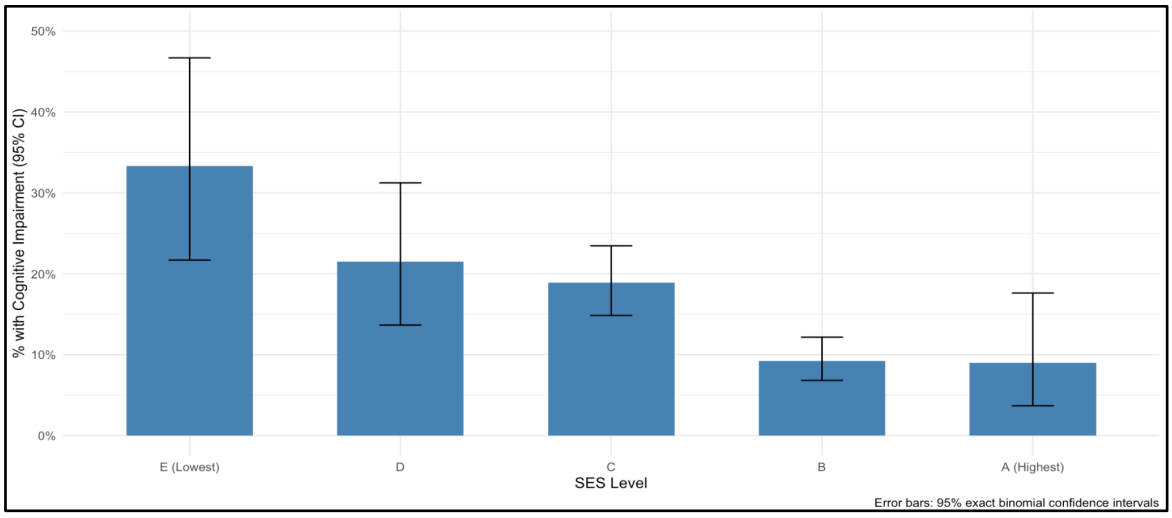

Figure 11 Relationship between socio-economic status and dementia status (n = 1,066). NSE E = most socio-economically deprived.

The two largest zones (MiPeru and PuenteP Estadio) are broadly similar in composition, which is relevant since they cover 81% of participants. Overall, while all zones are anchored in the NSE B and C range, Comas and Ventanilla show greater representation of lower SES categories, whereas Carab lacks this variation entirely (though n = 4, which limits its value for interpretation). The strong similarity between MiPeru and PuenteP Estadio supports treating them as compositionally comparable in SES.

This socioeconomic heterogeneity is clinically meaningful (Figure 11): cognitive impairment prevalence followed a clear dose-response gradient across SES levels, ranging from 33.3% in NSE E (95% CI 21.7–46.7%) to 9.0% in NSE A (95% CI 3.7–17.6%), with corresponding ACE score gradient from 73.0 in NSE E to 83.1 in NSE A, a difference of approximately 10 points across the full SES spectrum. RUDAS-PE scores, by contrast, showed a much flatter pattern across SES levels, ranging only from 23.6 in NSE D to 24.5 in both NSE E and NSE A, consistent with the instrument's design as a dementia screening tool with limited sensitivity to subtle cognitive variation in community samples (results not shown). The divergence between ACE and RUDAS-PE gradients across SES reinforces the analytic decision to treat them as distinct outcomes, and underscores the importance of accounting for SES when interpreting environmental exposure-cognition association in this sample.

Primary Analysis: Environmental Exposures and Cognitive Outcomes

No statistically significant associations were observed between any sensor-assigned environmental exposure (PM2.5, PM10, temperature, humidity) and cognitive outcomes in unadjusted or adjusted models. Age and sex adjusted estimates for the binary cognitive impairment outcome were: PM2.5 OR 0.91 (95% CI 0.75–1.11, p=0.370), PM10 OR 0.90 (95% CI 0.74–1.11, p=0.333), temperature OR 1.08 (95% CI 0.90–1.30, p=0.406), humidity OR 1.07 (95% CI 0.90–1.27, p=0.469). ACE models were null across all four exposures at all adjustment stages. One exception was humidity, which showed a significant association with RUDAS-PE scores in unadjusted (β −0.57, 95% CI −1.13 to −0.02, p=0.046) and age/sex adjusted (β −0.58, 95% CI −1.14 to −0.02, p=0.045) models; however, this attenuated to null after full covariate adjustment (β −0.42, 95% CI −0.95 to 0.11, p=0.122), suggesting the association was driven by sociodemographic factors rather than a direct meteorological effect on cognition. Forest plot presenting the air quality exposures and three cognitive outcomes across the three adjustment stages (unadjusted, age and sex adjusted, and fully adjusted) are shown in Figure 12. Fully adjusted models included: age, sex, SES, BMI, education, civil status, occupation, hypertension, glucose level, and chronic disease status. Comprehensive model results across all three adjustment stages are presented in Supplementary Tables 2-4.

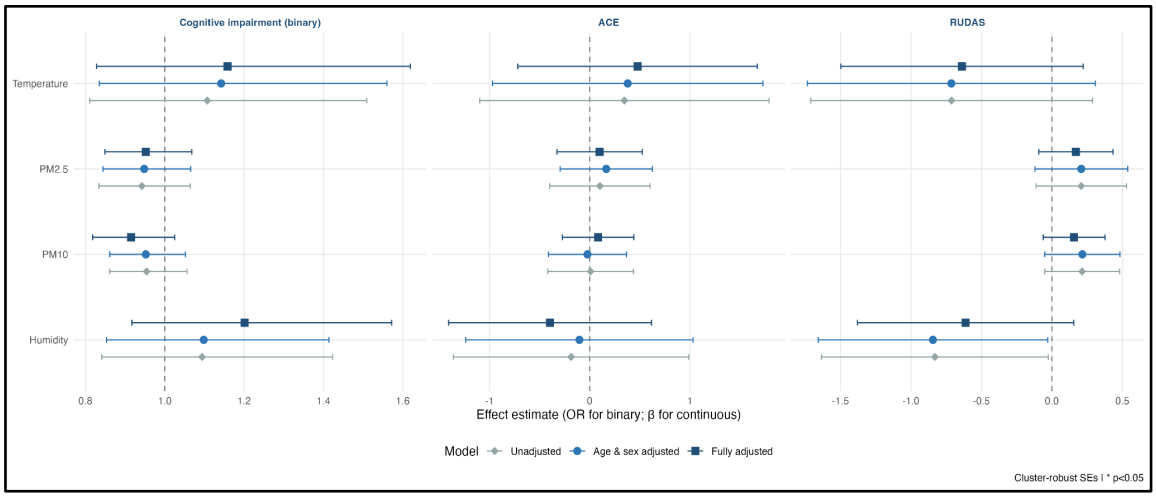

Figure 12 Air quality exposures and cognitive outcomes (binary dementia, ACE younger adults, RUDAS-PE older adults). Exposures standardized per 1 SD. Cluster-robust SE at sector x "conglomerado" level. (n = 1,066).

Ecological Confounding: Sensor Zone Comparison

No dose-response pattern (the expectation that higher pollution exposure leads to progressively worse cognitive outcomes) was observed between sensor-zone PM2.5 and cognitive impairment. Among the four sensors with adequate sample size, the highest PM2.5 zone (Comas, 40.1 μg/m^3) had the lowest rate of cognitive impairment (9.3%) and among the highest mean RUDAS-PE and ACE scores, while the lowest PM2.5 zones clustered around 15-16% cognitive impairment. This inverse pattern is an ecological confounding artifact: the bulk of participants are assigned to just two sensors, MiPeru (n = 501) and Puente Piedra Estadio (n = 361), which covers most of the study area and show nearly identical PM2.5 values (~32-34 μg/m^3). There is effectively no meaningful exposure gradient across participants. The sensor zones are not exchangeable populations, and any apparent association between sensor-assigned PM2.5 and cognition reflects compositional differences between zones rather than a pollution effect.

Road Proximity

Distance from participant conglomerates to the nearest major road ranged from 9 meters to 4.5 km (median 674m, mean 1,001m, right skewed distribution). Participants living within 500m of a major road had lower rates of cognitive impairment (12.2% v 16.4%) and higher ACE score (mean ACE 80.2 v 78.1) compared to those living farther away. RUDAS-PE score did not vary (mean RUDAS-PE 23.9 for within 500m and beyond 500m); this is consistent with the instrument's limited ability to detect subtle changes in cognition. Buffer zone distributions across all four distance categories are shown in Figure 13.

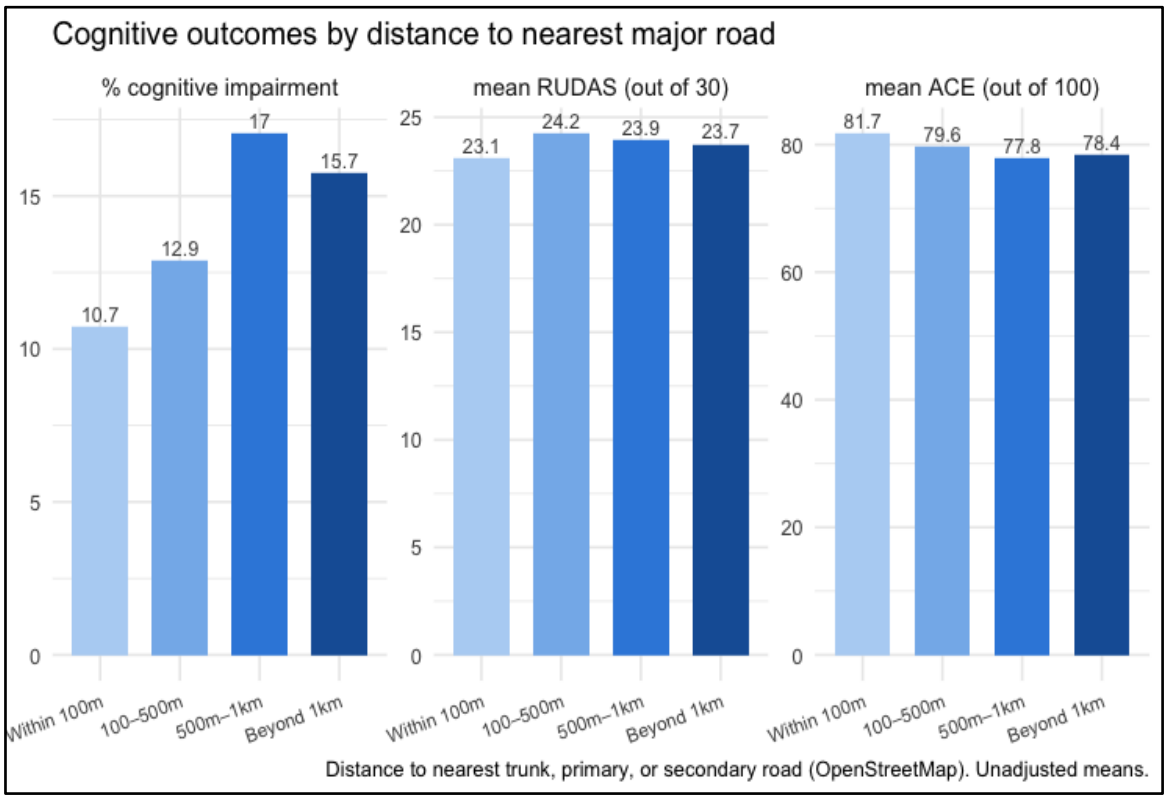

Figure 13 Cognitive outcomes by distance to nearest major road (buffer zones: within 100m, 100-500m, 500-1km, beyond 1km). Unadjusted means for % cognitive impairment, mean RUDAS-PE, and mean ACE.

To assess the strength of associations between road proximity and measured covariates, Spearman correlations between distance to nearest road and all available sociodemographic and health variables were computed. Correlations were uniformly weak ($|r| \leq 0.10$) across SES, education, health insurance type, occupation, chronic disease status, and BMI. A modest negative correlation was observed between road distance and age ($r = -0.19$), indicating that older participants tended to live closer to major roads; age was retained as a covariate in all adjusted models. Greater distance from major roads was associated with lower ACE scores in adults aged 30–59 (β −0.72, 95% CI −1.38 to −0.06, p=0.033 unadjusted; β −0.92, 95% CI −1.57 to −0.28, p=0.005 age/sex adjusted). This association attenuated after full covariate adjustment but remained marginal (β −0.54, 95% CI −1.15 to 0.06, p=0.079), indicating the relationship is not fully attributable to residential sorting by SES. Road proximity was not significantly associated with binary cognitive impairment (OR 1.07, 95% CI 0.93–1.24, p=0.336 age/sex adjusted) or RUDAS-PE scores in older adults (β 0.07, 95% CI −0.40 to 0.54, p=0.775 age/sex adjusted) across any adjustment stage. Forest plot presenting the road exposure and three cognitive outcomes across the three model adjustment stages (unadjusted, age and sex adjusted, and fully adjusted) are shown in Figure 14. Fully adjusted models included: age, sex, SES, BMI, education, civil status, occupation, hypertension, glucose level, and chronic disease status. Comprehensive results across all three adjustment stages are presented in Supplementary Tables 5-7.

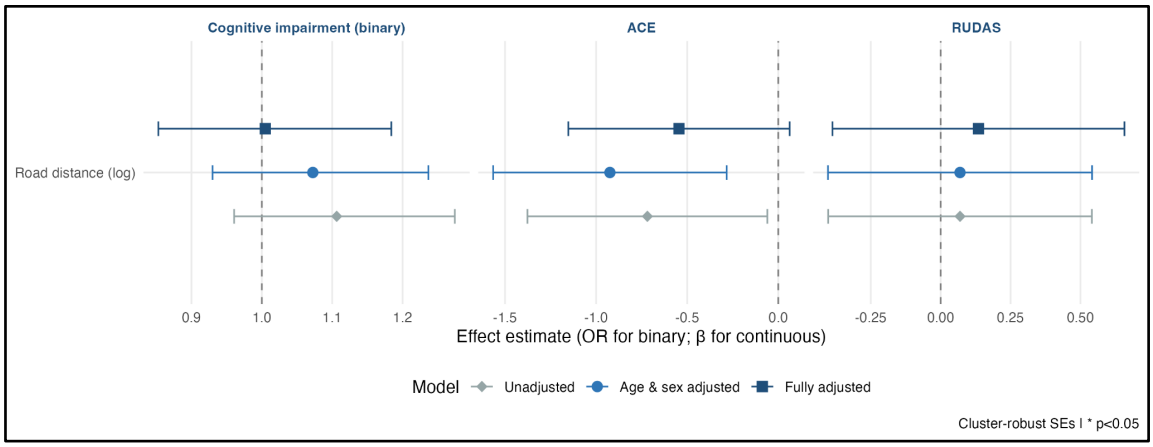

Figure 14 Road distance (log) and three cognitive outcomes (binary cognitive impairment, ACE, and RUDAS-PE) showing unadjusted, age and sex adjusted, and fully adjusted results (n = 1,066).

Socioeconomic Status as an Independent Determinant

SES showed an independent dose-response relationship with cognitive outcomes (Table 16). The rate of binary cognitive impairment increased monotonically from 8.9% in NSE A (highest SES) to 33.3% in NSE E (lowest SES). Mean ACE scores decreased by ~11 points across the SES gradient (83.1 in NSE A v 72.9 in NSE E). Across all sensor zones, there was no evidence that SES was associated with sensor-assigned PM2.5 concentrations (all within-zone ANOVA p-values > 0.10). Mean PM2.5 levels remained essentially stable across SES categories within each sensor (mean PM2.5 across NSE groups: ~33.2 to 34.2 μg/m³), supporting the assumption that SES is not systematically patterned by PM2.5 exposure in this sample.

Table 16 Cognitive outcomes by socioeconomic status level among adults in Puente Piedra, Peru. SES categories reflect the Peruvian NSE classification system, ranging from NSE A (highest) to NSE E (lowest). (n = 1,066).

SES Level	Mean ACE	SD ACE	Mean RUDAS	SD RUDAS	% Cognitive Impairment	n
NSE A	83.1	7.88	24.5	2.78	8.97	78
NSE B	81.5	9.79	23.9	3.55	9.24	487

NSE C	76.8	11.5	24.7	3.24	18.9	339
NSE D	73.1	14.6	24.6	2.92	21.5	93
NSE E	73.0	12.5	24.5	2.28	33.3	60
Mean ACE scores are reported for younger adults (ages 30–59); mean RUDAS-PE scores are reported for older adults (ages 60+). Percent cognitive impairment reflects the proportion meeting criteria for binary cognitive decline within each SES group.						

SES showed only a weak and inconsistent association with road proximity. In the categorical model, mean distance to major roads varied across SES groups (e.g., NSE E: 1,240 m; NSE A: 826 m), and overall differences were statistically significant ($R^2 = 0.011$, $p = 0.018$). However, the association was not monotonic, and there was no evidence of a linear trend (see Supplementary Table 8). Together, these results indicate that although small between-group differences exist, SES is only minimally and non-systematically related to road proximity, suggesting limited potential for confounding of the observed association with roadway distance.

SES adjustment attenuated the ACE road proximity effect, but did not fully explain it away, and the association remained statistically significant after age and sex adjusting and the full adjustment ($p = 0.004$ and $p = 0.090$, respectively). Road proximity was not significantly associated with binary cognitive impairment or RUDAS-PE in older adults with or without SES adjustment (all $p > 0.30$).

Sensitivity analyses

In road-type stratified sensitivity analyses, the inverse association between road proximity and ACE scores in younger adults was consistent for trunk (β −0.87, $p=0.048$) and secondary roads (β −0.83, $p=0.007$), suggesting the pooled result is

not attributable to any single road classification. The primary road estimate was in the opposite direction (β +1.15, p=0.081), possibly reflecting the distinct spatial distribution of primary roads in this peri-urban context. Dementia binary and RUDAS-PE results were null across all road types. Full sensitivity results are presented in Table 17.

*Table 17 Road type stratified sensitivity analyses: trunk, primary, secondary × dementia binary, RUDAS-PE, ACE. * p < 0.10, ** p < 0.05, *** p < 0.01.*

Outcome	Exposure	Estimate	CI Low	CI High	P Value
Dementia binary	Distance to trunk road (logged)	1.045	0.861	1.268	0.656
	Distance to primary road (logged)	0.948	0.704	1.277	0.727
	Distance to secondary road (logged)	1.032	0.895	1.190	0.663
RUDAS-PE	Distance to trunk road (logged)	-0.031	-0.663	0.600	0.922
	Distance to primary road (logged)	0.247	-1.425	1.919	0.773
	Distance to secondary road (logged)	0.255	-0.230	0.740	0.306
ACE	Distance to trunk road (logged)	-0.867	-1.722	-0.011	0.047**
	Distance to primary road (logged)	1.146	-0.138	2.430	0.081*
	Distance to secondary road (logged)	-0.828	-1.425	-0.231	0.007**

To test whether the road proximity effect on ACE differed by SES level, an interaction term between log-distance to nearest road and SES was included to assess effect modification of the road proximity–ACE association among younger adults (Figure 15). In the primary (non-interaction) model, greater distance from roads was associated with lower ACE scores overall – meaning participants living closer to roads tended to perform better cognitively, consistent with an urban access

advantage. The association between road distance and ACE scores differed across SES groups. Among the lowest SES group (NSE E), greater distance from roads was associated with lower ACE scores (β = 2.13, 95% CI: −0.34, 4.59, p = 0.091), suggesting that road proximity, and the access to services it may confer, benefits those with the fewest economic resources most. This association reversed for middle SES groups, with the strongest negative and statistically significant slope observed for NSE C (β = −1.38, 95% CI: −2.48, −0.27, p = 0.015), and a similar pattern for NSE D (β = −1.12, p = 0.178). NSE B and NSE A showed negligible associations (β = −0.32 and −0.13, respectively, both p > 0.40).

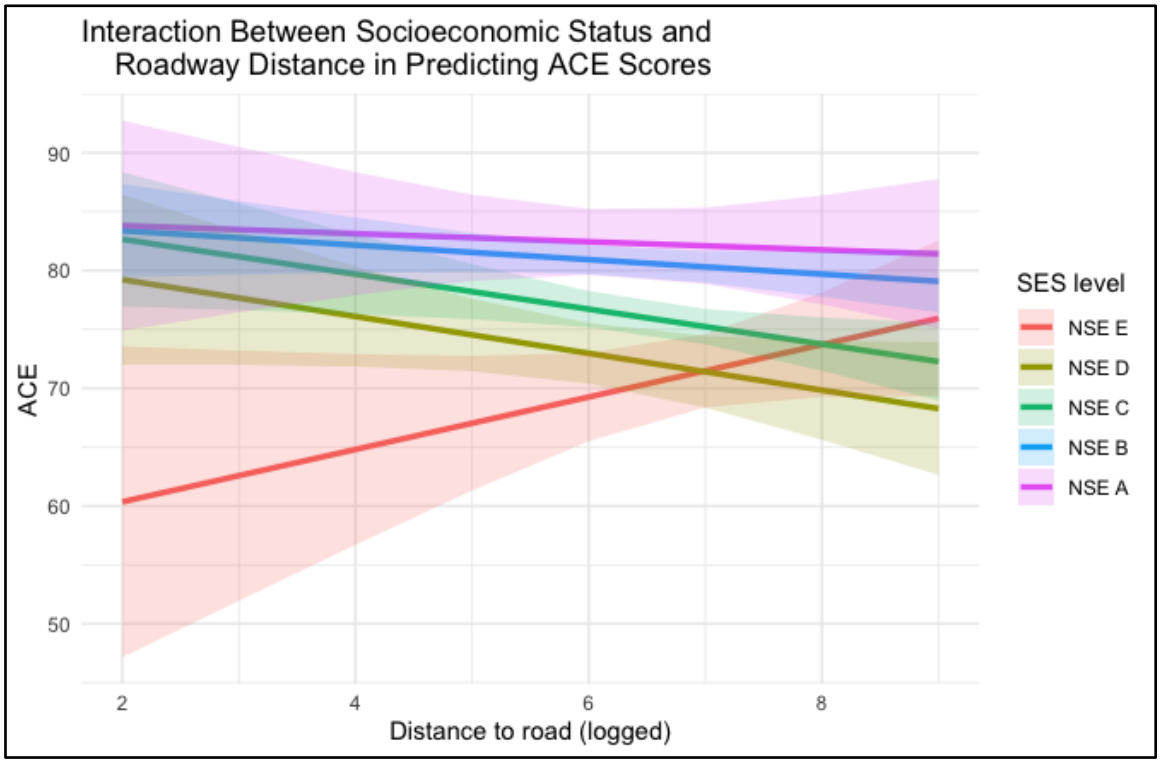

Figure 15 Predicted ACE scores from OLS regression adjusted for age and sex and with an interaction term between SES and roadway distance. NSE E = lowest category. Shaded bands reflect 95% CI. (n = 1,066).

Discussion & Limitations

This study examined associations between sensor-derived ambient exposures — PM2.5, PM10, temperature, and humidity — as well as proximity to major roadways, and cognitive outcomes in a community-based sample of adults in Puente Piedra, Peru. Given high collinearity across sensor-zone-assigned variables, each exposure was modeled separately, adjusted for age and sex. The primary findings are: (RQ1) no statistically significant associations between any sensor-assigned air quality variable and cognitive impairment; (RQ2) a significant association between greater distance from major roads and lower ACE scores (i.e. greater cognitive impairment) among younger adults (aged 30–59), which persisted after adjustment for socioeconomic status; and (RQ3) a strong, independent SES gradient across all cognitive outcomes. Taken together, these findings reveal as much about the methodological challenges of environmental epidemiology in peri-urban LMIC settings as they do about the complex interplay of pollution exposure and social determinants of cognitive health.

Puente Piedra is a district with significant internal socioeconomic variation. Higher-SES areas tend to have higher educational attainment, which builds cognitive reserve. That reserve can mask early cognitive impairment on standard tests, making people look cognitively healthier even under pollution exposure (Frndak et al., 2024). Sensors placed near industrial corridors or the main highway might be reading worse air, but those same corridors might have better infrastructure — paved roads, formal housing, more stable economic activity, better access to healthcare and nutrition. All of those are strong independent predictors of cognitive

health. Our PurpleAir sensor data with "better" air quality might be sitting in a more peripheral, informal settlement with lower SES and poorer cognitive health outcomes for largely non-air-quality reasons.

The absence of significant air pollution (PM2.5 and PM10) and cognition associations in this study does not necessarily rule out a meaningful relationship between air pollution and brain health in Puente Piedra, though it may also reflect a true null association in this context.

First, with only six unique sensor zones across 1,066 participants, sensor-assigned exposure effectively became a categorical variable with limited contrast — the PM2.5 range across zones was only 30.9–40.1 μg/m³, a span too narrow to reliably detect dose-response relationships. This is a fundamental limitation: without meaningful variation in the primary predictor, identifying a statistically or substantively significant association with any outcome is inherently difficult, regardless of sample size. If true within-zone exposure variability is greater than our sensor network captures, we are likely underestimating exposure contrast between participants, attenuating effect sizes toward null. Because all participants were exposed well above both WHO interim targets, the study is better positioned to characterize health effects at uniformly high exposure levels than to distinguish risk across a gradient — future studies should prioritize personal or higher-resolution spatial monitoring in this setting.

Second, the descriptive data reveal prominent ecological confounding: the highest PM2.5 zone (Comas, 40.1 μg/m^3) shows paradoxically better cognitive outcomes than lower PM2.5 zones. Although individual-level SES was measured and adjusted for in all models, this pattern likely reflects residual confounding by unmeasured factors operating at multiple levels, including neighborhood-level characteristics (local infrastructure, green space, access to healthcare, area-level economic activity) as well as household- and individual-level factors such as housing quality, time spent outdoors, occupational exposures, and commuting patterns, that individual SES does not fully capture. Participants assigned to the Comas sensor may reflect differences between neighborhoods and lifestyles (e.g., occupation, commuting patterns, indoor air quality) rather than a genuine protective effect of pollution exposure. More broadly, the available individual- and household-level measures in this study are unlikely to fully account for the complex social and environmental patterning of both pollution exposure and cognitive outcomes in this setting. This highlights a methodological limitation of nearest-sensor exposure assignment in settings with sparse monitoring infrastructure; when sensor zones are few and represent large geographical areas, they conflate exposure measurement with neighborhood identity, making causal inference at the exposure level severely limited without richer spatial data.

Taken together, these structural limitations do not negate the public health significance of the findings. All sensor-zone PM2.5 values (30.9-40.1μg/m^3) substantially exceeded the WHO 2021 annual guideline (World Health Organization, 2021b) of 5 μg/m^3, placing the entire study population in the range associated with

elevated health risk. The null findings in regression coexist with a population that *is* meaningfully exposed. This contrast highlights that population-level exposure burden and the ability to detect within-population exposure-response gradients are distinct problems, requiring monitoring infrastructure investment and sufficient exposure contrast in study design.

The finding that greater distance from major roads is associated with worse ACE scores in younger adults, and that participants living within 500m of roads have better, not worse, cognitive outcomes, is substantively important, and should not be dismissed as merely a null result for the pollution hypothesis. This finding runs counter to H2, which anticipated that road proximity would signal pollution harm; instead, proximity appears to operate as a marker of urban access in this setting. In high-income country epidemiology, road proximity is typically operationalized as a traffic-related air pollution proxy (Barzyk et al., 2009; S. Chen et al., 2016; Su et al., 2009), with the expected association being harmful. In the district of Puente Piedra, road proximity appears to operate primarily as a marker of integration into urban opportunity structures, (Iimi et al., 2016; C. Silva et al., 2023) access to employment, healthcare facilities, educational institutions, markets, and public transit. This is consistent with the broader urbanization-health literature from rapidly developing settings, where proximity to urban infrastructure often confers net-positive health advantages even in the presence of pollution co-exposure (Frndak et al., 2024; You et al., 2022). However, this interpretation should be treated cautiously, as unmeasured individual- and household-level characteristics, such as housing quality, occupation, lifestyle factors, or wealth beyond what the SES measure

captures, may partially or fully account for this association. This is consistent with the global literature on structural determinants of dementia risk, and with the Behavioral and Socioeconomics of Aging (BSEA) framework connecting macro-level socioeconomic structures to individual cognitive aging in sometimes novel ways (Figueroa et al., 2020; Hernandez et al., 2025; Lenart-Bugla et al., 2022; Udeh-Momoh et al., 2025).

The partial, but not complete, attenuation of the road proximity effect after SES adjustment conveys that SES and road proximity share overlapping pathways (i.e., reflecting urban access), yet are not redundant. The finding is specific to younger adults assessed with ACE, which has higher ceiling and greater sensitivity than RUDAS-PE, and whose age group likely retains sufficient cognitive reserve and score variance for environmental gradients to manifest (Cosarderelioglu et al., 2025; Frndak et al., 2024). Among older adults, age-related impairment may dominate and mask more subtle exposure effects. Data is lacking regarding the complex relationship between young adults, air pollution, and cognitive health. From the minimal body of work on this topic, the exposure-outcome dynamic is complex and sometimes contradictory, with some studies reporting an association between PM2.5 exposure and executive dysfunction, and others finding no clear effect (Thompson et al., 2023).

The SES gradient across all cognitive outcomes was substantial and exceeded any effects detected for environmental exposures in this study. The interaction between log-distance to road and SES was statistically significant. Among the lowest SES

group (NSE E), living closer to major roads was associated with better cognitive scores, consistent with an urban access advantage with those with the fewest resources. This benefit attenuated with increasing SES, suggesting that higher SES individuals maintain cognitive advantages regardless of road proximity, likely through individual, independent access to healthcare, education, and economic opportunity.

Recent work has highlighted the role of polygenic resilience factors in brain health, and the potential for interventions that improve cognitive trajectories in LMICs through whole-body health principles where resources are constrained and cultural diversity is high (Udeh-Momoh et al., 2025). Our findings may reflect a complementary dynamic: in Puente Piedra, the capacity for community-level resourcefulness and informal economic participation potentially interacts with biological and environmental vulnerabilities in ways that could both exacerbate and mitigate pollution-related cognitive risks. Disentangling these pathways requires measurement at multiple levels and settings simultaneously (i.e., more granular ambient air monitoring, and individual-level indoor air monitoring, documenting commuting patterns, gathering data on time use and activity spaces) – a direction for future work (Clouston, 2020; Jones et al., 2025). While our work was able to account for a handful of modifiable and non-modifiable risk factors for dementia – age, sex, SES, BMI, education, civil status, occupation, hypertension, glucose level, and chronic disease status – we were unable to capture data on where people work and where they spend their time; they may have more exposure to alternative districts' PM levels rather than in their home district. Collecting wearable mobility

data would be an informative next step for this work, even beyond the question of adequately capturing ambient air pollution. Collecting additional, longitudinal, individual-level data would allow us to investigate our ACE-roadway findings, which signals that possibly there are mechanisms at play that build or preserve resilience amidst the neurotoxic insults of air and roadway pollution.

While low-cost sensors have been validated as meeting U.S. EPA monitoring standards, it is known that they may produce over- or underestimates in environments with high particulate matter concentrations, they are sensitive to relative humidity, which can affect accuracy, and generally perform best in low-pollution environments (Ilenič et al., 2025). Additionally, our nearest-sensor exposure assignment does not account for wind direction or topographic channeling of pollutants. Lima's air quality is shaped by a complex interplay of meteorological and traffic-related factors (Carbajal-Arroyo et al., 2007; Underhill et al., 2015) that vary substantially by season, time of day, and location within the metropolitan area. The city experiences two distinct seasons: a warm, dry season from December to April characterized by calm winds, higher temperatures, and low rainfall, and a cool, humid, cloudy season from June to October with stronger winds and light precipitation (J. Silva et al., 2017; Warren et al., 2021). These seasonal patterns drive meaningful variation in particulate matter concentrations (Galindo et al., 2011). PM10 peaks in summer in the central and northern areas of Lima, while PM2.5 concentrations are higher in winter, likely due to thermal inversion and domestic heating emissions (Warren et al., 2021). The relationship between humidity and PM concentrations is not linear or consistent; in summer mornings, decreasing humidity

is associated with rising PM2.5 and PM10, while afternoon humidity between 65–80% tends to suppress PM2.5 as particle growth promotes dry deposition(Warren et al., 2021; L. Zhang et al., 2017). In winter, these dynamics shift and vary spatially, with the northern area, where the district of Puente Piedra is located, behaves differently from central and eastern zones (J. Silva et al., 2017; Warren et al., 2021). The direction of the humidity-PM relationship depends on season, time of day, and neighborhood.

This study reveals several methodological constraints that are likely to affect environmental epidemiology in similar LMIC peri-urban settings. The qAIRa sensor, though framed as filling Lima's monitoring gap, has no sensors in Puente Piedra and its coverage skews toward wealthier districts – a spatial inequity in environmental data infrastructure that mirrors the health inequities it aims to measure (see Supplementary Figure 1) (*Calidad Del Aire y Mapeo Digital Con Drones LiDAR*, n.d.). The Peru's government's air quality monitoring program has one sensor in the district of Puente Piedra (see Supplementary Figure 2). The Lima air quality monitoring stations are managed by the Ministry of Environment (MINAM) and The National Service of Meteorology and Hydrology (SENAMHI). Six PurpleAir citizen science sensors in the vicinity of the district of Puente Piedra represent substantial improvement over one single regulatory monitor, but remain insufficient for individual-level exposure regression when residential clustering produces little within-zone variability.

In order to overcome the lack of data available, there are some geostatistical interpolation methods that can be used. Kriging is a technique that estimates values at unsampled locations by weighting nearby measured values, yet unlike simple averaging, it weights them based on the spatial autocorrelation structure of the data. It creates a semi-variogram curve reflecting how similarity in measures decays with distance. It estimates pollution levels at every point in between known points, and provides uncertainty estimates alongside those predictions. Kriging and other spatial interpolation methods could theoretically be used to generate address-level PM2.5 estimates from sensor data, but their reliability is bounded by sensor density, the assumption of spatial stationarity, and the distinction between ambient concentration and personal exposure (which depends on time indoors, commuting patterns, and building characteristics). In Lima's complex topography, where altitude shapes atmospheric pollutant dispersion and the dry season concentrates particulate matter in the northern cone, these limitations are particularly acute (Warren et al., 2021). Someone "near" the cleaner sensor might actually sit in a pocket of worse air due to topography or wind patterns that our sensor network cannot capture. In a paper that examines air pollution estimation in Lima using Kriging methodology, they still report a room mean square error of 3.5 $\mu g/m^3$, which matters when WHO guidelines state that values above 5 $\mu g/m^3$ is harmful to health.(Romero-Baylón et al., 2024; World Health Organization, 2021b) While kriging can be used to generate continuous exposure surfaces, given the sparse sensor network and Lima's complex topography, such methods continue to carry substantial uncertainty.

Conclusion

This study makes three contributions. First, it characterized the air quality landscape of Puente Piedra using the PurpleAir sensor network, demonstrating that PM2.5 concentrations substantially exceed WHO guidelines across the district while showing little variability between sensors. This uniform exposure ceiling, with all zones ranging only from 30.9 to 40.1 μg/m³, likely explains the absence of a detectable association between sensor-assigned air quality variables and cognitive outcomes (RQ1). When an entire population sits well above the threshold of harm with minimal contrast between them, within-sample gradients cannot be identified regardless of sample size. Second, it documents that road proximity operates as a marker of urban access rather than pollution harm in this setting (RQ2) — a finding that runs counter to the expected direction and to standard traffic-related air pollution frameworks from high-income contexts. In Puente Piedra, where roads bring both traffic emissions and connectivity to services, ecological confounding patterns mean that assigning exposures based on nearest sensor zone alone produces an incomplete and potentially misleading picture, with direct implications for environmental epidemiology methods in LMIC peri-urban contexts. Third, it reveals that SES moderates the association between road proximity and cognitive outcomes (RQ3), with road access appearing most beneficial for those with the fewest economic resources — a finding with potential relevance for urban planning and public health policy in rapidly developing settings. Future work requires denser sensor networks, personal exposure monitors, and GPS-tracked mobility data to capture true individual exposure alongside the social and structural determinants that shape it. Both physical and social exposures across the life course have the

potential to have immediate and latent effects on neurological health, impacting the aging trajectory (Hernandez et al., 2025; Lenart-Bugla et al., 2022; Roy & D'Angiulli, 2024). Addressing these questions requires longitudinal, multi-level data — and the infrastructure to collect it equitably. The fundamental challenge, that the places with the worst air and the most concentrated poverty are precisely the places with the least monitoring infrastructure, is not a methodological limitation to footnote, but a structural problem to bring to light, and intervene upon.

CONCLUSION

This dissertation explored the phthalate-gut-brain nexus through several lines of investigation: (1) examining broad population-level longitudinal phthalate exposure and non-clinical, validated measures of ADRD risk; (2) developing a method for detecting phthalates in fecal samples using UPLC-MS, thereby laying the groundwork for future studies to connect fecal phthalate levels with gut microbiome composition, function, and ultimately brain biomarkers; and (3) investigating air pollution and cognitive health in an under-resourced population in Lima, by combining publicly available and citizen science air pollution measurements with a door-to-door, population-based cognitive health study to address a critical data gap in a vulnerable population.

Individuals experiencing socioeconomic disadvantage may face both higher environmental exposure burdens and greater biological vulnerability to those exposures due to chronic stress, poorer housing conditions, limited healthcare access, disrupted sleep, reduced access to green space, and nutritional inequities. In contrast, individuals with greater socioeconomic resources may possess protective factors that buffer the physiological consequences of similar exposures. Thus, the same conditions that increase exposure likelihood may also amplify susceptibility to exposure-related harm. Although these interrelated pathways complicate causal inference, they also suggest that interventions targeting structural determinants may simultaneously reduce exposure burden and strengthen resilience.

Within the United States, the total number of people living with dementia has grown as the population ages – unsurprising, given that age is one of its strongest

predictors. However, the *rate* of dementia has declined substantially over the last 40 years, even in the absence of any effective medical treatment (Stallard et al., 2025). In 1984, approximately 30% of people in the U.S. aged 80-85 had dementia; by 2024, that figure had dropped to approximately 10% for the same age group (Stallard et al., 2025). Much of this decline is attributed to population-wide improvements in educational attainment, cardiovascular health, and early-life infection rates, driven by greater vaccine accessibility and comprehensive immunization programs (Eyting et al., 2025; Livingston et al., 2020; Mistridis et al., 2017; Polisky et al., 2025). This is a partial success story within the U.S. It requires continual investment in these dementia-reducing factors.

Additionally, the downward trend is not a complete story; disaggregating the data *is* important to understand the full picture. Black Americans have an increasing prevalence rate of dementia. Black Americans are roughly twice as likely to have ADRD than White Americans, and Hispanic Americans are one and a half times more likely to have ADRD (*Alzheimer's Disease Facts and Figures*, 2025). Beyond disparities in access to health-promoting behaviors and care, it is unknown what causes these differences in prevalence of dementia among Blacks and Hispanics compared to Whites.

These disparities extend beyond U.S. borders. An estimated 60% of people living with dementia reside in low-and-middle-income countries, regions that are already under-resourced for diagnosis, care, and research. These regions are home to roughly 85% of the global population, yet have historically accounted for only about

10% of population-based dementia research. This mismatch between burden and scientific attention is a driver of inequity. Without adequate data from these regions, modifiable risk factors go unidentified and interventions are unable to be translated across contexts. As LMIC populations age, this burden is projected to grow to 71% by 2050 (Kalaria et al., 2024). This highlights the urgent need to improve access to interventions that reduce modifiable risk factors (e.g., low education, poor heart health, pollution, infections). The findings in this dissertation set the stage for a research trajectory that directly confronts these challenges. This research trajectory emphasizes geo-social determinants of health, integrates multiple forms of data at differing spatial levels (large national datasets, ADRC biomarker data, and neighborhood-level studies), and prioritizes interdisciplinary collaboration with international partners. Ultimately, this work aims to identify non-invasive, non-pharmacological approaches to report and intervene on modifiable risk factors for ADRD that is translatable to a global population.

Together, these chapters trace a pathway from structurally patterned environmental exposure to gut-level biological embodiment and add data points to the conversation around socially differentiated cognitive aging outcomes.

Chapter 1 used linked PSID, EPA Toxic Release Inventory, and U.S. Census data and found that long-term exposure to emissions from plastics and rubber manufacturing facilities is associated with increased risk of ADRD, independent of individual socioeconomic factors and neighborhood disadvantage. Emissions intensity (lbs of chemicals produced by the factory), rather than proximity (distance in kilometers)

alone, is associated with ADRD risk, highlighting the importance of measuring environmental exposure using facility-specific emissions data. Neighborhood disadvantage is a strong independent predictor of ADRD risk, underscoring the importance of structural and environmental determinants of cognitive aging.

Chapter 2 used MARS cohort data to develop a method to analyze human fecal samples for phthalates, establishing that phthalates are detectable in fecal samples, and that freezing the samples does not limit the signal of the phthalates. With the small sample size, we are limited to what we can conclude in relation to other socio-cognitive characteristics of the ten individuals we sampled from, however, it lays the foundation for future work that can hone in on quantifying phthalates, characterizing the gut microbiome, and connecting the results with cognitive biomarkers. Recent work in mice showed that exposure to specific bacteria can serve as a mechanism to reduce or improve cognitive function. They specifically identified a bacteria called *Parabacteroides goldsteinii* as one that reduces cognitive performance (Cox et al., 2026). Additionally, transplanting the gut of a young mouse into that of an old mouse was able to improve their cognitive functioning to be on par with that of the young mice (Cox et al., 2026).

Chapter 3 used secondary, door-to-door, population survey data paired with PurpleAir and Open Street Map data as a case study of cognitive health in a vulnerable population. The entire study population has exposure to PM2.5 monitoring values of 30.9-40.1μg/m^3, which substantially exceeds the WHO 2021 annual guideline(World Health Organization, 2021) of 5 μg/m^3, placing them all at elevated health risk. The null findings observed between air pollution and cognitive

measures likely reflect that distinction between population-level exposure burden and the ability to detect within-population exposure-response gradients, requiring monitoring infrastructure investment and sufficient exposure contrast in study design. A secondary finding was that those living further than 500m from major roads demonstrated worse ACE scores Participants living within 500m of roads demonstrated better cognitive outcomes in this sample, potentially reflecting differences in access to resources, external stimulation, and the broader social connectivity. Road proximity may simultaneously increase pollution exposure. However, it may also improve access to employment, transportation, healthcare, and social engagement. Places with the least access to monitoring and mitigation efforts are largely left out of research, limiting knowledge of the problems and opportunities to effectively remedy the problems.

Environmental pollution represents a preventable contributor to dementia risk. Identifying exposures as a potential risk factor underscores the importance of environmental monitoring and regulation and calls for equitable neighborhood conditions as a key player in reducing dementia burden and promoting healthy aging.

The Finnish Geriatric Intervention Study to Prevent Cognitive Impairment and Disability (FINGER) study was the first large-scale randomized trial to demonstrate that multidomain lifestyle interventions can improve brain health and reduce risk of cognitive decline. More recently, the U.S. Protect Brain Health Through Lifestyle Intervention to Reduce Risk (POINTER) study extended these findings within a

more geographically, socially, racially, and behaviorally diverse population in the United States. Both studies demonstrated that interventions targeting multiple domains, including diet, exercise, cardiovascular health monitoring, and social and cognitive engagement improved cognitive outcomes, with the intervention participants experiencing significantly greater benefits than control participants (Ngandu et al., 2015, Baker et al., 2025).

Importantly, these studies suggest that meaningful reductions in dementia risk may be achievable through non-pharmacological interventions. However, as Dr. Krieger describes in *Epidemiology and the Peoples' Health,* the ability to adopt and sustain "healthy lifestyles" is shaped by broader social and structural conditions. Access to nutritious food, safe environments for physical activity, healthcare, social engagement, and time for restorative behaviors is unequally distributed across populations. Similarly, Dr. Baker has argued that the 'third chapter' is the critical next step: developing sustainable community-level systems capable of making the POINTER "Brain Health Recipe" broadly accessible (*Unpacking the U.S. POINTER Study*, 2026). The POINTER study's integration of public health professionals, community organizations, and stakeholders represents an important step toward translating dementia prevention strategies into equitable population-level interventions.

Another equity aspect directly related to healthcare is the potential role of vaccines in mitigating the risk of dementia associated with certain infections. Specifically, evidence increasingly suggests that repeated episodes of shingles may elevate

dementia risk. A study in Wales leveraged a policy change in shingles vaccine rollout to conduct a natural experiment using a regression discontinuity design that mirrors the rigor of a randomized trial. Initially they observed an approximately 20% reduced risk of dementia, particularly for women (Eyting et al., 2025). These findings were subsequently replicated in the U.S., further associating the shingles vaccine with a lower dementia risk for both women and men, though women continued to show a greater benefit (Polisky et al., 2025). Hypothesized explanations for this sex difference include variations in the immune system and disparities in healthcare engagement and health-promoting behaviors. Vaccine access and uptake represent another example of modifiable risk reduction that can be a target of public health efforts to reduce dementia. The landscape of understanding factors influencing ADRD is continuing to enlarge. Issues of equity, geography, access, and space will remain key contributors to this research.

Growing evidence suggests that widespread microplastic exposure may represent an emerging public health crisis. This dissertation contributes to emerging interdisciplinary research examining microplastic pollution, social inequities, gut microbiome disruption, and ADRD risk. Although the consequences of environmental exposures may become most apparent in older age, prevention begins much earlier across the life course (Adkins-Jackson et al., 2023; Adkins-Jackson et al., 2023; Homan, 2019; Karlsson et al., 2021; Marmot, 2015). Neighborhood and population level factors interact with individual health behavior to shape risk and health outcomes. Geo-social, structural, and spatial determinants of health are theoretical foundations that explain differential health outcomes and risks.

Addressing socio-demographic disparities in environmental exposures requires attention to the broader social and structural systems that shape exposure and vulnerability. This dissertation positions bridges multiple disciplines, including Geography, Neuroscience, and Demography, and integrates methodologies spanning spatial statistics, biochemical lab analysis of biomarkers, neighborhood effects, to advance understanding of ADRD and modifiable risk factors. As Dr. Baker emphasizes, multidomain interventions may produce synergistic effects that exceed the sum of their individual components.

An important question emerging from this dissertation work is whether elevated phthalate excretion reflects greater exposure burden, more effective elimination, or some combination of the two. While the ideal scenario is clearly no exposure to phthalates and thus no excretion, this is entirely unattainable in our industrial society. Therefore, given our current circumstances, the most effective approach may be to focus on enhancing the excretion of these compounds, or better yet, promoting their retention within the gut lumen during transit (in parallel with policy changes to reduce overall exposure). Future work may build upon the framework in Chapter 2 by integrating multiple biomarkers (e.g., urine, blood, sweat, feces) to assess environmental exposures, gut microbiome function, and cognitive health. Such approaches may help piece together components of the communication between the gut and the brain.

An important extension of this work would be a longitudinal study tracking the input and output of various compounds in human participants over time. Wearable technology and AI assisted tracking could capture diet, physical activity, sleep,

physiological indicators, medication use, and environmental exposures in near real time. These input/contextual data could be paired with daily biomarkers from urine, feces, blood, and sweat. This intensive data collection would be conducted daily for a full month to capture both the male 24-hour hormonal cycle and the approximate 28 day female cycle (Heller et al., 2025; Taylor et al., 2019). While the use of wearables and AI would make data collection as passive as possible, the biomarker collection is inevitably labor-intensive, requiring a passionate participant pool and adequate financial compensation. Ultimately, such a comprehensive, dense-sampling study would provide the necessary data foundation to determine if high phthalate excretion is a marker of effective detoxification or simply high exposure, thus guiding future public health recommendations and policy decisions.

Ultimately, understanding how environmental exposures are biologically processed, socially patterned, and differentially experienced across populations will be critical for developing equitable strategies to reduce dementia risk across the life course.

REFERENCES

Adkins-Jackson, P. B., Kraal, A. Z., Hill-Jarrett, T. G., George, K. M., Deters, K. D., Besser, L. M., Avila-Rieger, J. F., Turney, I., & Manly, J. J. (2023). Riding the merry-go-round of racial disparities in ADRD research. Alzheimer's & Dementia, 19(10), 4735–4742. https://doi.org/10.1002/alz.13359

Adkins-Jackson, P. B., George, K. M., Besser, L. M., Hyun, J., Lamar, M., Hill-Jarrett, T. G., Bubu, O. M., Flatt, J. D., Heyn, P. C., Cicero, E. C., Zarina Kraal, A., Pushpalata Zanwar, P., Peterson, R., Kim, B., Turner, R. W., Viswanathan, J., Kulick, E. R., Zuelsdorff, M., Stites, S. D., … Babulal, G. (2023). The structural and social determinants of Alzheimer's disease related dementias. Alzheimer's & Dementia, 19(7), 3171–3185. https://doi.org/10.1002/alz.13027

Alzheimer's Association. (2020). The number of Americans living with Alzheimer's is growing and growing fast. https://aaic.alz.org/downloads2020/2020_Facts_and_Figures_Fact_Sheet.pdf

Alzheimer's Disease Facts and Figures. (2025). Alzheimer's Association. Retrieved April 28, 2026, from https://www.alz.org/alzheimers-dementia/facts-figures

Alzheimer's Disease International. (2020). Dementia Statistics. Alzheimer's Disease International. https://www.alzint.org/about/dementia-facts-figures/dementia-statistics/

ARUP Laboratories. (2025). Phospho-Tau 217, Plasma. Laboratory Test Directory; ARUP Laboratories. https://ltd.aruplab.com/api/ltd/pdf/174

Arumugam, M., Raes, J., Pelletier, E., Le Paslier, D., Yamada, T., Mende, D. R., Fernandes, G. R., Tap, J., Bruls, T., Batto, J.-M., Bertalan, M., Borruel, N., Casellas, F., Fernandez, L., Gautier, L., Hansen, T., Hattori, M., Hayashi, T., Kleerebezem, M., … Bork, P. (2011). Enterotypes of the human gut microbiome. Nature, 473(7346), 174–180. https://doi.org/10.1038/nature09944

Aubert, N.; Ameller, T.; Legrand, J. J. Systemic exposure to parabens: pharmacokinetics, tissue distribution, excretion balance and plasma metabolites of [14C]-methyl-, propyl- and butylparaben in rats after oral, topical or subcutaneous administration. Food. Chem. Toxicol. 2012, 50 (3–4), 445– 454, DOI: 10.1016/j.fct.2011.12.045

Air quality database. (n.d.). Retrieved April 22, 2026, from https://www.who.int/data/gho/data/themes/air-pollution/who-air-quality-database

Arias-Pérez, R. D., Taborda, N. A., Gómez, D. M., Narvaez, J. F., Porras, J., & Hernandez, J. C. (2020). Inflammatory effects of particulate matter air pollution. Environmental Science and Pollution Research, 27(34), 42390–42404. https://doi.org/10.1007/s11356-020-10574-w

Agin, A., Blanc, F., Bousiges, O., Villette, C., Philippi, N., Demuynck, C., Martin-Hunyadi, C., Cretin, B., Lang, S., Zumsteg, J., Namer, I. J., & Heintz, D. (2020). Environmental exposure to phthalates and dementia with Lewy bodies: Contribution of metabolomics. Journal of Neurology, Neurosurgery & Psychiatry, 91(9), 968–974. https://doi.org/10.1136/jnnp-2020-322815

Anderson, M. J. (2001). A new method for non-parametric multivariate analysis of variance. Austral Ecology, 26(1), 32–46. https://doi.org/10.1111/j.1442-9993.2001.01070.pp.x

Arumugam, M., Raes, J., Pelletier, E., Le Paslier, D., Yamada, T., Mende, D. R., Fernandes, G. R., Tap, J., Bruls, T., Batto, J.-M., Bertalan, M., Borruel, N., Casellas, F., Fernandez, L., Gautier, L., Hansen, T., Hattori, M., Hayashi, T., Kleerebezem, M., … Bork, P. (2011). Enterotypes of the human gut microbiome. Nature, 473(7346), 174–180. https://doi.org/10.1038/nature09944

Braveman, P., Egerter, S., & Williams, D. R. (2011). The Social Determinants of Health: Coming of Age. Annual Review of Public Health, 32(1), 381–398. https://doi.org/10.1146/annurev-publhealth-031210-101218

Baker, L. D., Espeland, M. A., Whitmer, R. A., Snyder, H. M., Leng, X., Lovato, L., Papp, K. V., Yu, M., Kivipelto, M., Alexander, A. S., Antkowiak, S., Cleveland, M., Day, C., Elbein, R., Tomaszewski Farias, S., Felton, D., Garcia, K. R., Gitelman, D. R., Graef, S., … Carrillo, M. C. (2025). Structured vs Self-Guided Multidomain Lifestyle Interventions for Global Cognitive Function: The US POINTER Randomized Clinical Trial. JAMA, 334(8), 681–691. https://doi.org/10.1001/jama.2025.12923

Baka, J. (2025). Cracking Appalachia: A Political-Industrial Ecology Perspective. Annals of the American Association of Geographers, 115(4), 743–763. https://doi.org/10.1080/24694452.2025.2452554

Barcellos, S. H., Carvalho, L., Langa, K., Nimmagadda, S., & Turley, P. (2025). Education and Dementia Risk (Working Paper 33430). National Bureau of Economic Research. https://doi.org/10.3386/w33430

Boehm, T., & Schlottmann, A. (2004). Wealth Accumulation and Homeownership: Evidence for Low-Income Households.

https://www.huduser.gov/publications/pdf/wealthaccumulationandhomeownership.pdf

Bornehag, C.-G., Sundell, J., Weschler, C. J., Sigsgaard, T., Lundgren, B., Hasselgren, M., & Hägerhed E. L. (2004). The Association between Asthma and Allergic Symptoms in Children and Phthalates in House Dust: A Nested Case–Control Study. Environmental Health Perspectives, 112(14), 1393–1397. https://doi.org/10.1289/ehp.7187

Baez, S., Nabil, Y., & Ibanez, A. (2026). Childhood adversities and the exposome in dementia risk and brain health. Current Opinion in Psychiatry, 39(2), 136. https://doi.org/10.1097/YCO.0000000000001057

Barnes, L. L., Dhana, K., Liu, X., Carey, V. J., Ventrelle, J., Johnson, K., Hollings, C. S., Bishop, L., Laranjo, N., Stubbs, B. J., Reilly, X., Agarwal, P., Zhang, S., Grodstein, F., Tangney, C. C., Holland, T. M., Aggarwal, N. T., Arfanakis, K., Morris, M. C., & Sacks, F. M. (2023). Trial of the MIND Diet for Prevention of Cognitive Decline in Older Persons. The New England Journal of Medicine, 389(7), 602–611. https://doi.org/10.1056/NEJMoa2302368

Bauer, K. C., Huus, K. E., & Finlay, B. B. (2016). Microbes and the mind: Emerging hallmarks of the gut microbiota–brain axis. Cellular Microbiology, 18(5), 632–644. https://doi.org/10.1111/cmi.12585

Burstein, H. J., Cirrincione, C. T., Barry, W. T., Chew, H. K., Tolaney, S. M., Lake, D. E., Ma, C., Blackwell, K. L., Winer, E. P., & Hudis, C. A. (2014). Endocrine Therapy With or Without Inhibition of Epidermal Growth Factor Receptor and Human Epidermal Growth Factor Receptor 2: A Randomized, Double-Blind, Placebo-Controlled Phase III Trial of Fulvestrant With or Without Lapatinib for Postmenopausal Women With Hormone Receptor–Positive Advanced Breast Cancer—CALGB 40302 (Alliance). Journal of Clinical Oncology, 32(35), 3959–3966. https://doi.org/10.1200/JCO.2014.56.7941

Barzyk, T. M., George, B. J., Vette, A. F., Williams, R. W., Croghan, C. W., & Stevens, C. D. (2009). Development of a distance-to-roadway proximity metric to compare near-road pollutant levels to a central site monitor. Atmospheric Environment, 43(4), 787–797. https://doi.org/10.1016/j.atmosenv.2008.11.002

Bruno, D., & Schurmann Vignaga, S. (2019). Addenbrooke's cognitive examination III in the diagnosis of dementia: A critical review. Neuropsychiatric Disease and Treatment, 15, 441–447. https://doi.org/10.2147/NDT.S151253

Butler, H. M., Keller, E., McCrorey, M., Keceli, G., Combs, C. K., Kayed, R., Namakkal-S, R., Paolocci, N., Jacobs Wolf, B., Wold, L. E., & Del Monte, F. (2025). Particulate matter and co-occurring genetic risk induce oxidative

stress and cardiac and brain Alzheimer's pathology. Communications Biology, 8(1), 603. https://doi.org/10.1038/s42003-025-07701-z

Bray, J. R., & Curtis, J. T. (1957). An ordination of the upland forest communities of southern Wisconsin. Ecological Monographs, 27(4), 325–349. https://doi.org/10.2307/1942268

Campanale, C., Massarelli, C., Savino, I., Locaputo, V., & Uricchio, V. F. (2020). A Detailed Review Study on Potential Effects of Microplastics and Additives of Concern on Human Health. International Journal of Environmental Research and Public Health, 17(4), 1212. https://doi.org/10.3390/ijerph17041212

Cox, K. D., Covernton, G. A., Davies, H. L., Dower, J. F., Juanes, F., & Dudas, S. E. (2019). Human Consumption of Microplastics. Environmental Science & Technology, 53(12), 7068–7074. https://doi.org/10.1021/acs.est.9b01517

Cox, T. O., Devason, A. S., de Araujo, A., Mason, S., Subramanian, M., Salvador, A. F. M., Descamps, H. C., Kim, J., Zhu, Y., Litichevskiy, L., Jung, S., Song, W.-S., Cortés-Martín, A., Henderson, N. T., Huang, K.-P., Nguyen, T., Sae-Lee, W., Umana, I. C., Sacta, M., … Thaiss, C. A. (2026). Intestinal interoceptive dysfunction drives age-associated cognitive decline. Nature, 652(8109), 442–450. https://doi.org/10.1038/s41586-026-10191-6

Census Bureau (2022). Surveys and Programs, Geography Program, Glossary. Census.gov. https://www.census.gov/programs-surveys/geography/about/glossary.html

Centers for Disease Control and Prevention. (2022). Social Determinants of Health at CDC. Centers for Disease Control and Prevention. Retrieved from https://www.cdc.gov/about/sdoh/index.html

Centers for Disease Control and Prevention (CDC). (2017-2018). Phthalates and phthalate alternative metabolites laboratory method manual (NHANES). U.S. Department of Health and Human Services. https://wwwn.cdc.gov/nchs/data/nhanes/public/2017/labmethods/PHTHTE-J-MET-508.pdf

Chang-Liao, W.-L., Hou, M.-L., Chang, L.-W., Lee, C.-J., Tsai, Y.-M., Lin, L.-C., & Tsai, T.-H. (2013). Determination and Pharmacokinetics of Di-(2-ethylhexyl) Phthalate in Rats by Ultra Performance Liquid Chromatography with Tandem Mass Spectrometry. Molecules, 18(9), 11452–11466. https://doi.org/10.3390/molecules180911452

Chen, M., et al. (2012). Simultaneous determination of multiple phthalate metabolites and bisphenol-A in human urine by liquid chromatography–tandem mass spectrometry. Journal of Chromatography B: Analytical

Technologies in the Biomedical and Life Sciences, 901, 68–74. https://pubmed.ncbi.nlm.nih.gov/22884473/

Chen, T., Wang, L., Xie, G., Kristal, B. S., Zheng, X., Sun, T., Arnold, M., Louie, G., Li, M., Wu, L., Mahmoudiandehkordi, S., Sniatynski, M. J., Borkowski, K., Guo, Q., Kuang, J., Wang, J., Nho, K., Ren, Z., Kueider-Paisley, A., … Alzheimer's Disease Neuroimaging Initiative (ADNI) and the Alzheimer Disease Metabolomics Consortium (ADMC). (2024). Serum Bile Acids Improve Prediction of Alzheimer's Progression in a Sex-Dependent Manner. Advanced Science, 11(9), e2306576. https://doi.org/10.1002/advs.202306576

Cheng, K., Brunius, C., Fristedt, R., & Landberg, R. (2020). An LC-QToF MS based method for untargeted metabolomics of human fecal samples. Metabolomics, 16(4), 46. https://doi.org/10.1007/s11306-020-01669-z

Claus, S. P., Guillou, H., & Ellero-Simatos, S. (2016). The gut microbiota: A major player in the toxicity of environmental pollutants? Npj Biofilms and Microbiomes, 2(1), 1–11. https://doi.org/10.1038/npjbiofilms.2016.3

Calidad del Aire y Mapeo Digital con Drones LiDAR. (n.d.). Retrieved April 17, 2026, from https://www.qairadrones.com/

Carbajal-Arroyo, L., Barraza-Villarreal, A., Durand-Pardo, R., Moreno-Macías, H., Espinoza-Laín, R., Chiarella-Ortigosa, P., & Romieu, I. (2007). Impact of Traffic Flow on the Asthma Prevalence Among School Children in Lima, Peru. Journal of Asthma, 44(3), 197–202. https://doi.org/10.1080/02770900701209756

Carrasco-Escobar, G., Schwalb, A., Tello-Lizarraga, K., Vega-Guerovich, P., & Ugarte-Gil, C. (2020). Spatio-temporal co-occurrence of hotspots of tuberculosis, poverty and air pollution in Lima, Peru. Infectious Diseases of Poverty, 09(02), 84–89. https://doi.org/10.1186/s40249-020-00647-w

Chen, D., Long, Y., Ma, Y., Sha, W., Zhang, L., Ma, Y., Li, Q., Feng, J., Zeng, R., Luo, D., Huang, W., Wu, Y., Meng, M., Leung, F. W., Duan, C., Tian, Y., & Chen, H. (2025). Atmospheric Pollutants, Cardiometabolic Disorders, and Dementia in Trajectory Analysis: A 13-Year Longitudinal Cohort Study. Journal of the American Heart Association, 14(9), e040844. https://doi.org/10.1161/JAHA.124.040844

Chen, S., Bekhor, S., Yuval, & Broday, D. M. (2016). Aggregated GPS tracking of vehicles and its use as a proxy of traffic-related air pollution emissions. Atmospheric Environment, 142, 351–359. https://doi.org/10.1016/j.atmosenv.2016.08.015

Clouston, M. K., Samuel E. Gandy,Jaymie R. Meliker,Benjamin J. Luft,Sean A. P. (2020). Acute versus Chronic Exposures to Inhaled Particulate Matter and Neurocognitive Dysfunction: Pathways to Alzheimer's Disease or a Related Dementia - Minos Kritikos, Samuel E. Gandy, Jaymie R. Meliker, Benjamin J. Luft, Sean A.P. Clouston, 2020. Journal of Alzheimer's Disease. https://journals.sagepub.com/doi/full/10.3233/JAD-200679

Cosardereliogl u, C., Walston, J. D., & Abadir, P. M. (2025). From frailty to resilience: Exploring adaptive capacity and reserve in older adults–a narrative review. Frontiers in Aging, 6. https://doi.org/10.3389/fragi.2025.1520842

Custodio, N., Montesinos, R., Diaz, M. M., Herrera-Perez, E., Chavez, K., Alva-Diaz, C., Reynoso-Guzman, W., Pintado-Caipa, M., Cuenca, J., Gamboa, C., & Lanata, S. (2021). Performance of the Rowland Universal Dementia Assessment Scale for the Detection of Mild Cognitive Impairment and Dementia in a Diverse Cohort of Illiterate Persons From Rural Communities in Peru. Frontiers in Neurology, 12, 629325. https://doi.org/10.3389/fneur.2021.629325

Dementia. (n.d.). Retrieved April 28, 2026, from https://www.who.int/news-room/fact-sheets/detail/dementia

Deng, Y., Zhang, Y., Lemos, B., & Ren, H. (2017). Tissue accumulation of microplastics in mice and biomarker responses suggest widespread health risks of exposure. Scientific Reports, 7, 46687. https://doi.org/10.1038/srep46687

Deng, Z., Li, L., Jing, Z., Luo, X., Yu, F., Zeng, W., Bi, W., & Zou, J. (2024). Association between environmental phthalates exposure and gut microbiota and metabolome in dementia with Lewy bodies. Environment International, 190, 108806. https://doi.org/10.1016/j.envint.2024.108806

Diez Roux, A. V. (2022). Social Epidemiology: Past, Present, and Future. Annual Review of Public Health, 43(1), 79–98. https://doi.org/10.1146/annurev-publhealth-060220-042648

Di Spirito, F., Folliero, V., Di Palo, M. P., De Benedetto, G., Aulisio, L., Martina, S., Rinaldi, L., & Franci, G. (2025). Micro- and Nanoplastics and the Oral Cavity: Implications for Oral and Systemic Health, Dental Practice, and the Environment—A Narrative Review. Journal of Functional Biomaterials, 16(9), 332. https://doi.org/10.3390/jfb16090332

Dutta, S., Haggerty, D. K., Rappolee, D. A., & Ruden, D. M. (2020). Phthalate Exposure and Long-Term Epigenomic Consequences: A Review. Frontiers in Genetics, 11, 405. https://doi.org/10.3389/fgene.2020.00405

Diez Roux, A. V. (2001). Investigating neighborhood and area effects on health. American journal of public health, 91(11), 1783-1789.

Deda, O., Gika, H. G., Wilson, I. D., & Theodoridis, G. A. (2015). An overview of fecal sample preparation for global metabolic profiling. Journal of Pharmaceutical and Biomedical Analysis, REVIEW 2015, 113, 137–150. https://doi.org/10.1016/j.jpba.2015.02.006

Deng, Z., Li, L., Jing, Z., Luo, X., Yu, F., Zeng, W., Bi, W., & Zou, J. (2024). Association between environmental phthalates exposure and gut microbiota and metabolome in dementia with Lewy bodies. Environment International, 190, 108806. https://doi.org/10.1016/j.envint.2024.108806

Dementia Statistics. (2021). Alzheimer's Disease International. https://www.alzint.org/about/dementia-facts-figures/dementia-statistics/

Eyting, M., Xie, M., Michalik, F., Heß, S., Chung, S., & Geldsetzer, P. (2025). A natural experiment on the effect of herpes zoster vaccination on dementia. Nature, 641(8062), 438–446. https://doi.org/10.1038/s41586-025-08800-x

Engel, S. M., Patisaul, H. B., Brody, C., Hauser, R., Zota, A. R., Bennet, D. H., Swanson, M., & Whyatt, R. M. (2021). Neurotoxicity of Ortho-Phthalates: Recommendations for Critical Policy Reforms to Protect Brain Development in Children. American Journal of Public Health, 111(4), 687–695. https://doi.org/10.2105/AJPH.2020.306014

Environmental Protection Agency. (2017). Toxics Release Inventory (TRI) Data for the year 2017. Retrieved from https://www.epa.gov/toxics-release-inventory-tri-program/tri-basic-data-files-calendar-years-1987-2017

EPA Announces Intent to Regulate Dozens of Uses of Five Phthalate Chemicals to Protect Workers and Environment | US EPA. (2025, December 31). US EPA.

Environmental Protection Agency (2017). Biomonitoring: Phthalates. America's Children and the Environment | Third Edition. https://www.epa.gov/sites/default/files/2017-08/documents/phthalates_updates_live_file_508_0.pdf

Erben, V., Poschet, G., Schrotz-King, P., & Brenner, H. (2021). Evaluation of different stool extraction methods for metabolomics measurements in human faecal samples. BMJ Nutrition, Prevention & Health, 4(2), 374–384. https://doi.org/10.1136/bmjnph-2020-000202

Eren, A. M., Sogin, M. L., Morrison, H. G., Vineis, J. H., Fisher, J. C., Newton, R. J., & McLellan, S. L. (2015). A single genus in the gut microbiome reflects host preference and specificity. The ISME Journal, 9(1), 90–100. https://doi.org/10.1038/ismej.2014.97

ELS, L. C. (2024, May 15). Prebiotics: Understanding their role in gut health. Harvard Health. https://www.health.harvard.edu/diet-and-nutrition/prebiotics-understanding-their-role-in-gut-health

Fox, A. (2026, March 16). Human-Made Chemicals Found Throughout Ocean Environments | Scripps Institution of Oceanography. https://scripps.ucsd.edu/news/human-made-chemicals-found-throughout-ocean-environments

Fricker, R. D. (n.d.). Environmental equity and the distribution of toxic release inventory and other environmentally undesirable sites in metropolitan New York City.

Farsetta, D. (2020, October 27). Taking Stress in STRIDE: Learning How to Support Brain Health. Center for Aging Research and Education; UW Madison School of Nursing. https://care.nursing.wisc.edu/2020/10/27/taking-stress-in-stride-learning-how-to-support-brain-health/

Freedman, V., McFall B. H., Ryan, L. (2019). Adding the AD8 Dementia Screen to the Panel Study of Income Dynamics (Technical Series Paper #19-01). University of Michigan, Institute for Social Research.

Frey, Christopher H. (2022). EPA Researchers Release Cumulative Impacts Report, Prioritizing Environmental Justice in New Research Cycle. Environmental Protection Agency. Science Matters.

Figueroa, J. F., Frakt, A. B., & Jha, A. K. (2020). Addressing Social Determinants of Health: Time for a Polysocial Risk Score. JAMA, 323(16), 1553–1554. https://doi.org/10.1001/jama.2020.2436

Frndak, S., Cudjoe, T., Thorpe, R. J., Deng, Z., Ward-Caviness, C. K., Clarke, K. A., & Dickerson, A. S. (2024). Social cohesion as a modifier of joint air pollution exposure and incident dementia. Science of The Total Environment, 949, 175149.

Galvin, J. E., Roe, C. M., Xiong, C., & Morris, J. C. (2006). Validity and reliability of the AD8 informant interview in dementia. Neurology, 67(11), 1942–1948. https://doi.org/10.1212/01.wnl.0000247042.15547.eb

Gower, J. C. (1966). Some distance properties of latent root and vector methods used in multivariate analysis. Biometrika, 53(3–4), 325–338. https://doi.org/10.1093/biomet/53.3-4.325

GeoLytics & Urban Institute. (2023). Neighborhood Change Database (NCDB) 1990–2020. GeoLytics, Inc. and The Urban Institute.

Goodrich, J. K., Waters, J. L., Poole, A. C., Sutter, J. L., Koren, O., Blekhman, R., Beaumont, M., Van Treuren, W., Knight, R., Bell, J. T., Spector, T. D., Clark, A. G., & Ley, R. E. (2014). Human Genetics Shape the Gut Microbiome. Cell, 159(4), 789–799. https://doi.org/10.1016/j.cell.2014.09.053

Genuis, S. J., Beesoon, S., Lobo, R. A., & Birkholz, D. (2012). Human Elimination of Phthalate Compounds: Blood, Urine, and Sweat (BUS) Study. The Scientific World Journal, 2012, 615068. https://doi.org/10.1100/2012/615068

Guo, Z., Feng, Y.-L., & Wang, J. (2019). A new strategy for non-targeted screening of phthalate metabolites using liquid chromatography-high resolution mass spectrometry. International Journal of Mass Spectrometry, 443, 46–52. https://doi.org/10.1016/j.ijms.2019.06.003

Galindo, N., Varea, M., Gil-Moltó, J., Yubero, E., & Nicolás, J. (2011). The Influence of Meteorology on Particulate Matter Concentrations at an Urban Mediterranean Location. Water, Air, & Soil Pollution, 215(1), 365–372. https://doi.org/10.1007/s11270-010-0484-z

Gimeno-Ferrer, F., Porschen, L. T., Matthes, F., Gohlsch, K., & Meissner, A. (2026). Airborne particulates and brain health: The role of PM2.5 in blood–brain-barrier dysfunction. Journal of Cerebral Blood Flow & Metabolism, 0271678X261418925. https://doi.org/10.1177/0271678X261418925

Hernandez, H., Santamaria-Garcia, H., Moguilner, S., Farina, F. R., Legaz, A., Prado, P., Cuadros, J., Gonzalez, L., Gonzalez-Gomez, R., Migeot, J., Coronel-Oliveros, C., Tagliazucchi, E., Maito, M. A., Godoy, M. E., Cruzat, J., Shaheen, A., Farombi, T., Salazar, D., Da Ros, L. U., … Ibanez, A. (2025). The exposome of healthy and accelerated aging across 40 countries. Nature Medicine, 31(9), 3089–3100. https://doi.org/10.1038/s41591-025-03808-2

Herrera-Perez, E., Custodio, N., Diaz, M., Montesinos, R., Chang, A., Villafuerte, M., & Lanata, S. (2023). Epidemiology of neurocognitive disorders in adults from urban-marginalized areas: A door-to-door population-based study in Puente Piedra, Lima, Peru. Frontiers in Public Health, 11, 1228008. https://doi.org/10.3389/fpubh.2023.1228008

Hasan, Md. M., Tama, R. T., Dona, H. A., Hoque, N. S., Rahaman, Md. A., & Alam, Md. A. (2025). Comprehensive review of phthalate exposure: Health implications, biomarker detection and regulatory standards. The Journal of Steroid Biochemistry and Molecular Biology, 247, 106671. https://doi.org/10.1016/j.jsbmb.2024.106671

Heston, M. B., Hanslik, K. L., Zarbock, K. R., Harding, S. J., Davenport-Sis, N. J., Kerby, R. L., Chin, N., Sun, Y., Hoeft, A., Deming, Y., Vogt, N. M., Betthauser, T. J., Johnson, S. C., Asthana, S., Kollmorgen, G., Suridjan, I., Wild, N., Zetterberg, H., Blennow, K., … Ulland, T. K. (2023). Gut inflammation associated with age and Alzheimer's disease pathology: A human cohort

study. Scientific Reports, 13(1), 18924. https://doi.org/10.1038/s41598-023-45929-z

Heudorf, U., Mersch-Sundermann, V., & Angerer, J. (2007). Phthalates: Toxicology and exposure. International Journal of Hygiene and Environmental Health, 210(5), 623–634. https://doi.org/10.1016/j.ijheh.2007.07.011

Hitha, P., Pillai, S.,, Butt, C., Lee, H., and Stahl-Zeng, J. (2023). Sensitive and precise quantitation of 29 phthalate esters in food simulants and beverages. SCIEX. DH Tech. Dev. Pte. Ltd. https://sciex.com/content/dam/SCIEX/pdf/tech-notes/food-and-beverage/food-and-beverage/MKT-27155-A_Phthalate_Esters_4500_Final2.pdf

Husøy, T., Andreassen, M., Hjertholm, H., Carlsen, M. H., Norberg, N., Sprong, C., Papadopoulou, E., Sakhi, A. K., Sabaredzovic, A., & Dirven, H. A. A. M. (2019). The Norwegian biomonitoring study from the EU project EuroMix: Levels of phenols and phthalates in 24-hour urine samples and exposure sources from food and personal care products. Environment International, 132, 105103. https://doi.org/10.1016/j.envint.2019.105103

Hamoudi, A., & Dowd, J. B. (2014). Housing Wealth, Psychological Well-being, and Cognitive Functioning of Older Americans. The Journals of Gerontology: Series B, 69(2), 253–262. https://doi.org/10.1093/geronb/gbt114

Human Rights Watch. (2024). US: Louisiana's "Cancer Alley" | Dire Health Crisis From Government Failure to Rein in Fossil Fuels. Human Rights Watch.

Hale, R. C., Seeley, M. E., La Guardia, M. J., Mai, L., & Zeng, E. Y. (2020). A Global Perspective on Microplastics. Journal of Geophysical Research: Oceans, 125(1), e2018JC014719. https://doi.org/10.1029/2018JC014719

Heston, M. B., Carlsson, C. M., Engelman, C. D., Jonaitis, E. M., Van Hulle, C. A., Deming, Y., Johnson, S. C., Asthana, S., Kollmorgen, G., Suridjan, I., Wild, N., Blennow, K., Zetterberg, H., Rey, F. E., & Bendlin, B. B. (2022). Gut microbe-modulated metabolites are longitudinally associated with higher neurodegeneration biomarkers in cerebrospinal fluid (CSF). Alzheimer's & Dementia, 18(S6), e067893. https://doi.org/10.1002/alz.067893

Husted, G., Cassels, S., Ackert, E., & Sweeney, S. (2024). Socio-demographic patterning of urinary mono-ethyl phthalate levels among children and adults in the U.S. (1999–2018). Environmental Research Communications, 6(8), 085012. https://doi.org/10.1088/2515-7620/ad6403

Heller, C., Güllmar, D., Colic, L., Pritschet, L., Gell, M., Javaheripour, N., de la Cruz, F., Rojczyk, P., Koeppel, C. J., Larsen, B., Ganjgahi, H., Lange, F. J., Buck, A.-C., Jesgarzewsky, T. L., Dahnke, R., Kiehntopf, M., Jacobs, E. G., Kikinis, Z.,

Walter, M., … Gaser, C. (2025). Hormonal milieu influences whole-brain structural dynamics across the menstrual cycle using dense sampling in multiple individuals. Nature Neuroscience, 28(12), 2588–2600. https://doi.org/10.1038/s41593-025-02066-2

Homan, P. (2019). Structural Sexism and Health in the United States: A New Perspective on Health Inequality and the Gender System. American Sociological Review, 84(3), 486–516. https://doi.org/10.1177/0003122419848723

Iimi, A., Ahmed, F., Anderson, E. C., Diehl, A. S., Maiyo, L., Peralta-Quirós, T., & Rao, K. (2016). New Rural Access Index: Main Determinants and Correlation to Poverty (SSRN Scholarly Paper No. 2867657). Social Science Research Network. https://papers.ssrn.com/abstract=2867657

Ilenič, A., Mauko Pranjić, A., Ščančar, J., Ščančar, R. M., & Kumar, P. (2025). Can low-cost sensors (LCS) enhance air quality monitoring for personal pollution exposure assessment? Environmental Research Communications, 7(9), 095007. https://doi.org/10.1088/2515-7620/ae02ef

Informe Nacional de la Calidad del Aire 2013—2014. (n.d.). Retrieved April 22, 2026, from https://www.gob.pe/institucion/minam/informes-publicaciones/2635-informe-nacional-de-la-calidad-del-aire-2013-2014

Is it Dementia or Mild Cognitive Impairment (MCI)? | alzfdn.org. (n.d.). Alzheimer's Foundation of America. Retrieved April 22, 2026, from https://alzfdn.org/dementia-or-mild-cognitive-impairment/

Jones, A., Ali, M. U., Mayhew, A., Aryal, K., Correia, R. H., Dash, D., Manis, D. R., Rehman, A., O'Connell, M. E., Taler, V., Costa, A. P., Hogan, D. B., Wolfson, C., Raina, P., & Griffith, L. (2025). Environmental risk factors for all-cause dementia, Alzheimer's disease dementia, vascular dementia, and mild cognitive impairment: An umbrella review and meta-analysis. Environmental Research, 270, 121007. https://doi.org/10.1016/j.envres.2025.121007

Jang, D., Lee, A.-H., Shin, H.-Y., Song, H.-R., Park, J.-H., Kang, T.-B., Lee, S.-R., & Yang, S.-H. (2021). The Role of Tumor Necrosis Factor Alpha (TNF-α) in Autoimmune Disease and Current TNF-α Inhibitors in Therapeutics. International Journal of Molecular Sciences, 22(5), 2719. https://doi.org/10.3390/ijms22052719

John R. Logan, Zengwang Xu, and Brian Stults. (2012). Interpolating US Decennial Census Tract Data from as Early as 1970 to 2010: A Longitudinal Tract Database. Professional Geographer, 66,3: 412-420.

Jagani, R., Chovatiya, J., Pulivarthi, D., Meher, A. K., Patel, D., Patel, H., Teraiya, S., & Andra, S. S. (2025). Multiclass Assays for Measuring Environmental

Chemical Mixture Exposure: Analytical Methodologies and Applications in Exposomics Research. Metabolites, 15(11), 742. https://doi.org/10.3390/metabo15110742

Jeong, S.-H., Jang, J.-H., Cho, H.-Y., & Lee, Y.-B. (2020). Toxicokinetics of diisobutyl phthalate and its major metabolite, monoisobutyl phthalate, in rats: UPLC-ESI-MS/MS method development for the simultaneous determination of diisobutyl phthalate and its major metabolite, monoisobutyl phthalate, in rat plasma, urine, feces, and 11 various tissues collected from a toxicokinetic study. Food and Chemical Toxicology, 145, 111747. https://doi.org/10.1016/j.fct.2020.111747

Jones, J., Reinke, S.N., Ali, A. et al. (2021) Fecal sample collection methods and time of day impact microbiome composition and short chain fatty acid concentrations. Sci Rep 11, 13964. https://doi.org/10.1038/s41598-021-93031-z

Jin, S., Cui, S., Mu, X., Liu, Z., Han, Y., Cui, T., Xiong, W., Xi, W., & Zhang, X. (2023). Exposure to phthalates and their alternatives in relation to biomarkers of inflammation and oxidative stress in adults: Evidence from NHANES 2017–2018. Environmental Science and Pollution Research, 30(59), 123770–123784. https://doi.org/10.1007/s11356-023-30924-8

Kaufman, L., & Rousseeuw, P. J. (1990). Finding groups in data: An introduction to cluster analysis. Wiley. https://doi.org/10.1002/9780470316801

Karlsson, O., Rocklöv, J., Lehoux, A. P., Bergquist, J., Rutgersson, A., Blunt, M. J., & Birnbaum, L. S. (2021). The human exposome and health in the Anthropocene. International Journal of Epidemiology, 50(2), 378–389. https://doi.org/10.1093/ije/dyaa231

Kalaria, R., Maestre, G., Mahinrad, S., Acosta, D. M., Akinyemi, R. O., Alladi, S., Allegri, R. F., Arshad, F., Babalola, D. O., Baiyewu, O., Bak, T. H., Bellaj, T., Brodie-Mends, D. K., Carrillo, M. C., Celestin, K.-K.-M., Damasceno, A., de Silva, R. K., de Silva, R., Djibuti, M., … Ismail, O. (2024). The 2022 symposium on dementia and brain aging in low- and middle-income countries: Highlights on research, diagnosis, care, and impact. Alzheimer's & Dementia, 20(6), 4290–4314. https://doi.org/10.1002/alz.13836

Keyes, T., Domingo, R., Dynowski, S., Graves, R., Klein, M., Leonard, M., Pilgrim, J., Sanchirico, A., & Trinkaus, K. (2023). Low-cost PM2.5 sensors can help identify driving factors of poor air quality and benefit communities. Heliyon, 9(9), E19876.

Krieger, N. (2011). Epidemiology and the People's Health: Theory and Context. Oxford University Press. https://doi.org/10.1093/acprof:oso/9780195383874.001.0001

Karakose, S., Luchetti, M., Stephan, Y., Sutin, A. R., & Terracciano, A. (2025). Marital status and risk of dementia over 18 years: Surprising findings from the National Alzheimer's Coordinating Center. Alzheimer's & dementia : the journal of the Alzheimer's Association, 21(3), e70072. https://doi.org/10.1002/alz.70072

Kind, A. J. H., & Buckingham, W. (2018). Making neighborhood disadvantage metrics accessible: The neighborhood atlas. New England Journal of Medicine, 378, 2456-2458. https://doi.org/10.1056/NEJMp1802313

Kravitz-Wirtz, N., Crowder, K., Hajat, A., & Sass, V. (2016). The Long-term Dynamics of Racial/Ethnic Inequality in Neighborhood Air Pollution Exposure, 1990-2009. Du Bois Review : Social Science Research on Race, 13(2), 237–259. https://doi.org/10.1017/S1742058X16000205

Kushel, M. B., Gupta, R., Gee, L., & Haas, J. S. (2006). Housing instability and food insecurity as barriers to health care among low-income americans. Journal of General Internal Medicine, 21(1), 71–77. https://doi.org/10.1111/j.1525-1497.2005.00278.x

Khasanov, S., Tolibov, M., & Daminova, N. (2026). Bridging the gaps in Alzheimer's disease biomarker research: From multi-omics integration to point-of-care diagnostics, a comprehensive review. Clinica Chimica Acta, 589, 121046. https://doi.org/10.1016/j.cca.2026.121046

Kato, K., Silva, M. J., Needham, L. L., & Calafat, A. M. (2006). Quantifying Phthalate Metabolites in Human Meconium and Semen Using Automated Off-Line Solid-Phase Extraction Coupled with On-Line SPE and Isotope-Dilution High-Performance Liquid Chromatography–Tandem Mass Spectrometry. Analytical Chemistry, 78(18), 6651–6655. https://doi.org/10.1021/ac0608220

Kelly, P. E., Ng, H. J., Farrell, G., McKirdy, S., Russell, R. K., Hansen, R., Rattray, Z. R., & Gerasimidis, K. (2022). An optimised monophasic faecal extraction method for LC-MS analysis and its application in gastrointestinal disease. Metabolites, 12(11), 1110. https://doi.org/10.3390/metabo12111110

Kind, A. J. H., Bendlin, B. B., Keller, S. A., & Powell, W. R. (2020). Adverse Social Exposome by Area Deprivation Index (ADI) and Alzheimer's Disease and Related Dementias (ADRD) Neuropathology for a National Cohort of Brain Donors within the Neighborhoods Study.

Koch, H.M., Gonzalez-Reche, L.M., Angerer, J., 2003a. Online cleanup by multidimensional LC-ESI-MS/MS for high throughput quantification of primary and secondary phthalate metabolites in human urine. J. Chromatogr. B 784, 169–182.

Koch, H. M., & Calafat, A. M. (2009). Human body burdens of chemicals used in plastic manufacture. Philosophical Transactions of the Royal Society B: Biological Sciences, 364(1526), 2063–2078. https://doi.org/10.1098/rstb.2008.0208

Kowalski, K., & Mulak, A. (2019). Brain-Gut-Microbiota Axis in Alzheimer's Disease. Journal of Neurogastroenterology and Motility, 25(1), 48–60. https://doi.org/10.5056/jnm18087

Kunde, H., Ioannou, E. I., Chovatiya, J., Jagani, R., Charisiadis, P., Arora, M., Andra, S. S., & Makris, K. C. (2025). An exposomics analysis of 125 biomarkers of exposure to food contaminants and biomarkers of oxidative stress: A randomized cross-over chrononutrition trial of healthy adults. Environment International, 202, 109682. https://doi.org/10.1016/j.envint.2025.109682

Kwak, S., Usyk, M., Beggs, D., Choi, H., Ahdoot, D., Wu, F., Maceda, L., Li, H., Im, E.-O., Han, H.-R., Lee, E., Wu, A. H., Hayes, R. B., & Ahn, J. (2024). Sociobiome—Individual and neighborhood socioeconomic status influence the gut microbiome in a multi-ethnic population in the US. Npj Biofilms and Microbiomes, 10(1), 19. https://doi.org/10.1038/s41522-024-00491-y

Lassalle, M. W. (2024) The present state of low-cost air quality sensors in Japan and their accuracy, International Journal of Environmental Studies, pp. 1–19.

Lei, M., Menon, R., Manteiga, S., Alden, N., Hunt, C., Alaniz, R. C., Lee, K., & Jayaraman, A. (2019). Environmental Chemical Diethylhexyl Phthalate Alters Intestinal Microbiota Community Structure and Metabolite Profile in Mice. mSystems, 4(6), 10.1128/msystems.00724-19. https://doi.org/10.1128/msystems.00724-19

Lim, U., & Park, S. Y. (2022). Racial and ethnic disparities in Alzheimer's dementia. Aging, 14(22), 8884–8885. https://doi.org/10.18632/aging.204421

Link, B. G., Phelan, J. C., Miech, R., & Westin, E. L. (2008). The Resources That Matter: Fundamental Social Causes of Health Disparities and the Challenge of Intelligence. Journal of Health and Social Behavior, 49(1), 72–91. https://doi.org/10.1177/002214650804900106

Livingston, G., Huntley, J., Sommerlad, A., Ames, D., Ballard, C., Banerjee, S., Brayne, C., Burns, A., Cohen-Mansfield, J., Cooper, C., Costafreda, S. G., Dias, A., Fox, N., Gitlin, L. N., Howard, R., Kales, H. C., Kivimäki, M., Larson, E. B., Ogunniyi, A., … Mukadam, N. (2020). Dementia prevention, intervention, and care: 2020 report of the Lancet Commission. The Lancet, 396(10248), 413–446. https://doi.org/10.1016/S0140-6736(20)30367-6

Larsen, D. A., Hill, D., Zhu, Y., Alazawi, M., Chatila, D., Dunham, C., Faruolo, C., Ferro, B., Godinez, A., Hanson, B., Insaf, T., Lang, D., Neigel, D., Neyra, M., Pulido, N., Wilder, M., Yang, N., Kmush, B., & Green, H. (2024). Non-detection of emerging and re-emerging pathogens in wastewater surveillance to confirm absence of transmission risk: A case study of polio in New York. PLOS Global Public Health, 4(12), e0002381. https://doi.org/10.1371/journal.pgph.0002381

Lee, S., Lee, K. M., Han, S. M., Lee, H.-J., Sung, C., Min, H., Im, H., Han, S. B., Cha, S., & Lee, J. (2022). Comprehensive LC-MS/MS method combined with tandem hybrid hydrolysis for multiple exposure assessment of multiclass environmental pollutants. Environmental Research, 211, 113053. https://doi.org/10.1016/j.envres.2022.113053

Li, Z.-M., & Kannan, K. (2024). Urinary and Fecal Excretion of 121 Environmental Chemicals in Pet Dogs and Cats: Significance of Feces in Biomonitoring of Exposures. Environmental Science & Technology, 58(32), 14169–14179. https://doi.org/10.1021/acs.est.4c05991

Liu, X., Mao, B., Gu, J., Wu, J., Cui, S., Wang, G., Zhao, J., Zhang, H., & Chen, W. (2021). Blautia—A new functional genus with potential probiotic properties? Gut Microbes, 13(1), 1875796. https://doi.org/10.1080/19490976.2021.1875796

Lenart-Bugla, M., Szcześniak, D., Bugla, B., Kowalski, K., Niwa, S., Rymaszewska, J., & Misiak, B. (2022). The association between allostatic load and brain: A systematic review. Psychoneuroendocrinology, 145, 105917. https://doi.org/10.1016/j.psyneuen.2022.105917

Lead and Children's Health. (2026, April 20). ArcGIS StoryMaps. https://storymaps.arcgis.com/stories/8c13aadca257491d9e99428b2c9f13db

Lim, X. (2021.). Microplastics are everywhere – but are they harmful? https://www.nature.com/articles/d41586-021-01143-3.

Maechler, M., Rousseeuw, P., Struyf, A., Hubert, M., & Hornik, K. (2024). cluster: Cluster analysis basics and extensions (R package version 2.1.6) [Computer software]. https://CRAN.R-project.org/package=cluster

Marmot, M. (2015). The health gap: The challenge of an unequal world. The Lancet, 386(10011), 2442–2444. https://doi.org/10.1016/S0140-6736(15)00150-6

Marmot, M. 2015. The Health Gap: The Challenge of an Unequal World. Bloomsbury Press

Marmot, M. (2017). The Health Gap: The Challenge of an Unequal World: the argument. International Journal of Epidemiology, 46(4), 1312–1318. https://doi.org/10.1093/ije/dyx163

Marmot, M (2004). Status Syndrome. Wiley Online Library. Retrieved April 18, 2023, from https://rss.onlinelibrary.wiley.com/doi/full/10.1111/j.1740-9713.2004.00058.x

Majoka, M. A., & Schimming, C. (2021). Effect of Social Determinants of Health on Cognition and Risk of Alzheimer Disease and Related Dementias. Clinical Therapeutics, 43(6), 922–929. https://doi.org/10.1016/j.clinthera.2021.05.005

MahmoudianDehkordi, S., Arnold, M., Nho, K., Ahmad, S., Jia, W., Xie, G., Louie, G., Kueider-Paisley, A., Moseley, M. A., Thompson, J. W., St John Williams, L., Tenenbaum, J. D., Blach, C., Baillie, R., Han, X., Bhattacharyya, S., Toledo, J. B., Schafferer, S., Klein, S., … for the Alzheimer's Disease Neuroimaging Initiative and the Alzheimer Disease Metabolomics Consortium. (2019). Altered bile acid profile associates with cognitive impairment in Alzheimer's disease—An emerging role for gut microbiome. Alzheimer's & Dementia, 15(1), 76–92. https://doi.org/10.1016/j.jalz.2018.07.217

Mistridis, P., Mata, J., Neuner-Jehle, S., Annoni, J.-M., Biedermann, A., Bopp-Kistler, I., Brand, D., Guevara, A. B., Decrey-Wick, H., Démonet, J.-F., Hemmeter, U., Kressig, R. W., Martin, B., Rampa, L., Savaskan, E., Stuck, A. E., Tschopp, P., Zekry, D., & Monsch, A. U. (2017). Use it or lose it! Cognitive activity as a protective factor for cognitive decline associated with Alzheimer's disease. Swiss Medical Weekly, 147(0910), w14407–w14407. https://doi.org/10.4414/smw.2017.14407

Martínez, I., Lattimer, J. M., Hubach, K. L., Case, J. A., Yang, J., Weber, C. G., Louk, J. A., Rose, D. J., Kyureghian, G., Peterson, D. A., Haub, M. D., & Walter, J. (2013). Gut microbiome composition is linked to whole grain-induced immunological improvements. The ISME Journal, 7(2), 269–280. https://doi.org/10.1038/ismej.2012.104

Maturana, J. L., & Cárdenas, J. P. (2021). Insights on the Evolutionary Genomics of the Blautia Genus: Potential New Species and Genetic Content Among Lineages. Frontiers in Microbiology, 12. https://doi.org/10.3389/fmicb.2021.660920

Mayo Foundation for Medical Education and Research. (2022). Glial Fibrillary Acidic Protein, Plasma - BioPharma Diagnostics. Testcatalog.org. https://biopharma.testcatalog.org/show/BGFAP

Moghazy, M., Papathanasiou, M., Tzoupis, H., Papavasileiou, K. D., Xing, C., Lauschke, V. M., Afantitis, A., & Melagraki, G. (2025). A Systematic Literature

Review of Reproductive Toxicological Studies on Phthalates. International Journal of Molecular Sciences, 26(18), 8761. https://doi.org/10.3390/ijms26188761

Moguilner, S., Baez, S., Hernandez, H., Migeot, J., Legaz, A., Gonzalez-Gomez, R., Farina, F. R., Prado, P., Cuadros, J., Tagliazucchi, E., Altschuler, F., Maito, M. A., Godoy, M. E., Cruzat, J., Valdes-Sosa, P. A., Lopera, F., Ochoa-Gómez, J. F., Hernandez, A. G., Bonilla-Santos, J., … Ibanez, A. (2024). Brain clocks capture diversity and disparities in aging and dementia across geographically diverse populations. Nature Medicine, 30(12), 3646–3657. https://doi.org/10.1038/s41591-024-03209-x

Nakashima, H., Shinohara, R., Emoto, T., Saito, Y., Yoshida, N., Hirata, K., Murakami, T., Mori, H., Toyoda, A., Sugiyama, T., Yamada, T., & Yamashita, T. (2025). Phocaeicola dorei andPhocaeicola vulgatus Protect against Atherosclerosis by Regulating Gut Immunity. Journal of Atherosclerosis and Thrombosis, 32(11), 1447–1463. https://doi.org/10.5551/jat.65460

Ngandu, T., Lehtisalo, J., Solomon, A., Levälahti, E., Ahtiluoto, S., Antikainen, R., Bäckman, L., Hänninen, T., Jula, A., Laatikainen, T., Lindström, J., Mangialasche, F., Paajanen, T., Pajala, S., Peltonen, M., Rauramaa, R., Stigsdotter-Neely, A., Strandberg, T., Tuomilehto, J., … Kivipelto, M. (2015). A 2 year multidomain intervention of diet, exercise, cognitive training, and vascular risk monitoring versus control to prevent cognitive decline in at-risk elderly people (FINGER): A randomised controlled trial. Lancet, 385(9984), 2255–2263. https://doi.org/10.1016/S0140-6736(15)60461-5

Neuman, S. (2019, August 22). WHO Study Finds No Evidence Of Health Concerns From Microplastics In Drinking Water. NPR. https://www.npr.org/2019/08/22/753324757/who-study-finds-no-evidence-of-health-concerns-from-microplastics-in-drinking-wa

Nihart, A. J., Garcia, M. A., El Hayek, E., Liu, R., Olewine, M., Kingston, J. D., Castillo, E. F., Gullapalli, R. R., Howard, T., Bleske, B., Scott, J., Gonzalez-Estrella, J., Gross, J. M., Spilde, M., Adolphi, N. L., Gallego, D. F., Jarrell, H. S., Dvorscak, G., Zuluaga-Ruiz, M. E., … Campen, M. J. (2025). Bioaccumulation of microplastics in decedent human brains. Nature Medicine, 31(4), 1114–1119. https://doi.org/10.1038/s41591-024-03453-1

Oksanen, J., Simpson, G. L., Blanchet, F. G., Kindt, R., Legendre, P., Minchin, P. R., O'Hara, R. B., Solymos, P., Stevens, M. H. H., Szoecs, E., Wagner, H., Barbour, M., Bedward, M., & Borcard, D. (2024). vegan: Community ecology package (R package version 2.6-6) [Computer software]. https://CRAN.R-project.org/package=vegan

Oh, J., Buckley, J. P., Kannan, K., Pellizzari, E., Miller, R. L., Bastain, T. M., Dunlop, A. L., Douglas, C., Gilliland, F. D., Herbstman, J. B., Karr, C., Porucznik, C. A.,

Hertz-Picciotto, I., Morello-Frosch, R., Sathyanarayana, S., Schmidt, R. J., Woodruff, T. J., & Bennett, D. H. (2025). Exposures to Contemporary and Emerging Chemicals among Children Aged 2 to 4 Years in the United States Environmental Influences on the Child Health Outcome (ECHO) Cohort. Environmental Science & Technology, 59(27), 13594–13610. https://doi.org/10.1021/acs.est.4c13605

O'Neal M. A. (2024). Women and the risk of Alzheimer's disease. Frontiers in global women's health, 4, 1324522. https://doi.org/10.3389/fgwh.2023.1324522

Polisky, V., Littmann, M., Triastcyn, A., Horn, M., Georgiou, A., Widenmaier, R., Anspach, B., Tahrat, H., Kumar, S., Buser-Doepner, C., Geldsetzer, P., Van Duijn, C. M., & Schwab, P. (2025). Varicella-zoster virus reactivation and the risk of dementia. Nature Medicine, 31(12), 4172–4179. https://doi.org/10.1038/s41591-025-03972-5

Pletz, M. (2022). Ingested microplastics: Do humans eat one credit card per week? Journal of Hazardous Materials Letters, 3, 100071. https://doi.org/10.1016/j.hazl.2022.100071

Pan, I., & Umapathy, S. (2024). Probiotics an emerging therapeutic approach towards gut-brain-axis oriented chronic health issues induced by microplastics: A comprehensive review. Heliyon, 10(11), e32004. https://doi.org/10.1016/j.heliyon.2024.e32004

Pope, R., Visconti, A., Zhang, X., Louca, P., Baleanu, A.-F., Lin, Y., Asnicar, F., Bermingham, K., Wong, K. E., Michelotti, G. A., Wolf, J., Segata, N., Berry, S. E., Spector, T. D., Leeming, E. R., Gibson, R., Menni, C., & Falchi, M. (2025). Faecal metabolites as a readout of habitual diet capture dietary interactions with the gut microbiome. Nature Communications, 16(1), 10051. https://doi.org/10.1038/s41467-025-66046-7

Parra, M. A., Baez, S., Sedeño, L., Gonzalez Campo, C., Santamaría-García, H., Aprahamian, I., Bertolucci, P. H., Bustin, J., Camargos Bicalho, M. A., Cano-Gutierrez, C., Caramelli, P., Chaves, M. L. F., Cogram, P., Beber, B. C., Court, F. A., de Souza, L. C., Custodio, N., Damian, A., de la Cruz, M., … Ibanez, A. (2021). Dementia in Latin America: Paving the way toward a regional action plan. Alzheimer's & Dementia, 17(2), 295–313. https://doi.org/10.1002/alz.12202

Pfeffer, R. I., Kurosaki, T. T., Harrah, C. H., Jr., Chance, J. M., & Filos, S. (1982). Measurement of Functional Activities in Older Adults in the Community1. Journal of Gerontology, 37(3), 323–329. https://doi.org/10.1093/geronj/37.3.323

Porta, A., Sanchez, E. Y., & Colman Lerner, J. E. (Eds.). (2018). Calidad del aire: Monitoreo y modelado de contaminantes atmosféricos. Efectos en la salud

pública. Editorial de la Universidad Nacional de La Plata (EDULP). https://doi.org/10.35537/10915/73756

PurpleAir in Research: Exploring Air Quality Across the Globe. (n.d.). PurpleAir. Retrieved April 22, 2026, from https://www2.purpleair.com/pages/exploring-air-quality-across-the-globe

Quince, C., Walker, A. W., Simpson, J. T., Loman, N. J., & Segata, N. (2017). Shotgun metagenomics, from sampling to analysis. Nature Biotechnology, 35(9), 833–844. https://doi.org/10.1038/nbt.3935

Rinninella E, Raoul P, Cintoni M, Franceschi F, Miggiano GAD, Gasbarrini A, Mele MC. (2019). What is the Healthy Gut Microbiota Composition? A Changing Ecosystem across Age, Environment, Diet, and Diseases. Microorganisms 7(1):14. https://doi.org/10.3390/microorganisms7010014. PMID: 30634578; PMCID: PMC6351938

Ribeiro, F., Teixeira-Santos, A. C., Caramelli, P., & Leist, A. K. (2022). Prevalence of dementia in Latin America and Caribbean countries: Systematic review and meta-analyses exploring age, sex, rurality, and education as possible determinants. Ageing Research Reviews, 81, 101703. https://doi.org/10.1016/j.arr.2022.101703

Romero-Baylón, A. A., Mayorga-Rojas, J. C., Del Valle, J. C., Diaz-Cartagena, W. J., Ccatamayo-Barrios, J. H., & Soto-Juscamayta, L. M. (2024). Spatial Localization of Air Pollutants in Lima: Air Quality Monitoring in the Troposphere. International Journal of Environmental Impacts, 7(3), 485–493. https://doi.org/10.18280/ijei.070310

Roy, R., & D'Angiulli, A. (2024). Air pollution and neurological diseases, current state highlights. Frontiers in Neuroscience, 18, 1351721. https://doi.org/10.3389/fnins.2024.1351721

Rappaport, S. M. (2011). Implications of the exposome for exposure science. Journal of Exposure Science & Environmental Epidemiology, 21(1), Article 1. https://doi.org/10.1038/jes.2010.50

Rousseeuw, P. J. (1987). Silhouettes: A graphical aid to the interpretation and validation of cluster analysis. Journal of Computational and Applied Mathematics, 20, 53–65. https://doi.org/10.1016/0377-0427(87)90125-7

Shannon, C. E. (1948). A mathematical theory of communication. Bell System Technical Journal, 27(3), 379–423. https://doi.org/10.1002/j.1538-7305.1948.tb01338.x

Stallard, P. J. E., Ukraintseva, S. V., & Doraiswamy, P. M. (2025). Changing Story of the Dementia Epidemic. JAMA, 333(18), 1579–1580. https://doi.org/10.1001/jama.2025.1897

Selling Smoke: Tobacco Advertising and Anti-Smoking Campaigns · Yale University Library Online Exhibitions. (n.d.). Retrieved April 28, 2026, from https://onlineexhibits.library.yale.edu/s/sellingsmoke/page/sellingsmoke

Sharkey, P., & Faber, J. W. (2014). Where, When, Why, and For Whom Do Residential Contexts Matter? Moving Away from the Dichotomous Understanding of Neighborhood Effects. Annual Review of Sociology, 40(1), 559–579. https://doi.org/10.1146/annurev-soc-071913-043350

Strehlow, C. D. (1972). The Use of Deciduous Teeth as Indicators of Lead Exposure [Ph.D., New York University, School of Engineering and Science]. https://www.proquest.com/docview/288021577/citation/688EA79DBB754528PQ/1

Saric, J., Wang, Y., Li, J., Coen, M., Utzinger, J., Marchesi, J. R., Keiser, J., Veselkov, K., Lindon, J. C., Nicholson, J. K., & Holmes, E. (2008). Species Variation in the Fecal Metabolome Gives Insight into Differential Gastrointestinal Function. Journal of Proteome Research, 7(1), 352–360. https://doi.org/10.1021/pr070340k

Senta, I., Rodríguez-Mozaz, S., Corominas, L., & Petrovic, M. (2020). Wastewater-based epidemiology to assess human exposure to personal care and household products – A review of biomarkers, analytical methods, and applications. Trends in Environmental Analytical Chemistry, 28, e00103. https://doi.org/10.1016/j.teac.2020.e00103

Sheridan, P., Martin, J. C., Lawley, T. D., Browne, H. P., Harris, H. M. B., Bernalier-Donadille, A., Duncan, S. H., O'Toole, P. W., P. Scott, K., & J. Flint, H. (2016). Polysaccharide utilization loci and nutritional specialization in a dominant group of butyrate-producing human colonic Firmicutes. Microbial Genomics, 2(2), e000043. https://doi.org/10.1099/mgen.0.000043

Silva, M. J., Samandar, E., Preau, J. L., Reidy, J. A., Needham, L. L., & Calafat, A. (2005). Automated solid-phase extraction and quantitative analysis of 14 phthalate metabolites in human serum using isotope dilution-high-performance liquid chromatography-tandem mass spectrometry. Journal of Analytical Toxicology, 29(8), 819–824. https://doi.org/10.1093/jat/29.8.819

Simrén, J., Andreasson, U., Gobom, J., Suarez Calvet, M., Borroni, B., Gillberg, C., Nyberg, L., Ghidoni, R., Fernell, E., Johnson, M., Depypere, H., Hansson, C., Jonsdottir, I. H., Zetterberg, H., & Blennow, K. (2022). Establishment of reference values for plasma neurofilament light based on healthy individuals

aged 5–90 years. Brain Communications, 4(4), fcac174. https://doi.org/10.1093/braincomms/fcac174

Somarelli, J. A., Arnold, J. W., & West, A. B. (2026). The carcinogenic consequences of the plastic pollution crisis. The Journal of Clinical Investigation, 136(4). https://doi.org/10.1172/JCI203775

Stavroulas, I., Grivas, G., Michalopoulos, P., Liakakou, E., Bougiatioti, A., Kalkavouras, P., Fameli, K. M., Hatzianastassiou, N., Mihalopoulos, N., & Gerasopoulos, E. (2020). Field Evaluation of Low-Cost PM Sensors (Purple Air PA-II) Under Variable Urban Air Quality Conditions, in Greece. Atmosphere, 11(9), 926.

Stokvis, E., Rosing, H., & Beijnen, J. H. (2005). Stable isotopically labeled internal standards in quantitative bioanalysis using liquid chromatography/mass spectrometry: necessity or not?. Rapid communications in mass spectrometry : RCM, 19(3), 401–407. https://doi.org/10.1002/rcm.1790

Survey Research Center, Institute for Social Research (2017). Panel Study of Income Dynamics, public use dataset. University of Michigan, Ann Arbor, MI. https://psidonline.isr.umich.edu/

Sadeghzadeh, C. (2024). We inhale a credit card's worth of microplastics each week. BBC.com. https://www.bbc.com/reel/video/p0h7vcts/we-inhale-a-credit-card-s-worth-of-microplastics-each-week

Subramanian, S. et al. (2014). Persistent gut microbiota immaturity in malnourished Bangladeshi children. Nature. 510, 417–421.

StataCorp. (2025). PCA postestimation — Postestimation tools for pca and pcamat — In Stata 19 multivariate statistics reference manual. StataCorp LLC. https://www.stata.com/manuals/mvpcapostestimation.pdf

Silva, C., Büttner, B., Seisenberger, S., & Rauli, A. (2023). Proximity-centred accessibility—A conceptual debate involving experts and planning practitioners. Journal of Urban Mobility, 4, 100060. https://doi.org/10.1016/j.urbmob.2023.100060

Silva, J., Rojas, J., Norabuena, M., Molina, C., Toro, R. A., & Leiva-Guzmán, M. A. (2017). Particulate matter levels in a South American megacity: The metropolitan area of Lima-Callao, Peru. Environmental Monitoring and Assessment, 189(12), 635. https://doi.org/10.1007/s10661-017-6327-2

Steenland, K., Vu, B., & Scovronick, N. (2022). Effect modification by maximum temperature of the association between PM2.5 and short-term cardiorespiratory mortality and emergency room visits in Lima, Peru, 2010-

2016. Journal of Exposure Science & Environmental Epidemiology, 32(4), 590–595. https://doi.org/10.1038/s41370-021-00393-7

Su, J. G., Jerrett, M., Beckerman, B., Wilhelm, M., Ghosh, J. K., & Ritz, B. (2009). Predicting traffic-related air pollution in Los Angeles using a distance decay regression selection strategy. Environmental Research, 109(6), 657–670. https://doi.org/10.1016/j.envres.2009.06.001

Taylor, C. M., Pritschet, L., Yu, S., & Jacobs, E. G. (2019). Applying a Women's Health Lens to the Study of the Aging Brain. Frontiers in Human Neuroscience, 13. https://doi.org/10.3389/fnhum.2019.00224

Ty, D. and Ahuja, R. (2022). Projected Prevalence and Cost of Dementia: 2022 Update Highlights. Milken Institute. https://milkeninstitute.org/sites/default/files/2022-11/Projected%20Prevalence%20and%20Cost%20of%20Dementia%202022%20Update_Highlights_FINAL_Nov.pdf

Terrell, K. A., & St Julien, G. (2022). Air pollution is linked to higher cancer rates among black or impoverished communities in Louisiana. Environmental Research Letters, 17(1), 014033. https://doi.org/10.1088/1748-9326/ac4360

Thompson, L. (2024). Dumped or Burned: Health and Environmental Impacts of Plastic Pollution on Earth. Webinar hosted by Alliance of Nurses for Healthy Environments (ANHE).

Ting, T. W., Cheng, C. N., Chen, C. C., & Kuo, C. H. (2025). Development of an untargeted metabolomics analytical protocol for fecal samples by liquid chromatography-mass spectrometry. Journal of food and drug analysis, 33(4), 460–470. https://doi.org/10.38212/2224-6614.3571

Tapia, V., Steenland, K., Vu, B., Liu, Y., Vásquez, V., & Gonzales, G. F. (2020). PM2.5 exposure on daily cardio-respiratory mortality in Lima, Peru, from 2010 to 2016. Environmental Health, 19(1), 63. https://doi.org/10.1186/s12940-020-00618-6

Thompson, R., Smith, R. B., Karim, Y. B., Shen, C., Drummond, K., Teng, C., & Toledano, M. B. (2023). Air pollution and human cognition: A systematic review and meta-analysis. Science of The Total Environment, 859, 160234. https://doi.org/10.1016/j.scitotenv.2022.160234

Unpacking the U.S. POINTER Study | Alzheimer's Disease Research Center. (n.d.-b). Retrieved April 30, 2026, from https://adrc.wisc.edu/dementia-matters/unpacking-us-pointer-study

Udeh-Momoh, C. T., Migeot, J., Blackmon, K., Mielke, M. M., Melloni, M., Cox, L., Yaffe, K., Santamaria-Garcia, H., Stern, Y., & Ibanez, A. (2025). Resilience

and brain health in global populations. Nature Medicine, 31(8), 2518–2531. https://doi.org/10.1038/s41591-025-03846-w

Underhill, L. J., Bose, S., Williams, D. L., Romero, K. M., Malpartida, G., Breysse, P. N., Klasen, E. M., Combe, J. M., Checkley, W., & Hansel, N. N. (2015). Association of Roadway Proximity with Indoor Air Pollution in a Peri-Urban Community in Lima, Peru. International Journal of Environmental Research and Public Health, 12(10), 13466–13481. https://doi.org/10.3390/ijerph121013466

US EPA, O. (2015a, September 21). Phthalates. US EPA. https://www.epa.gov/assessing-and-managing-chemicals-under-tsca/phthalates

US EPA, O. (2015b, September 21). Risk Management for Phthalates. US EPA. https://www.epa.gov/assessing-and-managing-chemicals-under-tsca/risk-management-phthalates

US EPA, O. (n.d.). Lead Poisoning: A Historical Perspective [Overviews and Factsheets]. Retrieved April 28, 2026, from https://www.epa.gov/archive/epa/aboutepa/lead-poisoning-historical-perspective.html

Vogt, N. M., Kerby, R. L., Dill-McFarland, K. A., Harding, S. J., Merluzzi, A. P., Johnson, S. C., Carlsson, C. M., Asthana, S., Zetterberg, H., Blennow, K., Bendlin, B. B., & Rey, F. E. (2017). Gut microbiome alterations in Alzheimer's disease. Scientific Reports, 7(1), Article 1. https://doi.org/10.1038/s41598-017-13601-y

Vara, A., Yates, S. J., González Prieto, C. A., Rivera-Rodriguez, C. L., & Cullum, S. (2022). The Rowland Universal Dementia Assessment Scale (RUDAS) for the detection of dementia in a variety of healthcare settings. The Cochrane Database of Systematic Reviews, 2022(4), CD014696. https://doi.org/10.1002/14651858.CD014696

Vatanen, T., Kostic, A. D., d'Hennezel, E. & Siljander, H. (2016). Variation in microbiome LPS immunogenicity contributes to autoimmunity in humans. Cell 165, 842–853.

Verdin, M. M. (2020). Cancer Alley: Istrouma to the Gulf of Mexico. Southern Cultures, 26(2), 80–95. https://doi.org/10.1353/scu.2020.0029

Valentino, V., De Filippis, F., Marotta, R., Pasolli, E., & Ercolini, D. (2024). Genomic features and prevalence of Ruminococcus species in humans are associated with age, lifestyle, and disease. Cell Reports, 43(12), 115018. https://doi.org/10.1016/j.celrep.2024.115018

Van der Kolk, B. A. (2014). The body keeps the score: Brain, mind, and body in the healing of trauma. Viking.

Voreades, N., Kozil, A., & Weir, T. L. (2014). Diet and the development of the human intestinal microbiome. Frontiers in Microbiology, 5. https://doi.org/10.3389/fmicb.2014.00494

Wallace, L., & Zhao, T. (2023). Spatial Variation of PM2.5 Indoors and Outdoors: Results from 261 Regulatory Monitors Compared to 14,000 Low-Cost Monitors in Three Western States over 4.7 Years. Sensors, 23(9), 4387.

Wild, C. P. (2005). Complementing the Genome with an "Exposome": The Outstanding Challenge of Environmental Exposure Measurement in Molecular Epidemiology. Cancer Epidemiology, Biomarkers & Prevention, 14(8), 1847–1850. https://doi.org/10.1158/1055-9965.EPI-05-0456

Wang, Y., & Qian, H. (2021). Phthalates and Their Impacts on Human Health. Healthcare (Basel, Switzerland), 9(5), 603. https://doi.org/10.3390/healthcare9050603

Wilson, S. M., Fraser-Rahim, H., Williams, E., Zhang, H., Rice, L., Svendsen, E., & Abara, W. (2012). Assessment of the Distribution of Toxic Release Inventory Facilities in Metropolitan Charleston: An Environmental Justice Case Study. American Journal of Public Health, 102(10), 1974–1980. https://doi.org/10.2105/AJPH.2012.300700

Wong W. (2020). Economic burden of Alzheimer disease and managed care considerations. The American journal of managed care, 26(8 Suppl), S177–S183. https://doi.org/10.37765/ajmc.2020.88482

Wang HX, Wang YP (2016) Gut microbiota-brain axis. Chin Med. J 129(19):2373–2380

West, A. B., Campen, M. J., Wiesner, M., Somarelli, J. A., & Arnold, J. W. (2026). The hidden world of nanoplastics colliding with neurodegenerative diseases. The Journal of Clinical Investigation, 136(4). https://doi.org/10.1172/JCI204824

Warren, R.-R., Walter, F. Z.-A., Sergio, P., Odón, R. S.-C., Alberto, E. G.-R., & Aldo, M. (2021). Behavior of the Average Concentrations As Well As Their PM10 and PM2.5 Variability in the Metropolitan Area of Lima, Peru: Case Study February and July 2016. International Journal of Environmental Science and Development, 12(7), 204–213. https://doi.org/10.18178/ijesd.2021.12.7.1341

World Health Organization. (2021a). Global status report on the public health response to dementia [Report].

https://iris.who.int/server/api/core/bitstreams/9e8aab50-ca34-45e0-9fb0-26e675746f65/content

World Health Organization. (2021b). WHO global air quality guidelines [Executive Summary]. https://iris.who.int/server/api/core/bitstreams/b729bbc4-7032-4799-898e-d112faa16f22/content

You, R., Ho, Y.-S., & Chang, R. C.-C. (2022). The pathogenic effects of particulate matter on neurodegeneration: A review. Journal of Biomedical Science, 29(1), 15. https://doi.org/10.1186/s12929-022-00799-x

Yung, P. F., Ken Kin Lam. (2020). Air Pollution and Alzheimer's Disease: A Systematic Review and Meta-Analysis - Pengfei Fu, Ken Kin Lam Yung, 2020. Sage Journals. https://journals.sagepub.com/doi/full/10.3233/JAD-200483

Yang, Y., Lane, B., Ravndal, D., & Sorkpor, S. K. (2025). Educational Attainment and Alzheimer's Disease and Related Dementias (ADRD) Risk Among Black Adults: A Comparative Analysis of U.S.-Born and Non-U.S.-born Populations in the All of Us Research Program. Journal of applied gerontology : the official journal of the Southern Gerontological Society, 7334648251359005. Advance online publication. https://doi.org/10.1177/07334648251359005

Yang, T.-C., Kim, S., Choi, S. E., Halloway, S., Mitchell, U. A., & Shaw, B. A. (2024). Neighborhood Features and Cognitive Function: Moderating Roles of Individual Socioeconomic Status. American Journal of Preventive Medicine, 66(3), 454–462. https://doi.org/10.1016/j.amepre.2023.10.012

Yan, Z., Liu, Y., Zhang, T., Zhang, F., Ren, H., & Zhang, Y. (2022). Analysis of Microplastics in Human Feces Reveals a Correlation between Fecal Microplastics and Inflammatory Bowel Disease Status. Environmental Science & Technology, 56(1), 414–421. https://doi.org/10.1021/acs.est.1c03924

Yan, Z., Zhao, H., Zhao, Y., Zhu, Q., Qiao, R., Ren, H., & Zhang, Y. (2020). An efficient method for extracting microplastics from feces of different species. Journal of Hazardous Materials, 384, 121489. https://doi.org/10.1016/j.jhazmat.2019.121489

Yeoh, Y. K., Sun, Y., Ip, L. Y. T., Wang, L., Chan, F. K. L., Miao, Y., & Ng, S. C. (2022). Prevotella species in the human gut is primarily comprised of Prevotella copri, Prevotella stercorea and related lineages. Scientific Reports, 12(1), 9055. https://doi.org/10.1038/s41598-022-12721-4

Zafar, H., & Saier, M. H. (2012). Gut Bacteroides species in health and disease. Gut Microbes, 13(1), 1848158. https://doi.org/10.1080/19490976.2020.1848158

Zarus, G. M., Muianga, C., Hunter, C. M., & Pappas, R. S. (2021). A review of data for quantifying human exposures to micro and nanoplastics and potential health risks. Science of The Total Environment, 756, 144010. https://doi.org/10.1016/j.scitotenv.2020.144010

Zou, Y., Lin, X., Xue, W., Tuo, L., Chen, M.-S., Chen, X.-H., Sun, C., Li, F., Liu, S., Dai, Y., Kristiansen, K., & Xiao, L. (2021). Characterization and description of Faecalibacterium butyricigenerans sp. Nov. And F. longum sp. Nov., isolated from human faeces. Scientific Reports, 11(1), 11340. https://doi.org/10.1038/s41598-021-90786-3

Zuniga-Chaves, I., Eggers, S., Kates, A. E., Safdar, N., Suen, G., & Malecki, K. M. C. (2023). Neighborhood socioeconomic status is associated with low diversity gut microbiomes and multi-drug resistant microorganism colonization. Npj Biofilms and Microbiomes, 9(1), 61. https://doi.org/10.1038/s41522-023-00430-3

Zetterberg, H., & Bendlin, B. B. (2021). Biomarkers for Alzheimer's disease – preparing for a new era of disease-modifying therapies. Molecular Psychiatry, 26(1), 296–308. https://doi.org/10.1038/s41380-020-0721-9

Zegarra-Valdivia, J., Pérez-Fernández, L., Casimiro-Arana, M., Arana-Nombera, H., Gallegos-Manayay, V. N., del Rosario Oliva-Piscoya, M., Alamo-Medina, R., Abanto-Saldaña, E., Vásquez-Zuñe, N., Pérez, L. D., Gutierrez-Flores, D., Tantarico, L. L., Hernández, N., Cruz-Ordinola, M. C., Paredes-Manrique, C., Chino-Vilca, B., Espinoza, G., Cabrejo, J., Castro-Suarez, S., & Custodio, N. (2025). Prevalence and risk factors of mild cognitive impairment and dementia in northern Peru. Frontiers in Public Health, 13. https://doi.org/10.3389/fpubh.2025.1567073

Zhang, B., Langa, K. M., Weuve, J., D'Souza, J., Szpiro, A., Faul, J., Mendes De Leon, C., Kaufman, J. D., Lisabeth, L., Hirth, R. A., & Adar, S. D. (2023). Hypertension and Stroke as Mediators of Air Pollution Exposure and Incident Dementia. JAMA Network Open, 6(9), e2333470. https://doi.org/10.1001/jamanetworkopen.2023.33470

Zhang, B., Weuve, J., Langa, K. M., D'Souza, J., Szpiro, A., Faul, J., Mendes De Leon, C., Gao, J., Kaufman, J. D., Sheppard, L., Lee, J., Kobayashi, L. C., Hirth, R., & Adar, S. D. (2023). Comparison of Particulate Air Pollution From Different Emission Sources and Incident Dementia in the US. JAMA Internal Medicine, 183(10), 1080. https://doi.org/10.1001/jamainternmed.2023.3300

Zhang, L., Cheng, Y., Zhang, Y., He, Y., Gu, Z., & Yu, C. (2017). Impact of Air Humidity Fluctuation on the Rise of PM Mass Concentration Based on the High-Resolution Monitoring Data. Aerosol and Air Quality Research, 17(2), 543–552. https://doi.org/10.4209/aaqr.2016.07.0296

Zheng, L., Su, B., Cui, F.-P., Li, D., Ma, Y., Xing, M., Tang, L., Wang, J., Tian, Y., & Zheng, X. (2025). Long-Term Exposure to PM2.5 Constituents, Genetic Susceptibility, and Incident Dementia: A Prospective Cohort Study among 0.2 Million Older Adults. Environmental Science & Technology, 59(9), 4493–4504. https://doi.org/10.1021/acs.est.4c08188

APPENDIX

Chapter 1 Appendix

Appendix Table A1. The eight-item AD8 dementia screening instrument. This table lists all eight questions from the AD8, a brief informant-based screening tool used to detect early signs of cognitive impairment. Each item reflects change in memory, orientation, judgment, or daily function. Responses are binary (yes/no), with endorsement of two or more items indicating possible cognitive decline. Copyright 2008 by Washington University in St. Louis, Missouri.

Eight Item Interview to Differentiate Aging and Dementia (AD8) Items in the PSID
Next, we'd like to know about changes that [you / [target person]] may have had in the last several years *[Target person is not respondent: because of a thinking or memory problem].* **In the last several years, has there been a change in:**
1. Problems [you / he / she] may have with judgment, for example, problems making decisions, making bad financial decisions, or with thinking?
1. Yes, a change
5. No, no change
2. The amount of interest [you / he / she] may have in hobbies or activities?
1. Yes, a change
5. No, no change
3. [Your / His / Her] repeating the same things over and over, such as questions, stories, or statements?
1. Yes, a change

5. No, no change
4. The trouble [you / he / she] may have learning how to use a tool, appliance or gadget like a TV remote?
1. Yes, a change
5. No, no change
5. [Your / His / Her] forgetting the correct month or year?
1. Yes, a change
5. No, no change
6. The trouble [you / he / she] may have handling complicated money matters, like balancing a checkbook or paying bills?
1. Yes, a change
5. No, no change
7. The trouble [you / he / she] may have remembering appointments?
1. Yes, a change
5. No, no change
8. Daily problems [you / he / she] may have with thinking and/or memory?
1. Yes, a change
5. No, no change

Appendix Table A2. Bivariate simple regression analyses. Significance levels: p < 0.05 *, p < 0.01 **, p < 0.001 ***

Variable	P Value
ADRD Risk Indicator (2017-2023)	- - -
Average Distance to Nearest Plastics/Rubber TRI Facility, km (1990-2017) *continuous*	0.669
Average Distance to Nearest Plastics/Rubber TRI Facility, km (1990-2017) *categorical*	
1 Near, 0.53-30.54 km (min up to 75th percentile)	
2 Moderate, 30.54-50.59 km (75th-90th percentile)	0.723
3 Far, 50.59+ km (90th+ percentile)	0.544
Average Exposure to Nearest Plastics/Rubber TRI Emissions, lbs (1990-2017) *continuous*	0.396
Average Exposure to Nearest Plastics/Rubber TRI Emissions, lbs (1990-2017) *categorical*	
0 None, 0 lbs	
1 Low, >0-7627.52 lbs (up to 75th percentile)	0.197
2 Moderate, 7627.52 lbs - 75797.66 lbs (75th-90th percentile)	0.009**
3 High, 75797.66+ lbs (90th+ percentile)	0.046*

Age (2023)	
65-70 y.o.	
71-80 y.o.	< 0.001***
81-90 y.o.	< 0.001***
91+ y.o.	< 0.001***
Sex (2023)	
Male	
Female	0.642
Race (2023)	
White	
Black	0.004**
All other	0.047*
Wtr Ever Married (2023)	
Never married	
Current/previously married	0.019*
Total Moves (1990-2017)	
0	
1-2	0.891
3-5	0.641
6-9	0.108
10+	0.001**
Home Ownership (1990-2017)	
Never a homeowner	
Current or previous homeowner	0.002**

Max Education Level (1990-2017)	
Less than 12 years	
12 years or more, less than 16 years	< 0.001***
16 years or more	< 0.001***
Household Average Income Percentile (1990-2017)	< 0.001***
Household Income Binary (recode of Household Average Income Percentile, 1990-2017)	< 0.001***
Bottom 50%	
Top 50%	
Mean Disadvantage Index, Standardized (1990-2017)	< 0.001***

Appendix 2. Explanation of neighborhood disadvantage index.

To measure neighborhood disadvantage, we constructed a composite census tract disadvantage index using eight census tract-level variables from the NCDB from years 1990-2017. We followed the framework and logic of the Neighborhood Atlas Area Deprivation Index, however, our selection of these 8 variables was determined by data availability, coverage, and alignment with our other variables we use in the PSID (Kind, A. J. H., & Buckingham, W., 2018). We chose to create our own Census Tract Disadvantage Index in order to have a comparison among our sample of participants, remaining hyper-local in our methodology.

Several variables required transformation prior to analysis. We calculated the proportion of elderly residents as the ratio of residents aged 65 and older to the total tract population, excluding tracts with zero or missing total population. We derived the proportion of non-white residents by subtracting the percentage of white residents from 100%. To create a low education indicator consistent with our disadvantage framework, we subtracted the percentage of college-educated residents from 100, so that higher values indicated lower educational attainment. The final set of variables included: poverty rate, unemployment rate, proportion elderly, proportion non-white, proportion of men never married, proportion of women never married, proportion with low college education, and proportion of renter-occupied housing units.

After geocoding PSID participants to census tracts and merging with NCDB data (1990-2017), we employed principal component analysis (PCA) to create a single disadvantage index using only the tracts where PSID participants in our analytic sample resided. This approach ensured the index optimally weighted the contribution of each variable based on the variation present within neighborhoods actually experienced by our study population. Prior to analysis, we assessed the appropriateness of PCA using the Kaiser-Meyer-Olkin (KMO) measure of sampling adequacy (StataCorp PCA Postestimation, 2025). The overall KMO value was 0.7150, meeting the recommended threshold of 0.70 and indicating good sampling adequacy. Individual variable KMO values ranged from 0.6119 (proportion of men never married) to 0.8314 (proportion of renter-occupied housing), all surpassing the minimum acceptable level of 0.50.

The PCA was based on 5,640 unique census tracts with data pooled across multiple years (1990-2017), resulting in 52,803 complete tract-year observations. We examined the correlation matrix and scree plot to ensure variables were appropriately intercorrelated and supported a single-factor solution. As shown in Appendix Figure 1, the scree plot indicates a strong one-factor structure underlying the census tract disadvantage index, with a steep drop between the first and second eigenvalues. This supports the use of the first principal component as a summary measure of neighborhood disadvantage. The resulting index provides a time-varying, tract-specific measure of disadvantage, with each tract receiving a score for each year of available data.

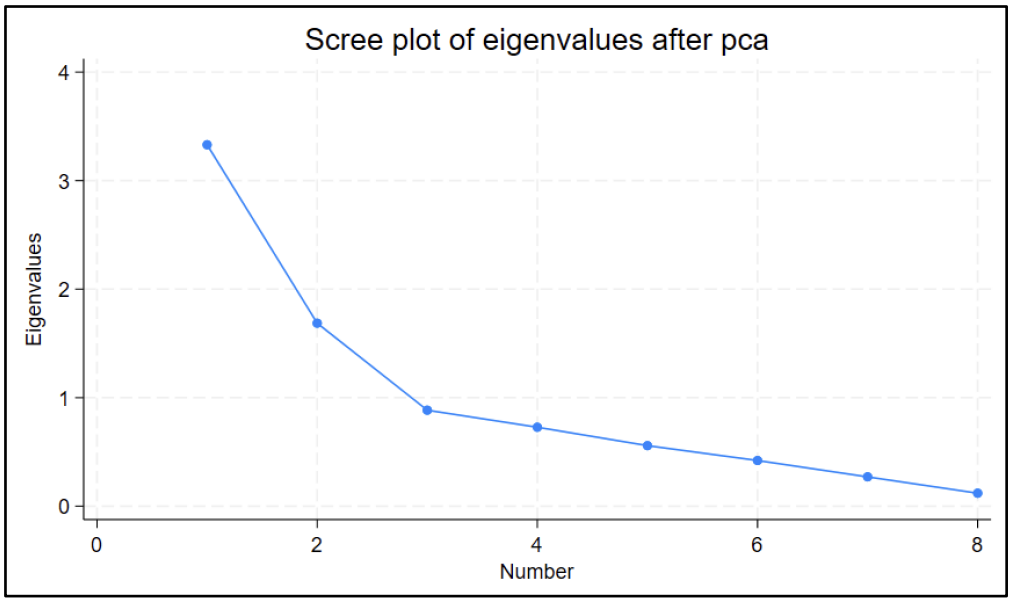

Appendix Figure 1. Scree plot of eigenvalues from principal component analysis (PCA) of eight tract-level disadvantage variables from the NCDB. The first component (eigenvalue = 3.33) explains the majority of shared variance, with a sharp drop to the second (1.68), supporting a one-factor solution. Data: NCDB, 1990–2020.

The first principal component explained 41.63% of the total variance across all eight variables, reflecting a coherent underlying construct of neighborhood disadvantage. Component loadings showed that the poverty rate (0.4090) and proportion of women never married (0.4014) contributed most strongly to the index, followed by proportion non-white (0.3946), proportion of men never married (0.3656), renter-occupied housing (0.3461), and unemployment rate (0.3611). The low college education variable showed a moderate loading (0.2725). Notably, the proportion of elderly residents had a negative loading (-0.2404), suggesting that neighborhoods with higher elderly populations tended to have lower disadvantage scores. This pattern is consistent with our sample geography, which included substantial representation from Florida and California, where elderly populations often reside in more affluent, established communities.

We generated standardized disadvantage index scores using the first principal component, with higher scores indicating greater neighborhood disadvantage. The standardized index (mean = 0, standard deviation = 1) provides an interpretable measure where positive values indicate above-average disadvantage and negative values indicate below-average disadvantage relative to all census tracts in the sample. This continuous variable is well-suited for multilevel modeling and allows for meaningful comparisons across census tracts. Appendix figure 2 presents the density distribution of the standardized neighborhood disadvantage index. The distribution illustrates variation in neighborhood disadvantage across 5,640 unique census tracts (52,803 complete observations over years 1990-2017) represented in

the PSID sample, with a roughly normal shape and some skewness toward higher disadvantage. The index captures a continuum of disadvantage consistent with the socio-demographic composition of neighborhoods.

The PCA results demonstrated strong construct validity. The single-factor solution, high proportion of variance explained, adequate sampling measures, and theoretically consistent factor loadings all support the use of this composite index as a valid measure of neighborhood disadvantage in our study context.

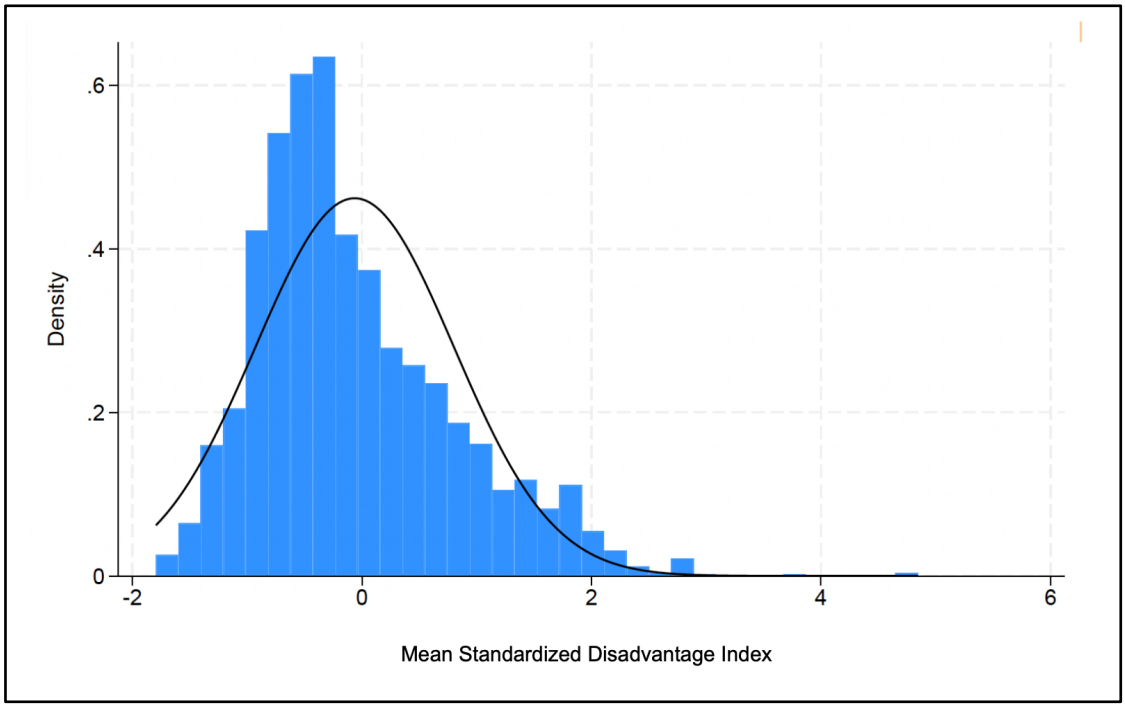

Appendix Figure 2. Distribution of the composite neighborhood disadvantage index derived from PCA of eight tract-level variables. Values are standardized (mean = 0, SD = 1). Data: NCDB, 1990–2020.

Appendix 3. Distance (km) based replication of the five models presented in the paper.

Variable	Model 1	Model 2	Model 3	Model 4	Model 5
Average Distance to Nearest Plastics/Rubber TRI Facility, km (1990-2017) *categorical*					
Ref = 1 Near, 0.53-30.54 km (min up to 75th percentile)					
2 Moderate, 30.54-50.59 km (75th-90th percentile)	0.956	0.879	0.887	0.968	0.88
3 Far, 50.59+ km (90th+ percentile)	1.094	0.906	0.955	1.071	0.96
Sex (2023)					
Ref = Male					
Female		0.897	0.901	0.925	0.904
Race (2023)					
Ref = White					
Black		1.032	0.914	0.972	0.924
All other		1.405	1.313	1.298	1.33
Age (2023)					
Ref = 65-70 y.o.					
71-80 y.o.		2.029***	2.063***	2.076***	2.073***
81-90 y.o.		3.819***	3.926***	4.184***	3.984***
91+ y.o.		11.163***	11.914***	12.892***	12.385***
Household Average Income Percentile (1990-2017)		0.981***	0.982***		0.983***

Total Moves (1990-2017)				
Ref = 0 moves				
1-2	1.19	1.196	1.196	1.194
3-5	1.22	1.212	1.246	1.172
6-9	1.440*	1.419*	1.484*	1.354
10+	2.223**	2.222**	2.539**	2.024*
Wtr Ever Married (2023)				
Ref = Never married				
Current/previously married	0.890	0.878	0.750	0.874
Home Ownership (1990-2017)				
Ref = Never a homeowner				
Current or previous homeowner	1.14	1.196	1.032	1.168
Max Education Level (1990-2017)				
Ref = Less than 12 years				
12 years or more, less than 16 years	0.826	0.854	0.766	0.843
16 years or more	0.833	0.861	0.683*	0.869
Mean Disadvantage Index, Standardized (1990-2017)		1.168*	1.218**	1.168*
Household Income Binary (recode of Household Average Income Percentile, 1990-2017)				
Ref = Bottom 50%				
Top 50%			0.589***	

Binary Income*Exposure to Emissions					
*Ref = Bottom 50% income*Low*					
Top 50% income*Moderate				0.909	
Top 50% income*High				0.929	
Average Exposure to Nearest Plastics/Rubber TRI Emissions, lbs (1990-2017) *categorical*					
Ref = 0 None, 0 lbs					
1 Low, >0-7627.52 lbs (up to 75th percentile)					1.141
2 Moderate, 7627.52 lbs - 75797.66 lbs (75th-90th percentile)					1.343*
3 High, 75797.66+ lbs (90th+ percentile)					1.202
_cons	0.343***	0.541*	0.485*	0.362**	0.452*
	m1	**m2**	**m3**	**m4**	**m5**
n	2627	2627	2627	2627	2627
aic	2992.985	2757.355	2754.23	2774.362	2754.968
bic	3010.606	2863.08	2865.828	2897.708	2884.187
ll	-1493.492	-1360.678	-1358.115	-1366.181	-1355.484

Appendix 4. Alternative Model Specifications

Note on Appendix 4A and 4B results: The results in Appendix 4B are identical to those in Appendix 4A. This reflects the underlying data distribution rather than error. Under the alternative categorization method (median and top 10%),

classifications based on pounds and kilometers produce identical groupings due to the highly skewed nature of the data. Every observation classified as "median" or "top 10%" by pounds receives the same classification by kilometers. This perfect correspondence further motivates the group-based percentile categorization approach employed in the main analysis, which provides greater differentiation across the distribution. Both appendices are retained for transparency in reporting all alternative specifications.

A. Pounds (lbs) exposure categorized by median and tail distribution.

Variable	Model 1	Model 2	Model 3	Model 4
Average Exposure to Nearest Plastics/Rubber TRI Emissions, lbs (1990-2017) *categorical*				
Ref = Low (≤ 50th)				
Mid (50-90th)	1.274*	1.236*	1.232	1.193
High (>90th)	1.347*	1.197	1.201	1.116
Sex (2023)				
Ref = Male				
Female		0.897	0.9	0.923
Race (2023)				
Ref = White				
Black		1.062	0.936	0.994
All other		1.431	1.338	1.329
Age (2023)				
Ref = 65-70 y.o.				
71-80 y.o.		2.031***	2.064***	2.079***

81-90 y.o.	3.879***	3.983***	4.240***
91+ y.o.	11.529***	12.296***	13.197***
Household Average Income Percentile (1990-2017)	0.982***	0.983***	
Total Moves (1990-2017)			
Ref = 0 moves			
1-2	1.187	1.192	1.188
3-5	1.188	1.176	1.204
6-9	1.367	1.344	1.408*
10+	2.018*	2.017*	2.334**
Wtr Ever Married (2023)			
Ref = Never married			
Current/previously married	0.887	0.876	0.752
Home Ownership (1990-2017)			
Ref = Never a homeowner			
Current or previous homeowner	1.095	1.156	1.012
Max Education Level (1990-2017)			
Ref = Less than 12 years			
12 years or more, less than 16 years	0.82	0.851	0.762
16 years or more	0.844	0.875	0.696*
Mean Disadvantage Index, Standardized (1990-2017)		1.170*	1.208**
Household Income Binary (recode of Household Average Income Percentile, 1990-2017)			
Ref = Bottom 50%			

Top 50%				0.549***
Binary Income*Exposure to Emissions				
*Ref = Bottom 50% income*None*				
Top 50% income*Mid				1.110
Top 50% income*High				1.227
_cons	0.308***	0.488*	0.440**	0.346***
n	2627	2627	2627	2627
aic	2985.423	2754.234	2750.87	2769.841
bic	3003.043	2859.959	2862.468	2893.186
ll	-1489.711	-1359.117	-1356.435	-1363.92

B. Distance (km) exposure categorized by median and tail distribution.

Variable	Model 1	Model 2	Model 3	Model 4
Average Distance to Nearest Plastics/Rubber TRI Facility, km (1990-2017) *categorical*				
Ref = Low (≤ 50th)				
Mid (50-90th)	1.274*	1.236*	1.232	1.193
High (>90th)	1.347*	1.197	1.201	1.116
Sex (2023)				
Ref = Male				
Female		0.897	0.9	0.923
Race (2023)				
Ref = White				
Black		1.062	0.936	0.994
All other		1.431	1.338	1.329

Age (2023)			
Ref = 65-70 y.o.			
71-80 y.o.	2.031***	2.064***	2.079***
81-90 y.o.	3.879***	3.983***	4.240***
91+ y.o.	11.529***	12.296***	13.197***
Household Average Income Percentile (1990-2017)	0.982***	0.983***	
Total Moves (1990-2017)			
Ref = 0 moves			
1-2	1.187	1.192	1.188
3-5	1.188	1.176	1.204
6-9	1.367	1.344	1.408*
10+	2.018*	2.017*	2.334**
Wtr Ever Married (2023)			
Ref = Never married			
Current/previously married	0.887	0.876	0.752
Home Ownership (1990-2017)			
Ref = Never a homeowner			
Current or previous homeowner	1.095	1.156	1.012
Max Education Level (1990-2017)			
Ref = Less than 12 years			
12 years or more, less than 16 years	0.82	0.851	0.762
16 years or more	0.844	0.875	0.696*
Mean Disadvantage Index, Standardized (1990-2017)		1.170*	1.208**

Household Income Binary (recode of Household Average Income Percentile, 1990-2017)				
Ref = Bottom 50%				
Top 50%				0.549***
Binary Income*Exposure to Emissions				
*Ref = Bottom 50% income*None*				
Top 50% income*Mid (50-90th)				1.110
Top 50% income*High (>90th)				1.227
_cons	0.308***	0.488*	0.440**	0.346***
n	2627	2627	2627	2627
aic	2985.423	2754.234	2750.87	2769.841
bic	3003.043	2859.959	2862.468	2893.186
ll	-1489.711	-1359.117	-1356.435	-1363.92

C. Log-transformed lbs exposure divided into quartiles.

The log transformation specification uses log(1+x) to avoid dropping observations with zero values. However, due to the highly skewed distribution of the exposure variable, half of all observations (the bottom 50%) have a value of zero. This prevents the quartile categorization from distinguishing between the first two quartiles. Consequently, only three categories (Q1, Q3, and Q4) are included in the log-transformed models, with Q1 serving as the reference category and representing the bottom 50% of the distribution.

Variable	**Model 1**	**Model 2**	**Model 3**	**Model 4**

Logged Average Exposure to Nearest Plastics/Rubber TRI Emissions, lbs (1990-2017) *categorical, quartiles*				
Ref = Q1				
Q2 - *omitted*	- - -	- - -	- - -	- - -
Q3	1.185	1.153	1.148	1.111
Q4	1.362**	1.274*	1.275*	1.211
Sex (2023)				
Ref = Male				
Female		0.898	0.902	0.925
Race (2023)				
Ref = White				
Black		1.066	0.938	0.999
All other		1.438	1.344	1.336
Age (2023)				
Ref = 65-70 y.o.				
71-80 y.o.		2.031***	2.065***	2.078***
81-90 y.o.		3.870***	3.975***	4.223***
91+ y.o.		11.563***	12.342***	13.242***
Household Average Income Percentile (1990-2017)		0.982***	0.983***	
Total Moves (1990-2017)				
Ref = 0 moves				
1-2		1.186	1.191	1.188
3-5		1.185	1.173	1.201
6-9		1.371	1.349	1.411*
10+		2.010*	2.010*	2.318**

Wtr Ever Married (2023)				
Ref = Never married				
Current/previously married		0.886	0.874	0.752
Home Ownership (1990-2017)				
Ref = Never a homeowner				
Current or previous homeowner		1.094	1.156	1.01
Max Education Level (1990-2017)				
Ref = Less than 12 years				
12 years or more, less than 16 years		0.823	0.854	0.766
16 years or more		0.847	0.877	0.699*
Mean Disadvantage Index, Standardized (1990-2017)			1.171*	1.208**
Household Income Binary (recode of Household Average Income Percentile, 1990-2017)				
Ref = Bottom 50%				
Top 50%				0.550***
Binary Income*Exposure to Emissions				
*Ref = Bottom 50% income*Q1*				
Top 50% income*Q3				1.109
Top 50% income*Q4				1.170
_cons	0.308***	0.485*	0.437**	0.345***
n	2627	2627	2627	2627
aic	2984.543	2753.81	2750.39	2769.402
bic	3002.164	2859.535	2861.989	2892.748
ll	-1489.271	-1358.905	-1356.195	-1363.701

D. Log-transformed km exposure divided into quartiles

Variable	Model 1	Model 2	Model 3	Model 4
Logged Average Distance to Nearest Plastics/Rubber TRI Facility, km (1990-2017) *categorical, quartiles*				
Ref = Q1				
Q2	0.807	0.876	0.912	1.081
Q3	1.01	1.154	1.22	1.301
Q4	0.948	0.901	0.956	1.135
Sex (2023)				
Ref = Male				
Female		0.899	0.903	0.927
Race (2023)				
Ref = White				
Black		1.048	0.925	0.986
All other		1.438	1.349	1.335
Age (2023)				
Ref = 65-70 y.o.				
71-80 y.o.		2.021***	2.054***	2.072***
81-90 y.o.		3.830***	3.933***	4.200***
91+ y.o.		11.384***	12.258***	13.465***
Household Average Income Percentile (1990-2017)		0.981***	0.982***	
Total Moves (1990-2017)				
Ref = 0 moves				

1-2	1.187	1.19	1.187
3-5	1.218	1.205	1.232
6-9	1.439*	1.410*	1.469*
10+	2.204**	2.201**	2.543**
Wtr Ever Married (2023)			
Ref = Never married			
Current/previously married	0.896	0.881	0.748
Home Ownership (1990-2017)			
Ref = Never a homeowner			
Current or previous homeowner	1.127	1.185	1.02
Max Education Level (1990-2017)			
Ref = Less than 12 years			
12 years or more, less than 16 years	0.831	0.865	0.778
16 years or more	0.837	0.871	0.695*
Mean Disadvantage Index, Standardized (1990-2017)		1.179*	1.231**
Household Income Binary (recode of Household Average Income Percentile, 1990-2017)			
Ref = Bottom 50%			
Top 50%			0.714
Binary Income*Exposure to Emissions			
*Ref = Bottom 50% income*None*			
Top 50% income*Q2			0.644
Top 50% income*Q3			0.852

Top 50% income*Q4				0.752
_cons	0.366***	0.534*	0.462*	0.323***
n	2627	2627	2627	2627
aic	2991.621	2755.3	2751.62	2770.894
bic	3015.115	2866.898	2869.092	2905.987
ll	-1491.81	-1358.65	-1355.81	-1362.447

Chapter 3 Appendix

Supplement Table 1: Post-hoc balance check across our sample sociodemographic and health characteristics using chi-square tests (categorical variables) and Kruskal-Wallis tests (continuous variables), with Monte Carlo p-values used throughout due to small expected cell counts in some zones.

Variable	**Test Statistic**	**P value**
Sex	5.07	0.440
Education	13.20	0.198
Civil status	8.15	0.592
Native language	5.56	0.347
Health Insurance	20.46	0.168
Occupation	14.38	0.147
Chronic disease	3.01	0.730
Glucose	15.85	0.100
Hypertension	5.33	0.385
SES Level	20.69	0.410
Age	4.67	0.458
BMI	6.95	0.225

Supplement Table 2: Full model output for exposures (Temperature, Humidity, PM2.5, PM10) and Dementia (binary). Model 1 = bivariate, Model 2 = Age and sex adjusted, Model 3 = Fully Adjusted.

Outcome: **binary dementia**

Table 2 A.
TEMPERATURE

M1	Est.	P	M2	Est.	P	M3	Est.	P
Temperature	1.061	0.522	Temperature	1.081	0.406	Temperature	1.09	0.391
			Age	0.987	0.024	Age	0.961	0.000
			Sex (male)	0.347	0.000	Sex (male)	0.579	0.055
						SES: NSE E	--	--
						SES: NSE D	0.607	0.26
						SES: NSE C	0.527	0.057
						SES: NSE B	0.296	0.000
						SES: NSE A	0.355	0.053
						BMI	1.024	0.196
						EDU: none	--	--
						EDU: primary	0.533	0.068
						EDU: sec+	0.099	0.000
						Civil Status: married	--	--
						Civil Status: single	1.01	0.965
						Civil Status: widows/sep	0.873	0.667
						Occup: employed	--	--
						Occup: homemaker	1.323	0.23
						Occup: not emp	0.863	0.644
						HTN: yes	1.405	0.153
						Glucose: Normal (<100)	--	--
						Glucose: prediab (<126)	1.038	0.88
						Glucose: Diab (≥ 126)	1.046	0.87

						Chr.Dis: yes	0.923	0.727

Table 2 B.
HUMIDITY

M1	Est.	P	M2	Est.	P	M3	Est.	P
Humidity	1.064	0.503	Humidity	1.067	0.469	Humidity	1.134	0.184
			Age	0.987	0.025	Age	0.961	0.000
			Sex (male)	0.348	0.000	Sex (male)	0.58	0.057
						SES: NSE E	--	--
						SES: NSE D	0.588	0.231
						SES: NSE C	0.519	0.053
						SES: NSE B	0.293	0.000
						SES: NSE A	0.358	0.055
						BMI	1.026	0.178
						EDU: none	--	--
						EDU: primary	0.56	0.093
						EDU: sec+	0.1	0.000
						Civil Status: married	--	--
						Civil Status: single	1.034	0.891
						Civil Status: widows/sep	0.891	0.713
						Occup: employed	--	--
						Occup: homemaker	1.306	0.254
						Occup: not emp	0.858	0.632
						HTN: yes	1.418	0.145
						Glucose: Normal (<100)	--	--
						Glucose: prediab (<126)	1.058	0.823
						Glucose: Diab (≥ 126)	1.073	0.798
						Chr.Dis: yes	0.921	0.72

Table 2 C. PM2.5

M1	Est.	P	M2	Est.	P	M3	Est.	P
PM2.5	0.903	0.336	PM2.5	0.913	0.37	PM2.5	0.92	0.405
			Age	0.987	0.027	Age	0.961	0.000
			Sex (male)	0.349	0.000	Sex (male)	0.58	0.056
						SES: NSE E	--	--
						SES: NSE D	0.61	0.264
						SES: NSE C	0.533	0.062
						SES: NSE B	0.302	0.001
						SES: NSE A	0.363	0.058
						BMI	1.024	0.2
						EDU: none	--	--
						EDU: primary	0.544	0.078
						EDU: sec+	0.1	0.000
						Civil Status: married	--	--
						Civil Status: single	1.018	0.94
						Civil Status: widows/sep	0.867	0.654
						Occup: employed	--	--
						Occup: homemaker	1.315	0.24
						Occup: not emp	0.868	0.657
						HTN: yes	1.415	0.146
						Glucose: Normal (<100)	--	--
						Glucose: prediab (<126)	1.048	0.848
						Glucose: Diab (≥ 126)	1.065	0.817
						Chr.Dis: yes	0.921	0.72

Table 2 D. PM10

M1	Est.	P	M2	Est.	P	M3	Est.	P
PM10	0.908	0.36	PM10	0.904	0.333	PM10	0.836	0.125
			Age	0.987	0.027	Age	0.961	0.000
			Sex (male)	0.347	0.000	Sex (male)	0.574	0.052

		SES: NSE E	--	--
		SES: NSE D	0.589	0.226
		SES: NSE C	0.517	0.049
		SES: NSE B	0.295	0.000
		SES: NSE A	0.355	0.052
		BMI	1.024	0.198
		EDU: none	--	--
		EDU: primary	0.545	0.075
		EDU: sec+	0.097	0.000
		Civil Status: married	--	--
		Civil Status: single	1.033	0.893
		Civil Status: widows/sep	0.876	0.676
		Occup: employed	--	--
		Occup: homemaker	1.288	0.281
		Occup: not emp	0.862	0.644
		HTN: yes	1.402	0.158
		Glucose: Normal (<100)	--	--
		Glucose: prediab (<126)	1.058	0.82
		Glucose: Diab (≥ 126)	1.081	0.778
		Chr.Dis: yes	0.915	0.697

Supplement Table 3: Full model output for exposures (Temperature, Humidity, PM2.5, PM10) and ACE. Model 1 = bivariate, Model 2 = Age and sex adjusted, Model 3 = Fully Adjusted.

Outcome: **ACE**

Table 3 A.
TEMPERATURE

M1	Est.	P	M2	Est.	P	M3	Est.	P
Temperature	0.203	0.639	Temperature	0.223	0.582	Temperature	0.281	0.434
			Age	-0.279	0.000	Age	-0.164	0.000
			Sex (male)	3.816	0.000	Sex (male)	1.237	0.174
						SES: NSE E	--	--
						SES: NSE D	0.962	0.703
						SES: NSE C	3.526	0.055
						SES: NSE B	6.696	0.000
						SES: NSE A	7.51	0.000
						BMI	-0.024	0.729
						EDU: none	--	--
						EDU: primary	18	0.000
						EDU: sec+	27.285	0.000
						Civil Status: married	--	--
						Civil Status: single	0.178	0.838
						Civil Status: widows/sep	0.365	0.77
						Occup: employed	--	--
						Occup: homemaker	-1.088	0.202
						Occup: not emp	-0.891	0.499
						HTN: yes	-2.209	0.026
						Glucose: Normal (<100)	--	--
						Glucose: prediab (<126)	-0.106	0.904
						Glucose: Diab (≥ 126)	0.566	0.578
						Chr.Dis: yes	0.863	0.274

Table 3 B.
HUMIDITY

M1	Est.	P	M2	Est.	P	M3	Est.	P
Humidity	-0.128	0.757	Humidity	-0.071	0.858	Humidity	-0.273	0.443

			Age	-0.279	0.000	Age	-0.162	0.000
			Sex (male)	3.824	0.000	Sex (male)	1.229	0.176
						SES: NSE E	--	--
						SES: NSE D	1.135	0.65
						SES: NSE C	3.613	0.047
						SES: NSE B	6.719	0.000
						SES: NSE A	7.566	0.000
						BMI	-0.024	0.733
						EDU: none	--	--
						EDU: primary	18.072	0.000
						EDU: sec+	27.394	0.000
						Civil Status: married	--	--
						Civil Status: single	0.133	0.879
						Civil Status: widows/sep	0.298	0.811
						Occup: employed	--	--
						Occup: homemaker	-1.105	0.194
						Occup: not emp	-0.906	0.492
						HTN: yes	-2.159	0.03
						Glucose: Normal (<100)	--	--
						Glucose: prediab (<126)	-0.104	0.906
						Glucose: Diab (≥ 126)	0.523	0.609
						Chr.Dis: yes	0.884	0.262

Table 3 C. PM2.5

M1	**Est.**	**P**	**M2**	**Est.**	**P**	**M3**	**Est.**	**P**
PM2.5	0.174	0.69	PM2.5	0.282	0.482	PM2.5	0.168	0.651
			Age	-0.281	0.000	Age	-0.165	0.000
			Sex (male)	3.814	0.000	Sex (male)	1.227	0.176
						SES: NSE E	--	--

						SES: NSE D	1.102	0.661
						SES: NSE C	3.592	0.049
						SES: NSE B	6.707	0.000
						SES: NSE A	7.565	0.000
						BMI	-0.019	0.78
						EDU: none	--	--
						EDU: primary	18.133	0.000
						EDU: sec+	27.4	0.000
						Civil Status: married	--	--
						Civil Status: single	0.161	0.853
						Civil Status: widows/sep	0.318	0.798
						Occup: employed	--	--
						Occup: homemaker	-1.106	0.195
						Occup: not emp	-0.901	0.492
						HTN: yes	-2.147	0.032
						Glucose: Normal (<100)	--	--
						Glucose: prediab (<126)	-0.102	0.908
						Glucose: Diab (≥ 126)	0.536	0.599
						Chr.Dis: yes	0.879	0.266

Table 3 D. PM10

M1	**Est.**	**P**	**M2**	**Est.**	**P**	**M3**	**Est.**	**P**
PM10	0.017	0.969	PM10	-0.046	0.91	PM10	0.169	0.647
			Age	-0.279	0.000	Age	-0.163	0.000
			Sex (male)	3.824	0.000	Sex (male)	1.226	0.177
						SES: NSE E	--	--
						SES: NSE D	1.109	0.657
						SES: NSE C	3.6	0.048
						SES: NSE B	6.719	0.000

		SES: NSE A	7.571	0.000
		BMI	-0.021	0.76
		EDU: none	--	--
		EDU: primary	18.124	0.000
		EDU: sec+	27.415	0.000
		Civil Status: married	--	--
		Civil Status: single	0.153	0.861
		Civil Status: widows/sep	0.319	0.797
		Occup: employed	--	--
		Occup: homemaker	-1.103	0.196
		Occup: not emp	-0.902	0.492
		HTN: yes	-2.149	0.031
		Glucose: Normal (<100)	--	--
		Glucose: prediab (<126)	-0.099	0.91
		Glucose: Diab (≥ 126)	0.539	0.598
		Chr.Dis: yes	0.877	0.266

Supplement Table 4: Full model output for exposures (Temperature, Humidity, PM2.5, PM10) and RUDAS-PE. Model 1 = bivariate, Model 2 = Age and sex adjusted, Model 3 = Fully Adjusted.

Outcome: **RUDAS**

Table 4 A.
TEMPERATURE

M1	**Est.**	**P**	**M2**	**Est.**	**P**	**M3**	**Est.**	**P**
Temperature	-0.419	0.166	Temperature	-0.42	0.175	Temperature	-0.375	0.15
			Age	0.005	0.931	Age	0.035	0.604
			Sex (male)	0.002	0.998	Sex (male)	-1.39	0.076
						SES: NSE E	--	--

						SES: NSE D	0.739	0.655
						SES: NSE C	1.22	0.451
						SES: NSE B	1.222	0.43
						SES: NSE A	1.776	0.28
						BMI	0.004	0.938
						EDU: none	--	--
						EDU: primary	0.265	0.842
						EDU: sec+	-0.585	0.611
						Civil Status: married	--	--
						Civil Status: single	1.63	0.13
						Civil Status: widows/sep	0.151	0.85
						Occup: employed	--	--
						Occup: homemaker	-3.206	0.017
						Occup: not emp	-0.729	0.395
						HTN: yes	0.18	0.791
						Glucose: Normal (<100)	--	--
						Glucose: prediab (<126)	0.103	0.914
						Glucose: Diab (≥ 126)	-0.332	0.734
						Chr.Dis: yes	-1.939	0.015

Table 4 B.
HUMIDITY

M1	**Est.**	**P**	**M2**	**Est.**	**P**	**M3**	**Est.**	**P**
Humidity	-0.572	0.046	Humidity	-0.581	0.045	Humidity	-0.422	0.122
			Age	0.008	0.891	Age	0.038	0.571
			Sex (male)	0.106	0.889	Sex (male)	-1.213	0.124
						SES: NSE E	--	--
						SES: NSE D	0.832	0.614
						SES: NSE C	1.308	0.408
						SES: NSE B	1.306	0.396

						SES: NSE A	2.058	0.198
						BMI	0.006	0.905
						EDU: none	--	--
						EDU: primary	0.202	0.877
						EDU: sec+	-0.754	0.51
						Civil Status: married	--	--
						Civil Status: single	1.435	0.181
						Civil Status: widows/sep	0.184	0.817
						Occup: employed	--	--
						Occup: homemaker	-2.937	0.032
						Occup: not emp	-0.754	0.37
						HTN: yes	0.226	0.745
						Glucose: Normal (<100)	--	--
						Glucose: prediab (<126)	0.199	0.836
						Glucose: Diab (≥ 126)	-0.309	0.751
						Chr.Dis: yes	-2.034	0.008

Table 4 C. PM2.5

M1	**Est.**	**P**	**M2**	**Est.**	**P**	**M3**	**Est.**	**P**
PM2.5	0.356	0.207	PM2.5	0.356	0.218	PM2.5	0.291	0.21
			Age	0.004	0.949	Age	0.035	0.601
			Sex (male)	0.000	1	Sex (male)	-1.342	0.086
						SES: NSE E	--	--
						SES: NSE D	0.817	0.621
						SES: NSE C	1.263	0.432
						SES: NSE B	1.236	0.424
						SES: NSE A	1.83	0.25
						BMI	0.004	0.946
						EDU: none	--	--

						EDU: primary	0.162	0.905
						EDU: sec+	-0.732	0.537
						Civil Status: married	--	--
						Civil Status: single	1.589	0.142
						Civil Status: widows/sep	0.172	0.829
						Occup: employed	--	--
						Occup: homemaker	-3.1	0.021
						Occup: not emp	-0.755	0.375
						HTN: yes	0.193	0.78
						Glucose: Normal (<100)	--	--
						Glucose: prediab (<126)	0.238	0.802
						Glucose: Diab (≥ 126)	-0.253	0.794
						Chr.Dis: yes	-2.02	0.009

Table 4 D. PM10

M1	**Est.**	**P**	**M2**	**Est.**	**P**	**M3**	**Est.**	**P**
PM10	0.435	0.117	PM10	0.438	0.117	PM10	0.319	0.164
			Age	0.006	0.915	Age	0.035	0.607
			Sex (male)	0.063	0.934	Sex (male)	-1.282	0.104
						SES: NSE E	--	--
						SES: NSE D	0.821	0.622
						SES: NSE C	1.365	0.398
						SES: NSE B	1.319	0.393
						SES: NSE A	2.042	0.207
						BMI	0.004	0.946
						EDU: none	--	--
						EDU: primary	0.231	0.86
						EDU: sec+	-0.661	0.559

						Civil Status: married	--	--
						Civil Status: single	1.572	0.141
						Civil Status: widows/sep	0.171	0.83
						Occup: employed	--	--
						Occup: homemaker	-3.062	0.023
						Occup: not emp	-0.728	0.39
						HTN: yes	0.21	0.76
						Glucose: Normal (<100)	--	--
						Glucose: prediab (<126)	0.173	0.857
						Glucose: Diab (≥ 126)	-0.279	0.776
						Chr.Dis: yes	-1.961	0.015

Supplement Table 5: Full model output for Road Proximity and Dementia (binary). Model 1 = bivariate, Model 2 = Age and sex adjusted, Model 3 = Fully Adjusted.

Outcome: **binary dementia**

Table 5. Road Proximity

M1	**Est.**	**P**	**M2**	**Est.**	**P**	**M3**	**Est.**	**P**
Dist to Road (logged)	1.106	0.161	Dist to Road (logged)	1.072	0.336	Dist to Road (logged)	1.005	0.953
			Age	0.988	0.031	Age	0.961	0.000
			Sex (male)	0.351	0.000	Sex (male)	0.583	0.059
						SES: NSE E	--	--
						SES: NSE D	0.619	0.282
						SES: NSE C	0.533	0.064

						SES: NSE B	0.298	0.001
						SES: NSE A	0.363	0.06
						BMI	1.025	0.182
						EDU: none	--	--
						EDU: primary	0.546	0.08
						EDU: sec+	0.100	0.000
						Civil Status: married	--	--
						Civil Status: single	1.009	0.971
						Civil Status: widows/sep	0.875	0.673
						Occup: employed	--	--
						Occup: homemaker	1.323	0.229
						Occup: not emp	0.861	0.638
						HTN: yes	1.426	0.141
						Glucose: Normal (<100)	--	--
						Glucose: prediab (<126)	1.046	0.856
						Glucose: Diab (≥ 126)	1.049	0.859
						Chr.Dis: yes	0.928	0.742

Supplement Table 6: Full model output for Road Proximity and ACE. Model 1 = bivariate, Model 2 = Age and sex adjusted, Model 3 = Fully Adjusted.

Outcome: **ACE**

Table 6. Road Proximity

M1	**Est.**	**P**	**M2**	**Est.**	**P**	**M3**	**Est.**	**P**
Dist to Road (logged)	-0.719	0.033	Dist to Road (logged)	-0.924	0.005	Dist to Road (logged)	-0.545	0.079
			Age	-0.296	0.000	Age	-0.174	0.000
			Sex (male)	3.71	0.000	Sex (male)	1.274	0.161
						SES: NSE E	--	--

						SES: NSE D	0.712	0.779
						SES: NSE C	3.486	0.06
						SES: NSE B	6.527	0.000
						SES: NSE A	7.314	0.000
						BMI	-0.02	0.769
						EDU: none	--	--
						EDU: primary	18.116	0.000
						EDU: sec+	27.244	0.000
						Civil Status: married	--	--
						Civil Status: single	0.13	0.881
						Civil Status: widows/sep	0.46	0.711
						Occup: employed	--	--
						Occup: homemaker	-1.055	0.216
						Occup: not emp	-0.815	0.53
						HTN: yes	-2.328	0.019
						Glucose: Normal (<100)	--	--
						Glucose: prediab (<126)	-0.131	0.882
						Glucose: Diab (≥ 126)	0.511	0.615
						Chr.Dis: yes	0.96	0.219

Supplement Table 7: Full model output for Road Proximity and RUDAS-PE.

Model 1 = bivariate, Model 2 = Age and sex adjusted, Model 3 = Fully Adjusted.

Outcome:
RUDAS

Table 4. Road Proximity

M1	**Est.**	**P**	**M2**	**Est.**	**P**	**M3**	**Est.**	**P**
Dist to Road (logged)	0.069	0.774	Dist to Road (logged)	0.069	0.775	Dist to Road (logged)	0.135	0.614
			Age	0.003	0.967	Age	0.036	0.599
			Sex (male)	0.04	0.959	Sex (male)	-1.392	0.076

		SES: NSE E	--	--
		SES: NSE D	0.599	0.73
		SES: NSE C	1.193	0.484
		SES: NSE B	1.155	0.483
		SES: NSE A	1.624	0.34
		BMI	0.003	0.96
		EDU: none	--	--
		EDU: primary	0.429	0.747
		EDU: sec+	-0.393	0.738
		Civil Status: married	--	--
		Civil Status: single	1.628	0.142
		Civil Status: widows/sep	0.162	0.841
		Occup: employed	--	--
		Occup: homemaker	-3.114	0.021
		Occup: not emp	-0.688	0.427
		HTN: yes	0.199	0.771
		Glucose: Normal (<100)	--	--
		Glucose: prediab (<126)	-0.008	0.993
		Glucose: Diab (≥ 126)	-0.38	0.699
		Chr.Dis: yes	-2.147	0.006

Supplement Table 8. Descriptive statistics of road proximity (meters) by SES category. R^2 = 0.011. p (overall) = 0.018

Predictor (reference: NSE E)	Estimate	p-value
NSE D	-431.7	0.009
NSE C	-157.5	0.259
NSE B	-265.2	0.052

NSE A	-414.1	0.016

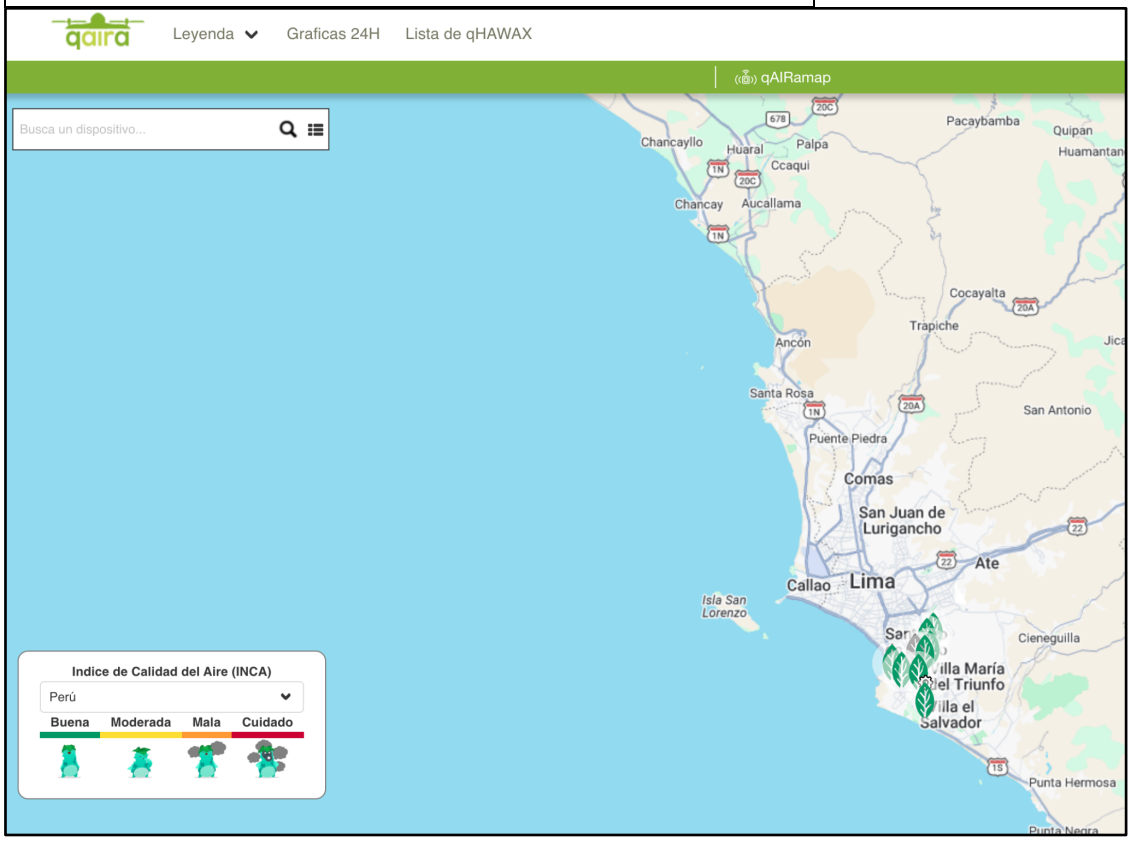

Supplementary Figure 1. Distribution of qAIRa air quality sensors across Lima, Peru, showing concentration in wealthier southern districts with no coverage in Puente Piedra (located north of central Lima)(*Calidad Del Aire y Mapeo Digital Con Drones LiDAR*, n.d.).

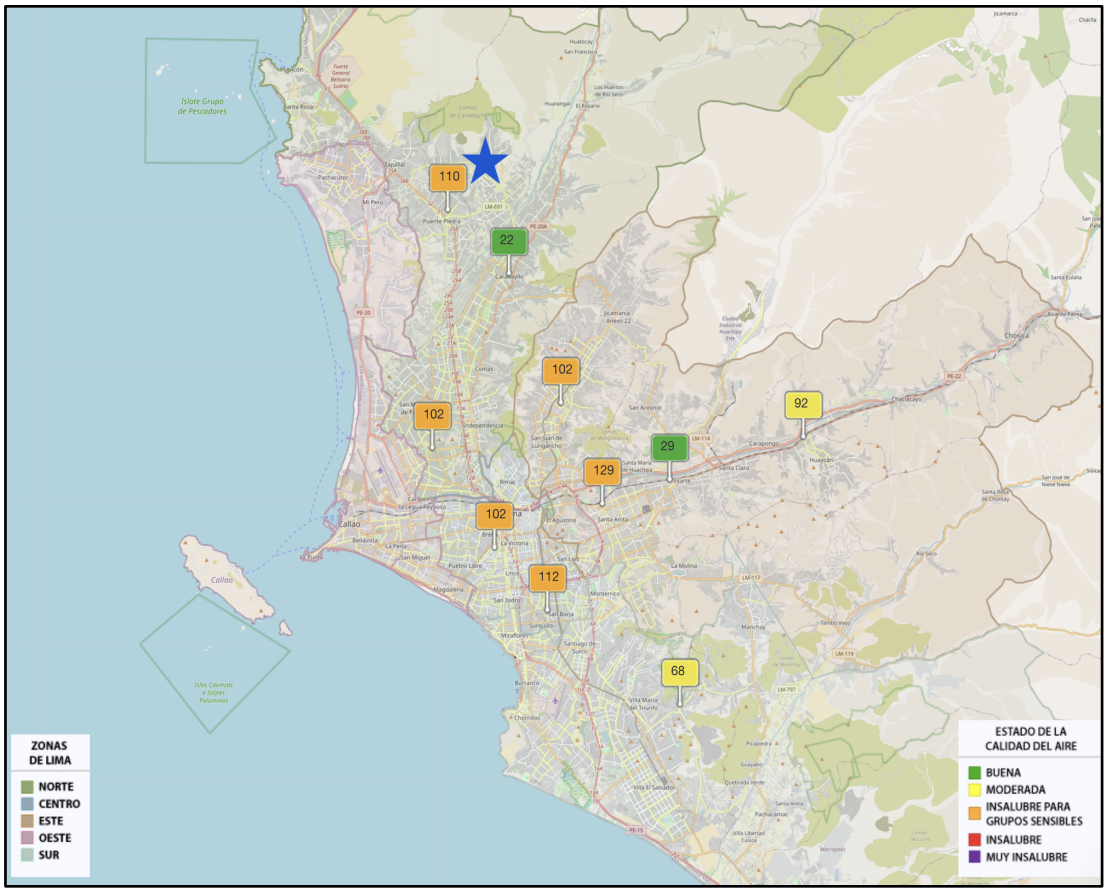

Supplementary Figure 2. Locations of air quality monitoring in Lima, Peru. Puente Piedra is indicated with the blue star. Accessed via Servicio Nacional de Meteorología e Hidrología del Perú.